CHARACTERIZATION AND MICROWAVE ASSISTED PYROLYSIS OF OKLAHOMA NATIVE MICROALGAE STRAINS FOR BIO-OIL PRODUCTION

By

NAN ZHOU

Bachelor of Science in Energy and Power Engineering

Xi'an Jiaotong University

Xi'an, China

2013

Submitted to the Faculty of the
Graduate College of the
Oklahoma State University
in partial fulfillment of
the requirements for
the Degree of
MASTER OF SCIENCE
December, 2015

CHARACTERIZATION AND MICROWAVE ASSISTED PYROLYSIS OF OKLAHOMA NATIVE MICROALGAE STRAINS FOR BIO-OIL PRODUCTION

Thesis Approved:

Dr. Nurhan Dunford

Thesis Advisor

Dr. Ajay Kumar

Dr. Mark Wilkins

ACKNOWLEDGEMENTS

First and foremost, I would like to express my sincere gratitude to my advisor Dr. Nurhan Dunford for her constant guidance, encouragement, and support during the past two and a half years. I am deeply impressed by Dr. Dunford's passion and diligence, which I believe will always motivate me to achieve my goals in the future. I would also like to thank my thesis committee members Dr. Mark Wilkins and Dr. Ajay Kumar for their valuable comments and suggestions. Their efforts and time are greatly appreciated.

I also want to thank my group friends. Dr. Meizhen Xie gave me invaluable trainings when I started my research from zero, and she also gave me constant support and encouragement whenever I need them. Thanks to Dr. Ran Ye and Qichen Ding, who provided me with advices and helped me make my lab work easier and more fun. The friendship between us is a precious gift to me.

Special thanks to Angie Lathrop who gave me encouragement and generous help with my GC-FID work, and Zixu Yang who helped me run the GC-MS experiments.

Last but not least, my deepest appreciation and love goes to my parents, Hongwei Zhou and Aiping Yu, my grandparents, Shiru Zhou and Sulan Xu, and my girlfriend, Yun Tang. You are the power that keeps me moving forward.

Name: NAN ZHOU

Date of Degree: DECEMBER, 2015

Title of Study: CHARACTERIZATION AND MICROWAVE ASSISTED PYROLYSIS OF OKLAHOMA NATIVE MICROALGAE STRAINS FOR BIO-OIL PRODUCTION

Major Field: BIOSYSTEMS ENGINEERING

Abstract:

Microalgae have received significant interest as a potential feedstock for the production of biofuel and other bioproducts. The main advantages of microalgae over the existing energy crops include the higher biomass production rate and not competing for resources needed for conventional agriculture. Selection of the appropriate algae species is crucial for the success of microalgae production systems. Pyrolysis is a thermochemical conversion technique in which biomass is thermally decomposed into bio-oil and other products.

In this study, seven algae strains isolated from the Great Salt Plains of Oklahoma, UTEX SP20, SP22, SP38, SP46, SP47, SP48, and SP50, were cultivated under controlled growth conditions. The growth parameters, chemical composition, and fatty acid profile of each strain were determined. Biomass thermal degradation behavior of each strain was examined by thermogravimetric analysis. Kinetic parameters were determined by using an iso-conversional approach. Algal biomass was used as feedstock for bio-oil production via microwave assisted pyrolysis, and the effects of final temperature on the product yields and bio-oil composition were evaluated.

Among the seven strains, SP46 produced the highest final biomass concentration (1.32 g/L), the highest biomass productivity (55.9 mg $L^{-1}day^{-1}$) and the lowest lipid content (9.2% based on ash free and dry weight). Due to these properties, SP46 was selected out of the seven strains for microwave assisted pyrolysis. Thermogravimetric analysis revealed that pyrolysis of algae biomass took place in three stages, with major weight loss occurring at the second stage from around 150 ^{o}C to 400 ^{o}C. The apparent activation energy was a function of degrees of conversion. Biomass of SP38 had the lowest average apparent activation energy, 102.8 kJ/mol, indicating that biomass of SP38 requires the least energy for pyrolysis among the seven strains. During the microwave assisted pyrolysis of SP46 biomass, the bio-oil yield increased from 4.6% to 22.5% with the increasing final temperature from 450 ^{o}C to 750 ^{o}C. The major compounds in the bio-oil included acids, aliphatic hydrocarbons, aromatic hydrocarbons, phenols, organic nitrogen compounds.

TABLE OF CONTENTS

Chapter Page

LIST OF TABLES

Table Page

.

LIST OF FIGURES

Figure Page

Figure Page

LIST OF PICTURES

CHAPTER I

INTRODUCTION

1.1 PROBLEM STATEMENT

Biofuel is a promising solution to the problems that have resulted from the utilization of conventional fuels such as fossil fuel depletion and environmental pollution. Microalgae have received increasing interest as a potential feedstock for the production of biofuels and other bioproducts. The main advantages of microalgae over the existing energy crops include higher productivity and minimal competition for resources needed for conventional agricultural production. Selection of the appropriate algae species is crucial for the success of microalgae production systems considering the diversity of algae species. Native algae strains tend to be more stable and adaptable for mass cultivation in regional conditions compared with non-native species. Therefore, it is necessary to characterize and select from native algae strains for the establishment of microalgae production systems in Oklahoma. In addition to strain selection, biomass conversion is also a critical step in the algal biofuel production pathway. Among various conversion techniques, microwave assisted pyrolysis has gained much attention mainly due to its high energy efficiency and easy control of the heating process. To the best of our knowledge, limited information is available regarding the growth characteristics, thermal degradation behavior and microwave assisted pyrolysis of biomass produced by

Oklahoma native algae strains. This information is essential for evaluating the potential of algal biomass as feedstock for bio-product manufacturing.

1.2 OBJECTIVES

The overall objective of this study is to evaluate the potential of seven Oklahoma native microalgae strains as feedstock for bio-oil production by studying their growth pattern, chemical composition, and pyrolysis behavior and selecting one strain as feedstock for bio-oil production via microwave assisted pyrolysis. The three specific objectives are as follows:

i. To characterize the growth patterns of the algae strains under standard laboratory batch culture conditions and analyze the chemical composition of the biomass including algal oil fatty acid composition.

ii. To characterize thermal degradation behavior of the algal biomass using thermogravimetric analysis, and calculate the pyrolysis kinetic parameters.

iii. To select and use one strain as feedstock for bio-oil production via microwave assisted pyrolysis, and evaluate the effect of pyrolysis temperature on the product yields and bio-oil composition.

CHAPTER II

LITERATURE REVIEW

2.1 ALGAE

Algae are a diverse group of organisms that are eukaryotic, chlorophyll-a containing, oxygenic photosynthetic, and relatively simple in vegetative and reproductive structures compared to higher plants. Depending on their sizes, algae fall into two broad categories: microalgae and macroalgae. Microalgae are microscopic organisms with sizes that typically range from 2 micrometers to 200 micrometers, while macroalgae such as kelp can reach as long as 80 meters. Although algal taxonomy is under constant debate mainly due to the advent of gene sequence phylogeny, in general, major groups of algae include: green algae (Phylum Chlorophyta), red algae (Phylum Rhodophyta), diatoms (Phylum Heterokontophyta, Class Bacillariophyceae), brown algae (Phylum Heterokontophyta, Class Phaeophyceae), Dinoflagellata, Euglenophyta, Cryptophyta, and Haptophyta (Richmond, 2008). Cyanobacteria, previously known as the blue-green algae, are a group of bacteria that are capable of photosynthesis. Therefore, within certain topics e.g. algal biofuel and applied phycology, the term microalgae may refer to the microscopic algae as mentioned above and the oxygenic photosynthetic bacteria, i.e. the cyanobacteria (DOE, 2010).

2.2 BIOFUEL FROM MICROALGAE

Due to a series of issues resulting from conventional fuel utilization such as fossil fuel depletion, environmental pollution, and global warming, finding sustainable and environmental-friendly alternatives to fossil fuels is among the top challenges facing humankind. Biofuel is one of the options that are currently being studied and implemented in practice. Biofuel is made from renewable biological sources through various conversion approaches. Examples of biofuel include bio-ethanol produced from fermentation of carbohydrate sources such as corn and sugarcane (Chisti, 2008), biodiesel from transesterification of oil and fat from soybean and waste cooking oil (Ma et al., 1999), and bio-oil from pyrolysis or liquefaction of various biomass feedstocks such as agricultural wastes and energy crops (Goyal et al., 2008). Among the various types of biofuel feedstocks, microalgae have received increasing attention during the past few decades. The advantages of microalgae over other biofuel feedstocks include:

1) Microalgae have high biomass productivity due to their simple cellular structure. Some oleaginous algae species contain high lipid content, mainly in the form of triglycerides, and have the potential to produce oil yield (weight per area) greatly exceeding that of the most productive oilseed crops such as palm;
2) Microalgae cultivation minimizes competition with conventional agriculture for resources such agricultural land, fertilizer, and fresh water, because microalgae can grow in saline or brackish water on non-arable land such as desert and utilize recycled nutrients from wastewater.
3) Certain microalgae species produce significant amounts of high value bioproducts such as proteins, polyunsaturated fatty acids (e.g. docosahexanenoic acid and

eicosapentaenoic acid) and carotenoids (β-carotene, astaxanthin, etc.). The biomass residue after extraction of high-value bioproducts can be used as feedstock for biofuel production.

Various pathways to produce biofuel from microalgae have been proposed during the past few decades. For example, biodiesel production from microalgae generally comprises the following steps: mass cultivation of microalgae, harvesting and dewatering microalgae cells from aquatic culture, lipid extraction from the biomass, and conversion (transesterification, in this case) of algal lipids to biodiesel. Biofuel production from microalgae is technically possible, but in order to compete with fossil fuel in the market, biofuel cost needs to be reduced to a competitive level. To achieve this goal, a series of technology challenges need to be overcome. Highly productive and lipid-rich algal strains need to be selected for outdoor mass cultivation. Monocultures of the selected species need to be protected from contamination during cultivation outdoors. Energy inputs in algae cultivation, harvesting, and processing steps need to be minimized to avoid negative energy balance.

2.3 STRAIN SELECTION AND CHARACTERIZATION

Strain selection is usually considered the first step in developing a process that utilizes microalgae as feedstock. Selecting the right algae species is crucial to the success of any algae mass production system. However, strain selection is time-consuming and challenging primarily due to the large number of algae species available. Algae are a much more phylogenetically diverse group compared to animals or terrestrial plants (Georgianna et al., 2012). A conservative estimate indicates that around 72,500 algal species currently exist in nature, and among them merely 32,260 have been described

(Guiry, 2012). However, most of the published studies focused on less than 20 species, which include green algae (*Chlamydomonas reinhardtii*, *Dunaliella salina*, various *Chlorella* species, and *Botryococcus braunii*), diatoms (*Phaeodactylum tricornutum* and *Thalassiosira pseudonana*), and some heterokonts including *Nannochloropsis* and *Isochrysis* spp. (Scott et al., 2010). Most of these species were selected out of a larger candidates pool such as around 3000 strains investigated during the Aquatic Species Program (Sheehan et al., 1998). Therefore, exploring algal biodiversity still remains an indispensable work which is far from complete (Larkum et al., 2012).

A variety of desirable characteristics of algae have been described in many studies. For example, an "ideal microalga" is depicted as possessing the following features: 1) high biomass and lipid yield on high light intensity, 2) large cells with thin membranes, 3) insensitivity to high oxygen concentrations, 4) capability to grow and produce lipids at the same time, 5) ability to form flocs, 6) capability to excrete oil outside cells, and 7) stability and resistance to biological contamination (Wijffels et al., 2010). Other features that could be added into this list include: 1) wide tolerance to outdoor conditions such as temperature, light, and salinity fluctuations; 2) capability to grow in wastewater which may contain inhibitory compounds to other species; and 3) containing high-value coproducts. However, it is unlikely for a single species to have all the desirable features, and it is also unrealistic to characterize all these features in one screening study, therefore prioritization is needed (Griffiths et al., 2009). Usually, high growth rate, high biomass density, and high content of desirable products are the three key parameters that most algae strain selection/characterization studies are looking for. Higher growth rates enable algae to out-compete potential contaminating strains or pathogens and shorten harvesting

cycles. Higher biomass density at the final stage of growth increases volumetric yield reducing water usage and harvesting cost. A high content of the desired cell components contributes to a higher productivity and thus reduces the cost of extraction (Borowitzka, 1992).

Strain selection work usually starts with isolating microalgae from their specific habitats, then each of the isolated strains is cultivated in a laboratory scale photobioreactor and a variety of cell growth parameters (i.e. cell density, specific growth rate, etc.) are measured to evaluate the potential of each strain for biofuel production. This work is time consuming and requires significant amounts of experimentation especially when the candidate pool is large. In order to speed up this process, researchers have been developing in-depth and high throughput screening methods such as using fluorescent analysis for in-situ lipid content measurement and flow cytometry for isolating algae cells (Montero et al., 2011; Pereira et al., 2011). However, the latter techniques are not as accurate as the conventional analytical methods.

It is worthwhile to point out that screening or selecting the best strains from copious wild species candidates might not result in the productivity required for economically feasible commercial production, thus further investigations need to be carried out for strain development. Breeding, a technology used for over a century to improve plant crop yields and to protect crops, is being investigated for algae because of its potential to considerably improve algal strains. The capability for sexual reproduction, the short life cycles and rapid growth rates that could be achieved through breeding could greatly enhance the economic viability of biofuel production from algae (Georgianna et al., 2012). In addition to breeding, the advent of novel genetic tools will allow scientists to

precisely analyze and manipulate many unique metabolic pathways of microalgae and finally improve the yield of desired products from microalgae (Radakovits et al., 2010). Mixed strains rather than monocultures should also be examined for their commercial feasibility to take advantage of the potential synergestic effects of various strains on cell growth and resistance to contamination.

2.4 ALGAE STRAINS EXAMINED IN THIS STUDY

The algae species investigated in this study were originally isolated from surface soil and brine pools in the Great Salt Plains (GSP) in Northwestern Oklahoma by the Salt Plains Microbial Observatory program. GSP is a terrestrial hypersaline environment (salinity > 5%) subject to wide temporal fluctuation in both salinity (fresh water to salt saturation) and temperature (daily variance of 15 ^{o}C), therefore considered as an "extreme" environment, where living conditions are hard for most life forms (Kirkwood et al., 2006). Compared to regular aquatic habitats, extreme environments such as hypersaline lakes and hot springs are ideal sampling sites for isolating microalgae for biofuel production. This is because algae living in these habitats tend to be robust and may have rare characteristics, thus will have better potential for adapting to the mass cultivation conditions (Sheehan et al., 1998).

2.5 FACTORS AFFECTING ALGAE GROWTH

Both biomass productivity and lipid accumulation capacity of microalgae cultures are affected by several factors including carbon source, nutrients, light conditions, temperature, pH, and salinity. Understanding the impact of these factors is essential for optimizing growth conditions of microalgae mass cultivation. It also helps interpreting the data collected from strain selection and characterization work.

2.5.1 Carbon Source

Carbon is the primary constituent element of algae biomass, therefore carbon source is one of the most critical factors for microalgae growth. Some microalgae strains are known to be photoautotrophic organisms. They can convert inorganic carbon such as CO_2 and bicarbonate into organic compounds by using the Calvin-Benson cycle of the photosynthesis pathway (Richmond, 2008). There are also microalgae species that are capable of heterotrophic growth, which means they can directly utilize organic carbon sources such as glucose, acetate, and other organic compounds. Many studies have shown that addition of organic carbon sources can significantly increase the biomass productivity of certain algae species (Lee et al., 1996). However, carbon dioxide remains the primary carbon source for photoautotrophic algae cultivation because economic and carbon neutral production of biofuels would be difficult to achieve without using CO_2 as the main carbon source (Yen et al., 2014). CO_2 supply rate should be controlled within a range that does not inhibit algae growth (Sobczuk et al., 2000). Studies have revealed that aeration with CO_2 enriched air would increase algae growth compared to aeration with air only (0.04% CO_2), which indicates that algae growth would be CO_2 limited under low CO_2 concentrations such as in nature (Tittel et al., 2005; Yang et al., 2003). However, it was also found that high CO_2 concentration (typically 5%-15% of air mixture) would decrease the biomass productivity for many species (Chiu et al., 2009; Sobczuk et al., 2000). Satoh et al. (2001) found that high CO_2 concentrations would decrease the intracellular pH level, thus inhibiting the overall photosynthesis process.

Strictly speaking, CO_2 concentration of the enriched air does not necessarily reflect the actual CO_2 amount supplied to algae. This is because when bubbled into the liquid

medium, CO_2 needs to be dissolved in water in order to be available to algae, and the undissolved portion will be lost to the atmosphere. According to Henry's law, the concentration of CO_2 dissolved in aqueous medium, [$CO_{2\ (aq)}$], is a function of the CO_2 concentration in the purged air. But CO_2 concentration in the solution also depends on many other conditions such as medium temperature, ionic strength, salinity, and especially pH. pH can greatly affect CO_2 availability because part of CO_2 dissociates into bicarbonate [HCO_3^-] and carbonate [CO_3^{2-}] in aqueous solutions, and the ratio of the ionic species in solution at equilibrium is mainly determined by pH. As Figure 1 shows, a pH shift from around 6 to 8 will reduce the dissolution of CO_2 (aq) from around 50% to almost zero (Baba et al., 2012). Therefore, pH is an important parameter when considering CO_2 availability for algae cultivation. Based on the carbonate equilibrium chemistry and the overall CO_2 volumetric mass transfer theory (Henry's law), the actual CO_2 uptake/loss rate can be theoretically calculated, and further manipulated by pH adjustment and/or addition of bicarbonate salt to growth media in order to improve algae biomass productivity (Peng et al., 2015).

2.5.2 Nutrients

Microalgae growth requires assimilation of various nutrients from aqueous media. Numerous artificial culture media have been developed and used for isolation and cultivation of microalgae. Some of them are extensively used today as the "standard media" in many algae biofuel studies. The examples include F/2 medium (Guillard, 1975), BG-11 medium (Hughes et al., 1958), and K medium (Keller et al., 1987). Although these "standard" media can serve as broad-spectrum media satisfying the growth requirement of a wide range of algae species to a certain extent, to obtain the

optimal growth of a specific algae species, culture media needs to be optimized. Many studies have tried to optimize the culture media composition based on the "standard media" recipe and obtained significant biomass productivity improvement (Fábregas et al., 2000; Gong et al., 1997). The other issue with using "standard media" might be that many nutrients, especially trace elements, in "standard media" prove to be surplus or even unnecessary, wasting resources and increasing cost of algal production (Cogne et al., 2003).

The nutrients in the artificial media generally fall into three groups: macronutrients [nitrogen (N), phosphorous (P), and silicate (Si)], trace elements (Cu, Fe, Zn, Co, Mn, etc.), and vitamins (vitamin B_1, vitamin B_{12}, and vitamin H as the most common three vitamins) (Andersen, 2005). Since N and P are the two major nutrients, one of the main objectives in optimizing culture medium is to find the best N: P mole ratio (Mayers et al., 2014; Rhee, 1978; Xin et al., 2010). Mayers et al. (2014) found that N:P ratio can be raised to 32:1 without compromising biomass productivity of *Nannochloropsis* sp. under specific experimental conditions. The latter study also confirmed that P can be absorbed excessively from medium and stored intracellularly by algae, which explains a common phenomenon that the uptake rate of P does not proportionally correspond to the biomass productivity. Therefore, the P concentration in many "standard media" can be reduced without limiting algal biomass productivity. The other common goal of medium optimization is to find the optimal concentrations of the nutrients. Increasing the concentrations of the nutrients does not necessarily lead to enhanced biomass productivity because nutrients will be "saturated" when increased to a certain level and other growth conditions such as light or CO_2 availability will become the new limiting

factor for algal growth (Fábregas et al., 2000). The classic Monod model is proven to well describe the relationship between the growth rate of a green alga and the initial N/P concentrations. The half-saturation constants of N and P uptake can also be calculated using Monod model (Xin et al., 2010). In terms of the N source, Chen et al. (2011) found that inorganic N in the form of nitrates was preferred over ammonium for optimal algae growth because high levels of ammonium inhibit algae growth.

Nutrient depletion is extensively reported to be of great influence on the chemical composition of algae cells, especially the lipid content. Among all the nutrients evaluated, N limitation is the most critical factor promoting lipid accumulation. The general trend of lipid accumulation in response to N starvation has been reported for an extensive range of algae species (Chen et al., 2011; Hu et al., 2008; Mayers et al., 2014; Rodolfi et al., 2009; Xin et al., 2010). Rodolfi et al. (2009) found that N deprivation increased the lipid content of *Nannochloropsis* cells from 15% to 50 %. The increase was mainly in saturated and mono-unsaturated fatty acids. Environmental stress (such as N deficiency) usually leads to a metabolism shift in which lipid is synthesized as a long-term energy storage mechanism. This also partially explains why an increase in lipid content is often observed during stationary phase of algae growth (Hu et al., 2008). Although N deprivation triggers lipid accumulation, it often stops cell division or even causes cell death at the same time. Therefore, N limitation may remarkably increase the lipid content but it might not be beneficial for improving lipid productivity to say the least (Xin et al., 2010).

2.5.3 Light

Light is the energy source for algae under photoautotrophic growth conditions. Photosynthetic organisms can only utilize a specific spectral wavelength range (400 nm to 700 nm) of solar radiance for photosynthesis. This wavelength range is called photosynthetically active radiance, PAR for short. PAR accounts for 42.3% of the total energy from solar irradiance on Earth (Brennan et al., 2010). According to the photosynthesis theory, it takes a minimum of 8 mol photons to fix one mol CO_2. This can be summarized by the reaction:

$$CO_2 + H_2O + 8\ \text{photons} \rightarrow (CH_2O) + O_2$$

With the following data: energy content of photons 218 kJ/mol, energy content of CH_2O 467 kJ/mol and 42.3% of the total photons (PAR) available for photosynthesis, the photosynthesis efficiency (PE) is estimated to be 11.3% (Brennan et al., 2010). This is just a rough estimation of the theoretical upper limit of PE without considering many complex factors that could significantly reduce the efficiency, such as photorespiration and photo-saturation. The literature shows a range of maximum PE predictions, ranging from 3.9 to 13 % (Bolton et al., 1991; Silva et al., 2015; Zhu et al., 2008). The actual PE is usually lower than the theoretical limit, with a global average estimate between 1-2% (Vasudevan et al., 2008). Microalgae are claimed to have higher PE values compared to higher plants because of their simple structure, and the typical PE are reported to be 4.15~8.66% (Brennan et al., 2010).

Light intensity is a critical factor affecting algae growth. As Figure 2 shows, there are generally three regimes of algae growth in response to light intensity. At illumination intensities above the light compensation point where the effects of respiration and

photosynthesis cancel out the rate of photosynthesis is largely proportional to light intensity. This is the light-limiting regime of algae growth. Light is considered "saturated" when light intensity reaches a level at which photosynthesis rate will not increase with increasing light intensity. At higher light intensities, the Photosystem II protein complex of the photosynthesis machinary where water splitting reactions occur will be damaged causing a decrease in biomass productivity. The latter conditions are referred to as the light-inhibited regime of algae growth. In addition to photo-inhibition, photo-oxidation and other irreversible damages will occur at high light intensities. Although microalgae are capable of photo-acclimation, a mechanism allowing microalgae cells to adapt to changing light conditions, a rapid light intensity change can cause damage within a few minutes. The saturation light intensities are species dependent and range from 62.5 to 2000 μmol $m^{-2}s^{-1}$ (Breuer et al., 2013; Gordillo et al., 1998; Wang et al., 2014). Light intensity not only influences biomass productivity but also plays a role in altering the chemical composition including lipid content and composition of algae cells. In general, low light intensities induce the formation of unsaturated fatty acids and polar lipids whereas high light intensities favor the formation of saturated fatty acids and neutral lipids (Hu et al., 2008). It is reported that an increase in the irradiance intensity as a stress condition can significantly improve the lipid content of many species (Ho et al., 2014).

Ideally, every cell in the culture needs to be exposed to the optimal light intensity to maximize bioproductivity. However, this is almost practically impossible because light attenuates exponentially along the light path. Cell shading effects along with intracellular light absorption and the ocasional surface biofilm formation greatly reduce the light

intensity within the algae culture, especailly when the cell density is high. Furthermore, as Figure 3 shows, the light conditions for outdoor algae cultivation is highly unstable because solar irradiance fluctuates both diurnally and seasonally and is susceptible to the weather. Therefore, to mitigate these effects on algae growth, mixing is indispensible for both cultures grown in a laboratory and large outdoor production (Yen et al., 2014).

2.5.4 Temperature

As a fundamental factor regulating all biochemical reactions, temperature plays a crucial role in microalgae cultivation. Temperature is highly correlated to growth rate of microalgae. Typically, the growth rate increases along with the temperature below the optimal level and significantly decreases above the optimum primarily due to the deactivation of essential proteins and enzymes. Converti et al. (2009) reported that the growth rate of *Nanochloropsis oculata* almost halved when the temperature shifted from the optimal temperature (20 ^{o}C) to non-optimal temperature (15 and 25 ^{o}C), whereas *Chlorella vulgaris* was able to maintain almost the same growth rate at 25, 30, and 35 ^{o}C. Therefore, the optimal temperature range for algal growth is strain specific.

It is also widely reported that temperature has a major effect on the biochemical composition of algae, especially lipid composition (Hu et al., 2008). A commonly observed trend is that unsaturation of fatty acids increases with decreasing temperature. It is speculated that the increased unsaturation of fatty acids increase the fluidity of cell membranes thus counteracting the effect of a lower temperature. However, the effect of increasing temperature on the total lipid content is not consistent among different species (Converti et al., 2009; Juneja et al., 2013).

2.5.5 pH

pH is a vital factor in algae cultivation mainly because it determines the solubility and availability of CO_2, as mentioned earlier, and other essential nutrients (Juneja et al., 2013). The pH of a culture without any control is normally in the range of 6-9 depending on the equilibrium between CO_2 feeding rate into the culture and the uptake of inorganic carbon by algae. The optimal pH for most algae species is found to be between 7 and 9 (Bartley et al., 2014; Breuer et al., 2013; Ho et al., 2011; Zhang et al., 2014). Alkaline pH above the optimal range induces lipid accumulation in some species at the cost of markedly decrease in growth rate (Breuer et al., 2013; Gardner et al., 2011). Similar to alkaline pH, acidic pH inhibits growth of many algae species. Bartley et al. (2014) found that acidic pH makes the *Nannochloropsis salina* culture more vulnerable to invading organisms such as ciliates.

2.5.6 Salinity

Similar to the other parameters discussed earlier, salinity plays an important role in the biochemical composition as well as the growth rate of algae. It is reported in several studies that exposing the algae to a higher salinity condition than previously adapted levels usually induces accumulation of lipids. Studies on fatty acid profile of algal lipids indicate that salinity stress increases the fraction of saturated and mono-unsaturated fatty acids, including palmitic (C16:0), stearic (C18:0), and oleic (C18:1) acids, which are considered better feedstock for biodiesel production than polyunsaturated fatty acids (Juneja et al., 2013; Rao et al., 2007; Takagi et al., 2006). The effects of higher salinity on fresh water algae growth rate depend upon the specific algae species. Yeesang et al. (2011) reported that growth rates decreased under high salinity for three *Botyococcus*

species newly isolated from freshwater environment while the growth rate remained unaffected for the other *Botryococcus* sp. under investigation. Increased growth rates in high salinity medium were reported for *Botryococcus braunii*, a well-known freshwater alga (Rao et al., 2007).

Algae differ in their adaptability and tolerance to salinity. Halotolerant algae, those capable of living in a wide range of salinity received considerable attention because of their potential for cultivation in brackish water. One of the well-known examples of halotolerant algae is the *Dunaliella*, which is the dominating chlorophyte found in various hypersaline environments (Kirkwood et al., 2006).These algae accumulate small molecules called osmoticants, such as glycerol and sucrose, to balance out the intracellular and extracellular osmotic pressure in response to varying salinity in the environment (Richmond, 2008).

2.6 ALGAL BIOMASS TO BIOFUEL CONVERSION TECHNIQUES

Various pathways have been proposed and investigated to convert algal biomass into target biofuels of diverse forms (Figure 4). Lipids, especially triacylglycerols, accumulated in microalgae cells can be extracted and then easily converted into biodiesel by transesterification. The biomass consisting of intact algae cells can also be biochemically converted to bioethanol or methane and hydrogen by means of fermentation and anaerobic digestion. Thermochemical conversion pathways mainly consist of torrefaction, gasification, liquefaction, and pyrolysis. Torrefaction is a process where biomass is heated at a temperature range of 200-300 ^{o}C in an inert atmosphere. Torrefaction is commonly used as a pre-treatment technology to obtain a solid fuel of higher caloric value than the original feedstock by dehydration and partial decomposition

(Wu et al., 2012). Pyrolysis also takes place under an inert atmosphere and is similar to torrefaction, but it is carried out at higher temperatures (usually >350 ^{o}C). The main products of pyrolysis consist of bio-oil, charcoal, and non-condensable gases (Marcilla et al., 2013). Liquefaction, such as hydrothermal liquefaction, is a process that can convert wet algae biomass into bio-oil and gases by using water at elevated temperatures (200-350 ^{o}C) and pressures (5-20 MPa) for normally 5-60 mins to keep the water in liquid phase (Brown et al., 2010). Finally, gasification of algal biomass produces H_2, CO, CH_4, and other combustible gases by partial oxidation at high temperatures, 800-1000 ^{o}C (Chen et al., 2015).

The choice of conversion technique for a given application depends on several factors, including the properties of feedstock, the desired end products, environmental standards, and economic considerations. Traditionally, algae based biofuel mainly refers to biodiesel due to the attractive lipid production potentials of certain algae species. However, biodiesel production is not necessarily the only plausible conversion pathway for all types of algal biomass. Many algae strains, though not good at lipid accumulation, demonstrate higher biomass productivity than most high lipid productivity strains. Some of the low lipid content algae strains may not require strictly controlled cultivation conditions in contrast with high lipid content algae strains (Williams et al., 2010). Biomass produced by these algae strains might not be good feedstock for biodiesel production due to the low lipid content, but it can be converted into other biofuels as long as an appropriate conversion pathway is selected. In addition, the residue after lipid extraction of oleaginous algae biomass contains significant amounts of carbohydrates and

proteins that also requires other conversion techniques to be fully exploited (Gai et al., 2015).

2.6.1 Pyrolysis

Among the aforementioned conversion strategies, pyrolysis is an important technology and has recently received wide attention for both research and commercial applications. Previously, pyrolysis was regarded as equal to carbonization (slow pyrolysis) in which the solid char was the primary product. Nowadays, pyrolysis as a term usually describes a process from which bio-oil is the preferred product (Fernández et al., 2011). To obtain a high yield of a desirable product, various operating parameters need to be optimized. Temperature, heating rate, and residence time (the time that hot vapors remain in the pyrolysis reactor) are the three critical factors for high bio-oil yield from pyrolysis (Bridgwater et al., 1999; Van de Velden et al., 2010; Yin, 2012).

Temperature, as an important parameter in all thermochemical conversion processes, determines the rate and the extent of biomass thermal decomposition. Thermogravimetric analysis shows that during biomass heating from 25 ^{o}C to 800 ^{o}C four distinct reactions take place during the pyrolytic process: (1) removal of moisture and some light volatiles (25–150 ^{o}C); (2) the main pyrolysis or devolatilization process due to the thermal decomposition of proteins and carbohydrates (200–430 ^{o}C); (3) thermal degradation of lipids (430–530 ^{o}C); and (4) slight but continuous weight loss of carbonaceous matters (530–800 ^{o}C) (Chen et al., 2014). In addition, temperatures above 500 ^{o}C significantly promote secondary cracking reactions during which larger molecular weight hydrocarbons are broken down to smaller ones, thus decreasing bio-oil yield (Yin, 2012). Heating rates also play an important role affecting the final product yields. Higher

heating rates not only increase the maximum thermal decomposition rates, but also enhance bio-oil production. However, size reduction of the feedstock is usually required to obtain high heating rates when conventional heating techniques are used (Mohan et al., 2006; Wu et al., 2014). Residence time is an important factor because a longer residence time of the vapor phase at high temperatures will lead to further decomposition of the vapor into lighter volatiles and eventually non-condensable gases by secondary pyrolysis (secondary decomposition reactions within the volatiles or between the volatile and the carbonaceous residue). Ideally, vapor needs to be expelled out of the reactor immediately upon formation and then rapidly condensed to bio-oil, but this is an engineering difficulty and requires careful reactor design and accurate temperature control (Bridgwater et al., 1999; Yin, 2012). In general, high temperatures and long residence time favor the formation of gas, while low temperatures and long residence time (i.e. slow pyrolysis) promote the formation of char. The preferred conditions for bio-oil production are fast heating rates, moderate temperatures, and rapid quenching of the primary vapors (low residence time). These parameters need to be optimized for each feedstock used for pyrolysis.

2.6.2 Microwave-assisted pyrolysis

Ever since the accidental discovery of the microwave's capability to heat food in the 1940s, research on microwave heating has expanded across various fields. Microwave assisted pyrolysis (MAP) has received increasing attention recently (Domínguez et al., 2006; Fernández et al., 2011; Wan et al., 2009). Microwaves are electromagnetic waves that lie between the infrared radiation and radio waves region within the electromagnetic spectrum. Microwave frequencies range from 0.3 to 300 GHz, and the specific

frequencies assigned to microwave heating are 0.915 GHz and 2.45 GHz (most commonly used in commercial microwaves) (Fernández et al., 2011). Microwave heating is based on the "dipole rotation/dielectric heating" effect. Microwave radiation makes polar molecules rotate continuously as the dipole (separation of positive and negative charges within a molecule) aligns itself with the alternating electric filed of the microwave. Heat is generated as the molecules rotate and interact with other molecules (Yin, 2012). Depending on their interactions with the microwave radiation, materials can be classified into three groups: 1) insulators through which microwaves can pass without any loss (e.g. quartz, Teflon), 2) conductors which completely reflect microwaves (e.g. metals), and 3) absorbers which absorb microwave energy and convert it to heat (e.g. water, salts). Biomass, in general, is not a good microwave absorber. However, biomass can be blended with microwave absorbers such as active carbon and char to obtain effective heating during a microwave-assisted pyrolysis process (Domínguez et al., 2006; Du et al., 2011; Wan et al., 2009).

The distinct nature of microwave heating gives rise to several advantages over conventional heating:

1) Microwave heating is more energy efficient compared to conventional heating. In conventional heating, an external environment of high temperature is needed to allow heat transfer from the surface to the center of the biomass particle. Heat transfer is limited by the thermal conductivity of biomass and the convection current within the reactor. In contrast heat flow from the center of biomass to the surface can be achieved with microwave heating resulting in uniform internal heating. In addition, conventional heating usually requires size reduction of the

feedstock and fluidization/agitation within the reactor to obtain high heating rates, whereas microwave heating mitigates these needs and thus saves considerable energy costs (Motasemi et al., 2013).

2) Microwave heating allows better process control. The energy input of microwave heating can be instantaneously started or stopped by turning the power on/off, which leads to rapid heating/cooling (Luque et al., 2012).
3) Under similar conditions, MAP produces gases containing significantly higher proportion of CO and H_2, and less CO_2 compared to conventional pyrolysis (Dominguez et al., 2007; Domínguez et al., 2006). Furthermore, bio-oil produced by MAP contains virtually no polycyclic aromatic hydrocarbons, which are carcinogenic and mutagenic products commonly found in conventional pyrolysis bio-oils (Luque et al., 2012).

The main disadvantage of MAP is the inherent issues of temperature measurement (Luque et al., 2012; Motasemi et al., 2013; Yin, 2012). The most commonly used sensors for high temperature measurement during pyrolysis processes are infrared pyrometers and thermocouples. Temperature measurement with infrared optical pyrometers requires a window in the reaction system that allows only the infrared but not microwaves to pass through, which usually leads to heat loss and thus an underestimate of the reaction temperature. In contrast, thermocouples often overestimate the temperature because the thermocouple tip can act as an antenna which creates a concentrated electric field and then generates a hot spot of a higher temperature than that of the bulk biomass (Luque et al., 2012). A combination of infrared optical pyrometers with thermocouple probes might

improve the reliability of the temperature measurement (Luque et al., 2012; Motasemi et al., 2013).

2.7 THERMOGRAVIMETRIC ANALYSIS

Pyrolysis not only serves as an effective approach to biomass energy conversion but also has a great potential for characterization of the biomass. Thermogravimetric analysis, TG-IR (thermogravimetric analysis-infrared spectroscopy) and Py-GC/MS (pyrolysis-gas chromatography/mass spectroscopy) are powerful analytical techniques related to pyrolysis (Marcilla et al., 2013).

Thermogravimetric analysis, or TGA for short, is a thermal analysis technique in which the sample weight is monitored against the programmed temperature under a specific atmosphere (Rizzo et al., 2013). TGA is a powerful tool in analyzing and understanding the thermal degradation behavior of biomass. One of the predominant uses of TGA is to analyze the solid-state decomposition kinetics of biomass. The kinetic data not only helps understanding the thermal degradation process but also can be used as input parameters to deduce the reaction mechanisms. This information will further provide insight into the highly complicated overall process of various thermochemical biomass conversion pathways such as direct combustion, pyrolysis, and gasification. In addition, the comparison of decomposition kinetic parameters among different biomass feedstocks provides valuable information in selecting feedstock for biofuel production.

Kinetics is the study of chemical reaction rates. For solid-state thermal decomposition, the rate is considered as a function of two variables: temperature (T), and fraction of conversion (α), as described in the following equation.

$$\frac{d\alpha}{dt} = k(T)f(\alpha)$$

Where; $f(\alpha)$ represents the dependence of reaction rate on the fraction of conversion, $k(T)$ is the reaction rate constant, which can be described through the Arrhenius equation as:

$$k(T) = A \exp\left(-\frac{E}{RT}\right)$$

where; A is the pre-exponential factor, E is the apparent activation energy, and R is the gas constant. A, E, and $f(\alpha)$ are often referred to as the kinetics triplicates: E is the minimal energy required for a chemical reaction to proceed, A is the vibration frequency of the activated complex, and $f(\alpha)$ is the function of the reaction mechanism (Vyazovkin et al., 2011).

The mathematical approaches to analyzing the TGA data and obtaining the kinetics triplets can be categorized in two groups: model-free methods and model fitting methods. Model fitting methods calculate all three kinetic parameters by fitting the experimental data into an assumed reaction model. However, the results might not be reliable due to the incorrect reaction order and model assumptions (Gai et al., 2013). In many cases model-fitting methods produced erroneous activation energy values due to the selection of wrong reaction models (Sharara et al., 2014). In contrast, model-free methods, as the name implies, do not need an assumption of a reaction model prior to calculating the parameters. Model free methods, with the exception of the Kissinger method, are based on the iso-conversional principle that the reaction rate at a particular fraction of conversion (α) is solely a function of temperature. Therefore, the results calculated by model-free methods are typically a set of kinetic parameters corresponding to each

fraction of conversion. The disadvantage of model-free methods, though, is that only E can be determined while the reaction model requires extra assumptions and steps to be determined (Sharara et al., 2014; Vyazovkin et al., 2011). Two methods, Ozawa-Flynn-Wall (OFW) method, and Kissinger-Akahira-Sunrose (KAS) method, are widely used for solid-state decomposition kinetic studies. A common practice in calculating the activation energy is to use both methods and compare the results (Chen et al., 2011; Sharara et al., 2014; Shuping et al., 2010). However, this comparison is not useful because these two methods are based on the same principle and the only difference is the different approximations applied. KAS method determines the activation energy with higher accuracy (Vyazovkin et al., 2011). TGA data can be collected in either isothermal (constant temperature) or non-isothermal (changing temperature, usually with constant heating rates) mode. Non-isothermal processes are usually preferred due to their broader temperature range coverage (Vyazovkin et al., 2011). Therefore, KAS method with non-isothermal temperature programs was adopted to determine the kinetics data in this study.

In addition to analyzing decomposition kinetics, TGA can be utilized to serve many other purposes, such as proximate analysis. Proximate analysis has traditionally been used to evaluate the quality of coals by measuring moisture, volatile matter, fixed carbon, and ash contents. Proximate analysis is now widely used as a basic characterization method to analyze the biomass feedstock for thermochemical production of biofuel. Usually, moisture, volatile matter, and ash are measured separately following published standards such as ASTM standards, e.g. ASTM E-871 for moisture, ASTM E-830 for ash, and ASTM E-1755 for volatile matter, and fixed carbon is determined by difference. These methods are not only time consuming but they also require a significant amount of

sample (Mayoral et al., 2001). As such, several studies have been carried out to develop a proximate analysis methodology based on TGA data because TGA only requires several milligrams of sample for each test and proximate composition of biomass can be determined using data from one test thus saving considerable amount of time (Cantrell et al., 2010; García et al., 2013; Mayoral et al., 2001; Saldarriaga et al., 2015).

CHAPTER III

MATERIALS AND METHODS

3.1 CHARACTERIZATION OF THE ALGAE STRAINS

3.1.1 Algae Strains and Culture Conditions

Seven algae strains (Table 1, Picture 1) investigated in this study were obtained from the Culture Collection of Algae at University of Texas at Austin (UTEX). SP 20 and SP 22 are unicellular green algae, and the other five strains (SP 38, SP 46, SP 47, SP 48, and SP 50) are filamentous cyanobacteria. SP 46, SP 47, and SP 48 belong to the same genus, *Pseudanabaena*, but the species information remains to be identified. The same media selected for culture maintenance at UTEX was used in this study. The chemical composition of each medium is provided in the Appendix.

Algae cultures were grown in 2L bioreactors (Picture 2.a), which were kept in a 30'×30'×60' growth chamber (Picture 2.b). The temperature of the chamber was maintained at 23±4 ^{o}C. Twelve soft white fluorescent bulbs (General Electric Company, Fairfield, CT) were installed on the ceiling of the growth chamber as the light source. The light intensity was measured at 4 different locations on the bioreactor surface by a quantum meter (model QMSW-SS, Apogee Instruments Inc., Logan, UT), and the average photosynthetic photon flux (PPF) was calculated to be 96 $\mu mol\, m^{-2}s^{-1}$. Cultures were cultivated under a cycle of a 12 h light period with aeration followed by a

12 h dark period without aeration. Each culture was purged with 50 ml/min of air enriched with 2% CO_2 (Industrial Carbon Dioxide, Airgas Inc., Stillwater, OK), which is controlled by gas flowmeters (Cole-Parmer, Vernon Hills, IL). Each strain was cultivated at least in duplicates. Stock cultures at the exponential growth phase were used as the inoculum for the cultivation at an inoculation rate of 0.5 % v/v. To minimize the risk of contamination, culture media together with the bioreactors were sterilized by autoclave before inoculation, and the growth chamber was disinfected regularly by spraying 70% ethanol solutions.

3.1.2 Characterization of the Growth Pattern

Samples were taken regularly with a syringe through opening #3 (Picture 2.a) of the bioreactor. The pH of each sample was measured by a pH meter (model AR20, Fisher Scientific, Waltham, MA), and absorbance (Abs) by a spectrophotometer (model DU 520, Beckman Coulter, Brea, CA) at 680 nm. Cell densities of the unicellular green algae cultures (SP 20 and SP 22) were determined regularly by counting the cells using a hemocytometer (Hausser Scientific, Horsham, PA) under a microscope (model T690C PL, Amscope, Irvine, CA). Cultures were harvested immediately after the Abs reached the maximum, which indicated the culture reached the stationary growth phase. The final dry biomass concentrations (X_{max}) were measured gravimetrically as follows (Zhu et al., 2013): 1) a glass fiber filter paper (GF/C 90 mm diameter 1.2 µm pore size, Whatman, ME14 2LE, UK) together with an aluminum dish were dried in a forced-air oven (model 1370 FM, VWR Science, Bristol, CT) at 105 ^{o}C for 2 h, cooled in a desiccator and then weighed; 2) 50 mL culture suspension was vacuum filtered through the filter paper, and then washed with about 50 mL of distilled water to remove extracellular inorganic salts

retained in the biomass (Zhu et al., 1997); 3) the wet filter paper and the aluminum dish were dried at 105 ^{o}C for at least 12 h until a constant weight was obtained; and finally 4) the dry biomass concentration was calculated as the weight difference / sample volume. A sample of each culture was diluted by different factors and the Abs was measured at each dilution rate to obtain a correlation between Abs and the dry biomass concentration. This linear correlation was used to convert the Abs data to dry biomass concentrations, and growth curves of each culture were obtained as dry biomass concentrations vs. time. Several important growth kinetic parameters, including the maximum specific growth rate (μ_{max}, 1/day), doubling time (t_d, day), and maximum biomass productivity (P_{max}, g/L/day) were calculated based on the growth curves (de Morais et al., 2007). The maximum specific growth rate was calculated as the slope of the linear regression line at the exponential phase of the growth curve [ln(X) vs. time], and the doubling time as $t_d = \ln2/\mu_{max}$. Average biomass productivity was determined according to the equation: $\Delta X = \frac{X_{max}}{t}$, where X_{max} is the maximum dry biomass concentration, and t is the time needed to obtain X_{max}.

3.1.3 Characterization of the Algae Biomass

3.1.3.1 Ash Content

The algae biomass was harvested by using a centrifuge (model Sorvall RC 5C plus, Kendro Laboratories Products, Newtown, CN) at 8000 rpm for 10 min each run. Ash content of each biomass sample was determined as the weight loss of pre-dried algae biomass after dry oxidation in a furnace at 575 ^{o}C for 3 h. In order to evaluate the influence of extracellular inorganic salts on the ash content, around 1 g of wet algae

slurry was re-suspended in 250 mL distilled water and centrifuged, and the ash test was performed after repeating this process three times.

3.1.3.2 Lipid Content

The procedure used to determine the lipid content of algae biomass was largely adopted from Lee et al. (1998): 1) about 120 mg biomass (dry weight) was first suspended in 5 mL of phosphate buffer (pH 7.4) and treated in a bead-beater (model HBB908, Hamilton Beach, Richmond, VA) half-filled with 1mm glass beads for 1 min; 2) the suspension was then transferred to a separatory funnel and 30 mL of chloroform: methanol (2:1, v/v) solution was added for lipid extraction; 3) the liquid mixture in the funnel was shaken vigorously for 20 min by an orbital shaker (model S500, VWR, Radnor, PA) and then left to stand for 30 min to achieve a clear phase separation. The bottom layer (organic phase containing lipid) was decanted and saved; 4) 20 mL solvent was added to the upper layer (aqueous layer containing residual cells) and step 3 was repeated; 5) the combined organic phases were washed with 20 mL of 5 % (w/v) sodium chloride solution in the separatory funnel; 6) the final organic layer (bottom layer) was decanted and transferred into a pre-weighed beaker, which was then placed in a RapidVap (LABCONCO Corporation, Kansas City, KS) to evaporate the solvent at 40 ^{o}C until a constant weight was obtained; and finally, 7) the lipid content was determined by the weight increase of the beaker /dry weight of the algae sample.

3.1.3.3 Fatty Acid Composition

The fatty acid composition of the algae biomass was analyzed in triplicates for each sample with GC-FID after a whole biomass *in situ* transesterification, a procedure based on the method developed by Van Wychen et al. (2013). A biomass sample of about 10

mg was transferred to a pre-weighed GC vial and dried in a vacuum oven at 40 ^{o}C overnight to remove moisture. Then, 20 µL of tridecanoic acid (C13:0) methyl ester surrogate standard (10 mg/mL), 200 µL of chloroform: methanol (2:1, v/v), and 300 µL of 0.6M HCl: methanol were added to the sample vial which was then sealed with a PTFE/silicone/PTFE crimp cap and vortexed vigorously. Sample vials were then heated at 85 ^{o}C for 1 h and cooled for 15 min at room temperature. After cooling, 1.0 mL HPLC grade n-hexane was added using a gas-tight syringe and mixed vigorously. The vials were left at room temperature for 1 h to allow a phase separation. The hexane layer was then diluted 5 times with hexane in a new GC vial to ensure the sample concentrations were within the calibration curves. Finally, 5 µL of pentadecane (1 mg/mL) was added as the internal standard. Fatty acid methyl esters (FAMEs) were analyzed by a gas chromatography-flame ionization detector (GC-FID) (model 6890N, Agilent technologies, Santa Clara, CA) equipped with a DB-WAX column (30 m length, 0.25 mm inner diameter, 0.25 µm thickness, Agilent Technologies, Santa Clara, CA). The sample (1 µL) was injected at 10:1 split ratio and inlet temperature of 250 °C. Hydrogen was used as the carrier gas with a constant flow rate of 1.25 mL/min. Oven temperature was programmed to be: 1) initial temperature of 100°C for 0.71 min, 2) 35.26 °C/min up to 200°C and hold for 0.71 min, and 3) 7°C/min up to 250°C and hold for 5 min. The detector temperature was set at 280 °C, and gas flow rates were as follows: 450 mL/min zero grade air, 40 mL/min H_2, and 30 mL/min helium. The FAME Mix, C4:0-C24:0, (37 compound calibration mix, Sigma Aldrich #18919) was used as the FAME standard.

3.2 THERMOGRAVIMETRIC ANALYSIS OF ALGAE BIOMASS

Thermogravimetric analysis of the algae biomass was performed in a TGA/SDTA 851e instrument (Mettler Toledo, Columbus, OH). Nitrogen (99.99% purity, Stillwater Steel and Supply, Stillwater, OK) was used as the purge gas at a flow rate of 50 mL/min. For each test biomass sample (5-10 mg) was transferred to a 70 µL platinum crucible. The temperature was ramped from 25 ^{o}C to 800 ^{o}C at three heating rates: 20, 40, and 80 ^{o}C /min. All tests were performed in duplicates, and an empty run (no sample in the crucible) was conducted to obtain the baseline of the signal for each heating rate.

3.2.1 Kinetic Analysis of Algae Biomass Pyrolysis

For solid-state thermal decomposition, the reaction rate can be expressed as:

$$\frac{d\alpha}{dt} = A \exp\left(-\frac{E}{RT}\right) f(\alpha)$$

Where; A is the pre-exponential factor, E the apparent activation energy, R, the gas constant, T, temperature, and α, the fraction of conversion, which is defined as:

$$\alpha = \frac{W_0 - W_t}{W_0 - W_\infty}$$

Where; W_0 is the initial weight of the biomass sample, W_t is the weight at time t, and W_∞ is the final weight of the biomass sample.

The temperature is a function of time,

$$T_t = T_0 + \beta \cdot t$$

Where; T_0 is the initial temperature (25 ^{o}C), and β is the heating rate. Using this equation, the conversion rate can be transformed into:

$$\frac{d\alpha}{dT} = \frac{A}{\beta} \exp\left(-\frac{E}{RT}\right) f(\alpha)$$

By rearranging this equation and then integrating, a new equation is obtained:

$$G(\alpha) = \int_0^{\alpha} \frac{d\alpha}{f(\alpha)} = \frac{A}{\beta} \int_{T_0}^{T} \exp\left(-\frac{E}{RT}\right) dT$$

Based on these equations, different methods have been developed to determine the kinetics of thermal decomposition. As introduced earlier, KAS method was used in this study, which is expressed as (Vyazovkin et al., 2011):

$$\ln\left(\frac{\beta}{T^2}\right) = \ln\frac{AR}{EG(\alpha)} - \frac{E}{RT}$$

E, the apparent activation energy, can be calculated from the slope of the line $\ln\left(\frac{\beta}{T^2}\right)$ vs. $\frac{1}{T}$ at a given α.

3.2.2 Proximate Analysis

Proximate analysis of the algae biomass was performed by a TGA method, which is modified based on the methods used by García et al. (2013) and Ross et al. (2008). As illustrated in Figure 5, the sample was heated from 25 ^{o}C to 110 ^{o}C at a heating rate of 20 ^{o}C/min under nitrogen atmosphere (flow rate 50 mL/min), and the temperature was held at 110 ^{o}C for 6 min. The weight loss at this stage corresponded to the moisture content of the sample. After the isothermal section, temperature was increased to 575 ^{o}C at 80 ^{o}C/min and held for 10 min, during which the weight loss was determined as the volatile matter. Then the atmosphere was switched from nitrogen to air (50 mL/min). The temperature was increased at a heating rate of 80 ^{o}C/min to 800 ^{o}C, and then maintained at this temperature until a constant sample weight was obtained. The weight loss at this stage was accounted as fixed carbon, and the remaining weight was ash. An estimation of

the higher heating value (HHV) was performed using the following equation proposed by Parikh et al. (2005):

HHV = 0.3536× FC (fixed carbon) + 0.1559×VM (volatile matter) - 0.0078× ASH (ash) MJ/kg, (dry basis)

3.3 MICROWAVE ASSISTED PYROLYSIS OF ALGAE BIOMASS

3.3.1 Sample Preparation

The algae biomass investigated in this study was *Pseudanabaena sp.* (UTEX SP 46) cultivated in 10 L reactors under the same growth conditions used in the screening study. Biomass harvested by centrifugation was dried in a forced air oven at 45 ^{o}C for 24 h. Then the biomass was pulverized with a mortar and pestle, and sieved with a 1 mm sieve and then saved in a freezer for later use. Proximate analysis of the biomass was performed by the TGA method mentioned earlier.

3.3.2 Experimental System Set-up

A microwave-assisted pyrolysis system, as shown in Figure 6, was constructed for the experiments. The microwave oven (BP 210) was custom made by Microwave Research and Applications, Inc. (Carol Stream, IL). Microwave frequency and the maximum output power of the system were 2.45 GHz and 2,100 W, respectively. The microwave oven was equipped with a process controller which enables accurate temperature control of the process by rapidly adjusting the microwave power based on the comparison between actual temperature and the temperature program. The process controller was linked to a computer to allow easier programming and data processing. Temperature was measured by inserting the tip of an ungrounded thermocouple (model TJ36-CAIN-18U-24, Omega Engineering, Inc., Stamford, CT) to the center of the

biomass sample held in a crucible. Due to the high pyrolysis reaction temperature (>450 ^{o}C), a muffle was used to protect the microwave oven from direct contact with the hot reactor. Two tubes within the oven cavity were made of fused quartz (strain point 1120 ^{o}C). To create and maintain an inert atmosphere required for pyrolysis, 1) N_2 was purged into the reactor at 100 mL/min starting at least 20 min before the experiment and lasting 10 min after the completion of each experiment, 2) ground tapered joints were used to ensure proper sealing of the connections between tubes, condensers, and the reactor, 3) connections were double-checked until gas bubbles came out of the tip submerged 5 cm in the water bottle (15) before any experiment was initiated. A condenser system was used to collect the liquid product (bio-oil + water) produced during pyrolysis. Water at 5 ^{o}C was circulated within the two condensers, and the three liquid collection flasks were submerged in an ice bath to improve the condensation effect.

3.3.3 Pyrolysis Experiments

Ten grams of algae biomass sample was used for each experiment. The temperature was ramped from room temperature to three different final temperatures (450, 600, and 750 ^{o}C) at a heating rate of 100 ^{o}C/min followed by an isothermal process of 20 min. The weight of the solid residue, char that remained in the crucible after the experiment was measured. While most of the liquid product was collected in the liquid collection flasks (#13 in Figure 6), some of the condensate stuck to the inner surfaces of the reactor and tubing. Therefore, the weight of liquid product was determined by the weight increase of the entire pyrolysis system (i.e. reactor, tubing, and the liquid collection flasks) after the experiment. Non-condensable gas, together with some light condensable volatiles,

escaped from the condenser system and was released into a fume hood. The weight of the gas product was determined by mass balance.

Methanol was used to wash out the condensate stuck on the inner surface of the pyrolysis system components. Then bio-oil was recovered by evaporating the solvent using a RapidVap (LABCONCO Corporation, Kansas City, KS) at 40 ^{o}C until a constant weight was obtained. Bio-oil yield was reported as the weight of the residue after solvent evaporation (Domínguez et al., 2006; Wan et al., 2009).

3.3.4 GC-MS Analysis of the Bio-oil

Both the bio-oil directly collected in the liquid collection flask (original bio-oil) and the bio-oil recovered after methanol washing of the system components (recovered bio-oil) were analyzed by GC-MS. Bio-oil samples were taken from the dark bottom phase (original bio-oil) of the liquid products (Picture 3) and the recovered bio-oil using a syringe. The Bio-oil samples were diluted 40 times using HPLC-grade dichloromethane (CH_2Cl_2). Each sample (1μL) was injected by a gas-tight syringe into a gas chromatography/mass spectrometer (Agilent 7890GC/5975MS) which was equipped with a DB-5 capillary column (30 m length, 0.32 mm inner diameter, 0.25 μm film thickness). The GC oven temperature was held at 40 ^{o}C for 4 min, and then increased at a rate of 5 ^{o}C/min to 280 ^{o}C and held for 20 min. The injector temperature was set at 250 ^{o}C, and the split ratio was 30:1. Helium (purity: 99.99%) was used as a carrier gas at a flow rate of 1 mL/min (Yang et al., 2014). The compounds were identified by comparison with the NIST Mass Spectral Data Library. A semi-quantitative evaluation of each component was performed by calculating the area percentage of each identified peak on the total ion chromatogram (TIC) (Domínguez et al., 2006).

3.4 STATISTICAL ANALYSIS

All the experiments were carried out at least in duplicates. Means were compared by Tukey's HSD test at a 95% confidence interval. The statistical analysis of the experimental data was performed using SAS 9.4 (SAS Institute Inc., Cary, NC). Linear regression equations to determine specific growth rates and apparent activation energies were calculated using Microsoft Office Excel 2013 (Microsoft Corporation, Redmond, WA).

CHAPTER IV

RESULTS AND DISCUSSION

4.1 CHARACTERIZAITON OF THE ALGAE STRAINS

4.1.1 Algae Growth

Two of the algae strains, SP20 and SP22, are unicellular green algae, and the remaining five strains, SP38, SP46, SP47, SP48, and SP50, are filamentous cyanobacteria. Algae cells of each strain were observed under microscope. The cells of the two green algae were found to have flagella, the structures algae use to swim. Therefore, these two algae strains were motile algae, and this explains why the cultures of these two strains were usually uniformly dispersed even without mixing. In contrast, the cultures of the five cyanobacteria had a tendency to form filaments and cell clumps when no mixing was applied, which is partially caused by the lack of cell motility. Clump formation can be a beneficial characteristic which could simplify the cell harvesting process and reduce the energy requirement for harvesting.

Growth curves were obtained for each algae strain as shown in Figures 7 to 13. These curves exhibit all the characteristic growth phases, including the lag phase (e.g. Day 0 to Day 3 of SP50, Figure 13), the exponential growth phase (e.g. Day 3 to Day 7 of SP20, Figure 7), the declining growth phase (e.g. Day 8 to Day 20 of SP48, Figure 12), the stationary phase (e.g. Day 26 to Day 33 of SP46, Figure 10), and the death phase (e.g.

Day 20 to Day 26 of SP47, Figure 11). The length of each growth phase was strain specific. Most of the cultures did not experience a visible lag phase (with the exception of SP20 in Figure 7 and SP50 in Figure 13) which indicates that cells in the inoculum immediately adapted to the growth conditions after inoculation. The exponential growth phase lasted for about 5 to 10 days for different stains. Following this phase, some cultures (e.g. SP20, Figure 7 and SP22, Figure 8) almost immediately reached the stationary phase, while other strains such as SP46 (Figure 10), SP47 (Figure 11), and SP48 (Figure 12) experienced a long declining growth phase before reaching the stationary phase. In regards to the death phase, it is worthwhile to mention that a rapid color change from green to brownish yellow was observed during the last several days of the cell growth in three cultures (SP38, SP47, and especially SP50). The color change corresponded to the sharp drop in biomass concentration observed right after the peaks shown in the growth curves of SP 38, SP 47, and SP50 (Figure 9, 11, and 13). This rapid loss of pigmentation reoccurred in subsequent replicated cultures of these three strains. No contaminating organisms, such as zooplankton, were found in these cultures indicating that the culture crash was caused by non-biological factors such as depletion of nutrients or accumulation of toxic metabolites (Richmond, 2008). The rapid pigmentation loss observed shortly after the peak biomass concentration suggests that SP38, SP47, and SP50 were not very stable during the stationary phase and need to be harvested as soon as the stationary phase is reached.

Semi-log coordinates were used to replot the growth curves in order to calculate the specific growth rates. A regression line was fitted through the first three data points following day 0 and the specific growth rate was obtained as the slope of the fitted line

(Li et al., 2011). As shown in Table 2, the fastest growing strain was SP20 (0.76/day), and it had a doubling time of 0.91 day and a maximum biomass concentration of 0.62 g/L. SP 46 is the second fastest growing strain (0.61/day), and it exhibited the highest maximum biomass concentration, 1.32 g/L. The average biomass productivity of SP20, SP46, and SP50 were not significantly different and were higher than the remaining four strains.

The specific growth rate as an inherent characteristic of a specific strain is widely used to make comparisons between different strains. However, the specific growth rate depends on not only the strain itself but also other growth conditions such as light intensity, temperature, media composition, and CO_2 supply rate. The specific growth rates can change under different growth conditions (Huesemann et al., 2013; Thiansathit et al., 2015; Xin et al., 2010). Therefore, the comparison of specific rates is only valid when the growth conditions are the same or similar which was the case in this study. The growth conditions (1:10 v/v inoculation ratio, 120 µmol PAR m-2s-1, f/2 medium, 12/12 h light/dark photoperiod) applied in a strain screening study by Duong et al. (2015) were similar to those of our study, and the highest specific growth rate obtained among 18 candidate strains was 0.64/day. In another strain screening study of 18 strains conducted by Renaud et al. (1999), similar growth conditions were used, and the highest specific growth rate obtained was 0.73/day. Therefore, the specific growth rates of SP20 and SP46 are within the range reported in literature.

The biomass productivity is another key parameter in selecting microalgae strains for mass cultivation. The average biomass productivity obtained in this study ranged from 17.9 to 55.9 mg L^{-1} day^{-1} which is much lower than that obtained by Rodolfi et al. (2009)

(40 mg L^{-1} day^{-1} of *Chaetoceros calcitrans* to 370 mg L^{-1} day^{-1} of *Porphyridium cruentum*) and Hempel et al. (2012) (50 mg L^{-1} day^{-1} of *Phaodactylum tricornutum* to 500 mg L^{-1} day^{-1} of *Chlorella* sp. 800). However, the difference between the experiment conditions must be considered in interpreting the difference in biomass productivity. Rodolfi et al. (2009) and Hempel et al. (2012) used smaller culture volumes (100 mL in a 250 mL flask), higher aeration rates (0.3 L/min 2% CO_2 – enriched air for 24 h) , higher light intensities (200 and 100 µmol PAR $m^{-2}s^{-1}$, respectively), and higher initial biomass concentrations (about 0.2 g/L). Therefore, higher biomass productivities are expected with these differences in growth conditions. The high specific growth rates do not contradict the low average biomass productivities. Biomass productivity is the product of growth rate and biomass concentration. The high specific growth rates were achieved only in the exponential phase which lasted for less than 7 days for most strains because of the limitations of the growth conditions. In addition, the initial biomass concentrations (inoculum rates) used in this study were rather low, less than 0.02 g/L. Therefore, these conditions determined the overall low biomass productivity. However, the comparisons made between algae strains in this study are valid since similar growth conditions were used for all the strains. Optimization of the growth conditions was not within the scope of this study and is not necessary for strain screening purposes.

4.1.2 Culture pH

The pH vs time curves of the algae cultures are shown in Figures14 to 20. The general trend of the pH curves was closely correlated to algae growth phases. The original pH of the culture media pH which was measured in day 0 before aeration started ranged from 7.8 to 8.1. A significant pH drop was observed following day 0 in most

cultures. This can be explained by the CO_2 enriched air feed to the culture. CO_2 dissolved in water formed carbonic acid which further dissociated and released H^+ into the medium. As algae population grew, an increasing amount of CO_2/CO_3^{2-} was taken up by algae cells, and pH level rose. This pH increase corresponded to the exponential and declining growth phases on the growth curves. The pH increase ended at almost the same time when the algae culture reached the stationary phase, followed by a slight or rapid pH drop depending on different strains. The correspondence between the pH curves and the growth curves suggests that medium pH can serve as an indirect indicator of algae growth phases.

4.1.3 Ash and Lipid Contents and Fatty Acid Composition

Ash content of the algae biomass was measured with and without cell washing. As Table 3 shows, biomass of SP50 contained the highest ash content, 34.0 % before cell washing and 7.5% after cell washing. The significant decrease in ash content indicates that a considerable amount of extracellular salt originated from the culture media remained in the biomass during harvest.

Lipid content was calculated on the ash free dry weight basis (Table 3). SP20 was the best lipid producer among the seven strains, with the highest lipid content of 18.9%. The lipid content ranged from 8.7 to 18.9%, which is within the range reported in other strain screening studies, 8.5% of *Tetraselmis suecica* to 39.8% of *Chaetoceros calcitrans* (Hempel et al., 2012; Rodolfi et al., 2009), yet again, the difference in experiment conditions must be recognized when making comparisons. The two green algae strains had higher lipid content than the five cyanobacteria. This finding is in agreement with the

previous knowledge that in general, cyanobacteria are not good lipid producers (Hu et al., 2008).

The fatty acid profiles of the seven strains are summarized in Table 4. Eighteen different fatty acids were identified in the oil samples extracted from algal biomass. The two green algae strains were found to have more types of fatty acids (i.e. 13 different fatty acids detected in the oil obtained from biomass produced by SP20) than those in the oil obtained from cyanobacteria (i.e. 6 fatty acids for SP50). The fatty acid composition varied greatly among different strains. The palmitic acid (C16:0) was the major fatty acid in all 7 strains, constituting 30.95 – 36.48% of the total fatty acids. Oleic and elaidic acids (C18:1 n9) were the other major fatty acids in all the algae strains except in SP20 and SP38. γ – Linolenic acid (C18:3 n6), however, was the second major fatty acid in SP20 (29.12%) and SP38 (35.95%). Linoleic acid (C18:2) was found in a significant amount (9.29 – 18.23%) in all the seven algae strains. Linoleic acid is an essential fatty acid for humans, which means the human body requires it for maintenance of good health but cannot synthesize it. Essential fatty acids need to be provided in diet. A significant amount (6.88%) of eicosapentaenoic acid (C20:5 n3, EPA), was detected in SP22. EPA is an important fatty acid involved in human physiology and is of high commercial value. All the seven strains, especially SP20 and SP38, with the exception of SP46, contained a high content of polyunsaturated fatty acids (PUFA). It is reported that biodiesel produced from feedstocks with high PUFA content has a much better cold-flow property compared with that made from all saturated fats (Hu et al., 2008). However, PUFAs are unstable due to their susceptibility to oxidation (Knothe, 2005).

Algal biodiesel is FAMEs derived from algal lipids through the transesterification processes. Not all lipid components in algae can be converted to FAMEs. Therefore the FAMEs content of algae biomass was measured as an indicator of the amount of lipids present in algal oils that is suitable for biodiesel production. Total FAMEs of each strain is shown in Table 3. SP22 produced the highest total FAMEs content, 10.4% on an ash free dry weight basis (AFDW), and SP20 was second with 7.76% AFDW. These findings were comparable to the highest FAMEs content obtained in another strain selection study, 8.1% (Hempel et al., 2012). The total FAMEs content, in general, is lower than the lipid content for the same algal biomass. This difference between the oil and the FAMEs content is likely to arise from the following two factors. First, as mentioned earlier, total lipids, measured gravimetrically after solvent extraction, contain non-lipid components such as pigments and carbohydrates. In a study conducted by Laurens et al. (2012), only 30.9% and 51.4% of the lipids extracted from *Chlorella vulgaris* and *Nannochloropsis* sp., respectively, were converted to FAMEs. Second, only 78.4 – 93.5% of the peaks in the GC-FID chromatograms could be identified that means about 10 – 20% of the peak area was not included in the calculations. Some of the unidentified peaks could have been FAMEs.

4.2 THERMOGRAVIMETRIC ANALYSIS OF ALGAE BIOMASS

4.2.1 Proximate Analysis

Proximate analyses of the seven algae biomass samples was conducted by a TGA method (García et al., 2013), and the higher heating values (HHV) were estimated based on proximate analysis results (Table 5). The volatile matter and fixed carbon contents of the biomass samples ranged from 61.9% to 67.5% and 10.6% to 26.0%, respectively,

which are comparable to the results for algae biomass reported in previous studies (Bi et al., 2013; Li et al., 2010; Maddi et al., 2011; Shuping et al., 2010). High volatile matter and fixed carbon contents are desirable features of algal biomass as a feedstock for thermochemical production of biofuel. SP 20 and SP48 showed the highest HHVs, 20.3 MJ/kg and 20.0 MJ/kg, respectively, while SP 38 had the lowest HHV, 16.2 MJ/kg.

4.2.2 Thermal Decomposition Characteristics of the Algae Biomass

Figures 21 to 27 show the thermogravimetric (TG) curves for the seven strains under the inert atmosphere at three different heating rates. As observed in many TGA characterization studies (Gai et al., 2013; Shuping et al., 2010), the TG curves showed three typical stages during the heating process. The first stage, from the initial temperature to around 150 ^{o}C – 200 ^{o}C, depending on different strains, indicated a minor weight loss (around 10% to 15%) which was due to the removal of moisture and some light volatiles (Shuping et al., 2010); therefore, the first stage is sometimes referred to as the dehydration stage. Afterwards, from around 150 ^{o}C to 400 ^{o}C, the major weight loss (about 45% to 60% for different strains) corresponding to the rapid drop in the TG curves occurred. The weight loss at this stage arises from the decomposition of the major organic components in algae biomass, e.g. carbohydrates, protein, and lipids (Gai et al., 2013). And finally, the third stage was characterized by a slow, but continuous weight loss that resulted from the decomposition of carbonaceous material in the residue. The fraction of solid residue that remained after the experiments represented the combined ash and fixed carbon content. In addition, it was found that a higher heating rate would shift the TG curve to the right (higher temperatures) and reduce the fraction of final solid residues. The latter trend was also observed in several other studies (Maiti et al., 2007;

Shuping et al., 2010). The main reason for the general shift to the higher temperatures is that higher heating rates will induce larger temperature gradients within the biomass particles which are not good heat conductors themselves; therefore, the overall temperature of the biomass particle will be slightly lower than the temperature measured externally. Lower fractions of the final solid residue obtained at higher heating rates could be attributed to the fact that higher heating rates would reduce the residence time inside the reactor and inhibit secondary reactions such as cracking and re-condensation that induce the formation of chars (Maiti et al., 2007; Shuping et al., 2010).

The first derivative of each TG curve was calculated to obtain the derivative thermogravimetric (DTG) curves for the algae biomass samples (Figures 28-34). Corresponding to the shift of TG curves as discussed earlier, DTG curves shift to higher temperatures with increasing heating rates. This shift can also be attributed to the temperature gradients within the biomass particles at high heating rates. DTG curves exhibited single peaks for SP 20, SP46, SP48, and SP 50, and multiple peaks for SP22, SP37, and SP38 within the temperature range of 150 ^{o}C to 400 ^{o}C (the second stage of pyrolysis as discussed earlier). The maximum weight loss rates and the corresponding temperatures of the pyrolysis at the heating rate of 20 ^{o}C/min are presented in Table 6. Among the four biomass samples that showed a single weight loss peak during pyrolysis, SP20 had the highest maximum weight loss rate, 0.93 %/^{o}C, and the lowest peak temperature, 226.3 ^{o}C, while SP48 had the lowest maximum weight loss rate, 0.53 %/^{o}C, and the highest peak temperature, 254.3 ^{o}C. This indicates that biomass of SP20 is superior to SP48 as a feedstock for thermochemical conversion because SP20 degraded at lower temperatures at higher rates than SP48. Compared to the pyrolysis of the other

samples, thermal degradation of SP38 generally occurred at low temperatures illustrated by the broad shape of its DTG curves and the temperature corresponding to the first peak, 177 ^{o}C, the lowest level among all the samples. The results obtained by the qualitative analyses here are in agreement with the quantitative results of kinetic parameters, which will be discussed later.

The shape of DTG curves is determined by the compositions of algae biomass. A pyrolysis curve of algae biomass encompasses thermal degradation of all individual components, e.g. carbohydrates, proteins, and lipids, each of them having distinct decomposition patterns. Maddi et al. (2011) found that hemicellulose mainly decomposes in the temperature range of 220 – 315 ^{o}C, cellulose in a range of 345 – 400 ^{o}C, and lignin in a much wider temperature range of 190 – 900 ^{o}C. Na et al. (2011) studied the decomposition behavior of *Chlorella* sp. biomass and found that the maximum weight loss rate of triacylglycerols occurred at around 390 ^{o}C. In our cases, the single weight loss peak for some strains might indicate that the biomass was composed of one dominant component, while the multiple peaks might suggest the biomass was composed of several major components.

4.2.3 Pyrolysis Kinetics

Apparent activation energies, E_{α}, of the thermal decomposition reactions were determined by KAS method at degrees of conversion ranging from 0.2 to 0.8 which covered the second stage of pyrolysis. Plots of $\ln(\beta/T^2)$ versus 1/T for each biomass sample are shown in Figures 35 to 41. The slopes of the fitted regression lines, $-E_{\alpha}/R$, were used to calculate the apparent activation energy, shown in Table 7. The high linear

correlation coefficients (R^2) indicate that the curve fits explained the experimental data well.

The calculated activation energies depended on the degrees of conversion. A similar trend was also observed in previous studies (Gai et al., 2013; Hu et al., 2015). Specifically, the activation energies remained constant or slightly increased when $\alpha \leq 0.6$ and dramatically increased when $\alpha > 0.6$. The change of activation energies with degrees of conversion reflects the continuous change of the biomass composition during the pyrolysis process (Hu et al., 2015). This specific variation trend of activation energies indicates that decomposition reactions of the algal biomass are single step reactions when $\alpha \leq 0.6$. In contrast, reactions at higher degrees of conversion ($\alpha > 0.6$) might involve multiple decomposition mechanisms which require higher activation energy than the single step reactions (Gai et al., 2013; Sharara et al., 2014).

A lower activation energy of a thermal decomposition reaction means less energy is required to thermally break down the components, hence, degradation is an easier process (Gai et al., 2013). The average activation energy of SP20 (130.1 kJ/mol) was lower than that of SP48 (187.1 kJ/mol), the highest level among the seven algae samples. The lowest average apparent activation energy was obtained with SP38 (102.8 kJ/mol) indicating that the decomposition occurred at lower temperatures than the other algae biomass samples. Therefore, the qualitative evaluations of the thermal degradation patterns are consistent with the quantitative results of the kinetics study. The average activation energies are within the ranges for algae biomass reported in previous studies using the same calculation method. Gai et al. (2013) studied the thermal decomposition behavior of two microalgae, and the average activation energies were found to be 77.02 and 91.56 kJ/mol

for *Chlorella pyrenoidosa* and *Spirulina platensis*, respectively. Sharara et al. (2014) determined the activation energy of two mixed algae consortia grown at two different water treatment systems as 213.4 and 247.8 kJ/mol, indicating the variations in biomass composition.

4.3 MICROWAVE ASSISTED PYROLYSIS

4.3.1 Temperature Profiles

The temperature profiles of the pyrolysis experiments are shown in Figure 36. Based on the preliminary experiments, the temperature was first raised to 100 ^{o}C followed by an isothermal process of 1 min in order to achieve better process control. Then, the temperature was increased at a rate of 100 ^{o}C/min until the set final temperature was reached, 450, 600, or 750 ^{o}C. The actual temperature profiles measured by the thermocouple inserted in the sample matched well with the set temperature programs in general. However, minor deviations were observed during the initial period of the final isothermal process. A similar trend was also observed by Zhao et al. (2012). This deviation might have been caused by the thermal inertia of the biomass sample and the imperfection of the process control. White smoke started coming out of the reactor and appeared in the quartz tube (No. 11 in Figure 6) when the temperature reached around 350 ^{o}C.

4.3.2 Product Yields

The microwave assisted pyrolysis of algae biomass produced three products in different forms, liquid (bio-oil + water), solid, and gas. The yield of each product is shown in Figure 43. With increasing final temperature from 450 ^{o}C to 750 ^{o}C, the yield of solid product decreased from 71.2% to 31.2%, while the yields of gas product and liquid

product increased from 7.4% and 21.6% to 23.9% and 45.1%, respectively. This is in agreement with the general trend reported in previous studies: lower temperature produces more char and higher temperature favors gasification reactions (Borges et al., 2014; Du et al., 2011; Pan et al., 2010). As shown in Picture 3, the liquid product collected in the flasks (No. 13 in Figure 6) contained both bio-oil (dark phase) and water (light-color phase). Due to the difficulty of directly recovering all the bio-oil from the system, the fraction condensed in the system was washed out using methanol. The weight of the bio-oil that remained after solvent evaporation was reported as the bio-oil yield. However, the GC-MS analysis of the bio-oil composition indicated that a number of compounds were not recovered by solvent washing or lost during the evaporation of the solvent. Therefore, the weight of the bio-oil after solvent washing and evaporation might be an underestimation of the actual bio-oil amount produced during pyrolysis. The bio-oil yield increased from 4.6% to 22.5% with increasing final temperature from 450 ^{o}C to 750 ^{o}C, which were within the range of bio-oil yields reported in literature (Du et al., 2011; Hu et al., 2012; Pan et al., 2010). Previous studies have found that optimal temperatures exist for bio-oil production because of the inadequate conversion of biomass at low temperatures and the secondary cracking reactions of volatiles at high temperatures (Borges et al., 2014; Du et al., 2011; Hu et al., 2012; Pan et al., 2010). Therefore, further experiments at higher final temperatures are needed to determine the optimal temperature for bio-oil production under the experimental conditions examined in this study.

A comparison of the results from microwave assisted pyrolysis and the TGA experiments with SP46 biomass indicates that the fractional yields of solid residue from microwave pyrolysis (71.2% and 51.5% at the final temperatures of 450 ^{o}C and 600 ^{o}C,

respectively) were higher than those from the TGA pyrolysis (32.8% and 30.3% at 450 ^{o}C and 600 ^{o}C, respectively) (Figure 24). One of the possible reasons for this difference is that the inner region of the biomass where the thermocouple was inserted had a much higher temperature than the outer region. Du et al. (2011) observed this difference to be 100-150 ^{o}C. This temperature difference can be caused by two factors: first, the internal heating characteristic of microwave heating, and second, the hot spot created by the thermocouple tip which can act as an antenna within a microwave field (Luque et al., 2012; Salema et al., 2011; Zhao et al., 2012). Therefore, the temperature measurement with a thermocouple might overestimate the average temperature of the biomass sample. Hence, microwave pyrolysis might have occurred at a lower temperature than that reported here, resulting in higher amount of solid residue than TGA experiments. A combination of thermocouple and pyrometer might improve the accuracy of temperature measurement during a microwave-assisted pyrolysis process (Luque et al., 2012).

4.3.3 GC-MS analysis of the bio-oils

Both the bio-oil collected after solvent washing and evaporation and the bio-oil directly collected in a flask were analyzed by GC-MS. The amount of each major compound was determined as the relative area percentage of the corresponding peak as compared to total peak area (Table 8). The identified compounds were grouped into the following groups: acids (mostly fatty acids), aliphatic hydrocarbons, aromatic hydrocarbons, phenols (including phenol and phenol derivatives), organic nitrogen compounds, and the other compounds (mostly oxygenates such as ketones and furans).

Hydrocarbons are the major components of fossil fuels such as gasoline and diesel and are, therefore, desirable components in bio-oil. Specifically, aromatic hydrocarbons

are of high value as they are important chemical feedstock, but polycyclic aromatic hydrocarbons (PAH) pose threats to human health and also the environment. The fraction of aromatic hydrocarbons obtained at 750 ^{o}C reached 6.23%, with no PAH identified. Phenol and its derivatives are also important chemicals in industry, and they represented 15.22 to 17.82 % of the bio-oil. Organic nitrogen compounds, including amines, nitriles, pyridines, and indoles, represented 20.47% to 30.27% of the bio-oil. These compounds are typical products of protein decomposition (Du et al., 2013). Nitrogen in these compounds is undesirable due to the potential NO_X emission during combustion. Acids, mostly fatty acids, accounted for 14.16% to 30.4% of the bio-oil. These fatty acids included palmitoleic acid (C16: 1), n-hexadecanoic acid (C16:0), and 9-Octadecenoic acid (oleic acid, C18:1), which is in agreement with the findings in GC-FID analysis of SP46 FAMEs (Table 4).

Bio-oil produced from algae biomass was distinct in composition compared with bio-oil from other lignocellulosic biomass reported in previous studies (Ates et al., 2008; Lei et al., 2009; Yang et al., 2014). For lignocellulosic bio-oil, the predominant compounds are oxygenates such as phenols, furans, and their derivatives, while algae derived bio-oil contained significant portions of aliphatic hydrocarbons, organic nitrogen compounds, and acids. This difference is determined by the different feedstock composition: lignocellulosic biomass is mainly composed of cellulose, hemicellulose, and lignin, while algae mainly consist of carbohydrates, proteins, and lipids.

The fraction of each chemical group varied under different pyrolysis temperatures. The fraction of acids increased from 14.16% to 30.40% with the pyrolysis temperature rising from 450 ^{o}C to 750 ^{o}C. This could be because triacylglycerols mainly decompose

into fatty acids at high temperatures. Although fatty acids can further decompose into short chain hydrocarbons according to Maher et al. (2007), the short residence time in the reactor might have limited the further decomposition process. The fraction of aromatic hydrocarbons increased with increasing temperature, which was also observed by Du et al. (2013). The fraction of organic nitrogen compounds reached the maximum, 30.27 %, at 600 ^{o}C and then decreased at 750 ^{o}C. The dependence of bio-oil composition on pyrolysis temperature suggests that bio-oil of higher quality can be obtained by controlling the temperature at the optimal levels.

The bio-oil produced at 600 ^{o}C and collected after solvent washing and evaporation did not contain several compounds [including 3-methyl-1-butene (C_5H_{10}), 2-cyclopropyl-propane (C_6H_{12}), toluene (C_7H_8), 1-methylethyl- oxirane ($C_5H_{10}O$), and 2-furanmethanol ($C_5H_6O_2$)] that were in the original bio-oil obtained at the same temperature (600 ^{o}C) but collected directly in the flask (Table 7). These compounds have low boiling points, therefore, they might have been removed from the bio-oil along with solvent and water evaporation. Therefore, the amount of the bio-oil that remained after solvent washing might be an underestimation of the actual weight of the bio-oil produced during pyrolysis.

CHAPTER V

CONCLUSIONS

In this study, seven algae strains isolated from the Great Salt Plains of Oklahoma, UTEX SP20 (*Dunaliella sp.*), SP22 (*Tetraselmis striata*), SP38 (*Phormidium keutzingianum*), SP46 (*Pseudanabaena sp.*), SP47 (*Pseudanabaena sp.*), SP48 (*Pseudanabaena sp.*), and SP50 (*Tychonema bornetii*), were cultivated under controlled growth conditions and the growth parameters and chemical composition of each strain were studied. SP20 had the highest oil content (18.9% AFDW), the highest specific growth rate (0.76/day), and the second highest total FAME content (7.76 % AFDW) among the seven strains; therefore, SP20 can be a viable strain for biofuel production, especially for biodiesel production. SP46 produced the highest final biomass concentration (1.32 g/L), the highest biomass productivity (55.9 mg $L^{-1}day^{-1}$) and the lowest lipid content (9.2% AFDW). Due to these properties, SP46 was selected out of the seven strains as the feedstock for bio-oil production via microwave assisted pyrolysis. Optimization of the growth conditions and outdoor large scale cultivation are recommended to ascertain the suitability of these two strains as feedstock for biofuel production. In addition, pH of the medium was found to be closely related to algae growth, therefore, pH may serve as an indicator of algae growth phases.

Thermal degradation behavior of each strain was examined by thermogravimetric analyses. Pyrolysis of algae biomass took place in three stages, with major weight loss occurring at the second stage of pyrolysis from around 150 ^{o}C to 400 ^{o}C. The qualitative information revealed in the TG and DTG curves were corroborated by the quantitative

results of the pyrolysis kinetic parameters. The apparent activation energy was calculated by using a model-free method. The apparent activation energy varied at different degrees of conversion; specifically, it dramatically increased when $\alpha>0.6$. Biomass of SP38 resulted in the lowest average apparent activation energy, 102.8 kJ/mol, indicating that pyrolysis of biomass from SP38 requires the least energy consumption among the seven strains.

During the microwave assisted pyrolysis of SP46 biomass, the bio-oil yield increased from 4.6% to 22.5% with the increasing final temperature from 450 ^{o}C to 750 ^{o}C. The major compounds in the bio-oil included acids, aliphatic hydrocarbons, aromatic hydrocarbons, phenols, organic nitrogen compounds, and other oxygenates. The fraction of each chemical group varied under different pyrolysis temperatures, The fractions of acids and aromatic hydrocarbons increased while that of aliphatic hydrocarbons decreased with the pyrolysis temperature rising from 450 ^{o}C to 750 ^{o}C. No polycyclic aromatic hydrocarbons were found in the bio-oils. The highest bio-oil yield was obtained at the final temperature of 750 ^{o}C. However, experiments at higher temperatures are recommended for a better understanding of the effect of temperature on microwave assisted pyrolysis. Modifications in the microwave pyrolysis system design could improve the temperature measurement accuracy and the bio-oil collection efficiency.

REFERENCES

Andersen, R. A. (2005). *Algal culturing techniques*: Academic press.

Ates, F., & Işıkdağ, M. j. A. (2008). Evaluation of the role of the pyrolysis temperature in straw biomass samples and characterization of the oils by GC/MS. *Energy & Fuels, 22*(3), 1936-1943.

Baba, M., & Shiraiwa, Y. (2012). High-CO2 response mechanisms in microalgae. *Advances in photosynthesis—fundamental aspects. InTech, Rijeka*, 299-320.

Bartley, M. L., Boeing, W. J., Dungan, B. N., Holguin, F. O., & Schaub, T. (2014). pH effects on growth and lipid accumulation of the biofuel microalgae Nannochloropsis salina and invading organisms. *Journal of Applied Phycology, 26*(3), 1431-1437.

Bi, Z., & He, B. (2013). Characterization of microalgae for the purpose of biofuel production. *Trans. ASABE, 56*(4), 1529-1539.

Bolton, J. R., & Hall, D. O. (1991). The maximum efficiency of photosynthesis. *Photochemistry and Photobiology, 53*(4), 545-548.

Borges, F. C., Xie, Q., Min, M., Muniz, L. A. R., Farenzena, M., Trierweiler, J. O., Ruan, R. (2014). Fast microwave-assisted pyrolysis of microalgae using microwave absorbent and HZSM-5 catalyst. *Bioresource technology, 166*, 518-526.

Borowitzka, M. A. (1992). Algal biotechnology products and processes—matching science and economics. *Journal of Applied Phycology, 4*(3), 267-279.

Brennan, L., & Owende, P. (2010). Biofuels from microalgae—a review of technologies for production, processing, and extractions of biofuels and co-products. *Renewable and sustainable energy reviews, 14*(2), 557-577.

Breuer, G., Lamers, P. P., Martens, D. E., Draaisma, R. B., & Wijffels, R. H. (2013). Effect of light intensity, pH, and temperature on triacylglycerol (TAG) accumulation induced by nitrogen starvation in Scenedesmus obliquus. *Bioresource technology, 143*, 1-9.

Bridgwater, A., Meier, D., & Radlein, D. (1999). An overview of fast pyrolysis of biomass. *Organic Geochemistry, 30*(12), 1479-1493.

Brown, T. M., Duan, P. G., & Savage, P. E. (2010). Hydrothermal Liquefaction and Gasification of Nannochloropsis sp. *Energy & Fuels, 24*, 3639-3646.

Cantrell, K., Martin, J., & Ro, K. (2010). Application of thermogravimetric analysis for the proximate analysis of livestock wastes. *Journal of ASTM International (JAI), 7*(3).

Chen, C., Ma, X., & Liu, K. (2011). Thermogravimetric analysis of microalgae combustion under different oxygen supply concentrations. *Applied Energy, 88*(9), 3189-3196.

Chen, M., Tang, H., Ma, H., Holland, T. C., Ng, K. S., & Salley, S. O. (2011). Effect of nutrients on growth and lipid accumulation in the green algae Dunaliella tertiolecta. *Bioresource technology, 102*(2), 1649-1655.

Chen, W.-H., Lin, B.-J., Huang, M.-Y., & Chang, J.-S. (2015). Thermochemical conversion of microalgal biomass into biofuels: A review. *Bioresource technology, 184*, 314-327.

Chen, W.-H., Wu, Z.-Y., & Chang, J.-S. (2014). Isothermal and non-isothermal torrefaction characteristics and kinetics of microalga Scenedesmus obliquus CNW-N. *Bioresource technology, 155*, 245-251.

Chisti, Y. (2008). Biodiesel from microalgae beats bioethanol. *Trends in biotechnology, 26*(3), 126-131.

Chiu, S.-Y., Kao, C.-Y., Tsai, M.-T., Ong, S.-C., Chen, C.-H., & Lin, C.-S. (2009). Lipid accumulation and CO 2 utilization of Nannochloropsis oculata in response to CO 2 aeration. *Bioresource technology, 100*(2), 833-838.

Cogne, G., Lehmann, B., Dussap, C. G., & Gros, J. B. (2003). Uptake of macrominerals and trace elements by the cyanobacterium Spirulina platensis (Arthrospira platensis PCC 8005) under photoautotrophic conditions: culture medium optimization. *Biotechnology and bioengineering, 81*(5), 588-593.

Converti, A., Casazza, A. A., Ortiz, E. Y., Perego, P., & Del Borghi, M. (2009). Effect of temperature and nitrogen concentration on the growth and lipid content of Nannochloropsis oculata and Chlorella vulgaris for biodiesel production. *Chemical Engineering and Processing, 48*(6), 1146-1151.

de Morais, M. G., & Costa, J. A. V. (2007). Isolation and selection of microalgae from coal fired thermoelectric power plant for biofixation of carbon dioxide. *Energy Conversion and Management, 48*(7), 2169-2173.

DOE, U. (2010). National algal biofuels technology roadmap. *US Department of Energy, Office of Energy Efficiency and Renewable Energy, Biomass Program*.

Dominguez, A., Menéndez, J., Fernandez, Y., Pis, J., Nabais, J. V., Carrott, P., & Carrott, M. R. (2007). Conventional and microwave induced pyrolysis of coffee hulls for

the production of a hydrogen rich fuel gas. *Journal of Analytical and Applied Pyrolysis, 79*(1), 128-135.

Domínguez, A., Menéndez, J., Inguanzo, M., & Pis, J. (2006). Production of bio-fuels by high temperature pyrolysis of sewage sludge using conventional and microwave heating. *Bioresource technology, 97*(10), 1185-1193.

Du, Z., Hu, B., Ma, X., Cheng, Y., Liu, Y., Lin, X., & Ruan, R. (2013). Catalytic pyrolysis of microalgae and their three major components: carbohydrates, proteins, and lipids. *Bioresource technology, 130*, 777-782.

Du, Z., Li, Y., Wang, X., Wan, Y., Chen, Q., Wang, C., & Ruan, R. (2011). Microwave-assisted pyrolysis of microalgae for biofuel production. *Bioresource technology, 102*(7), 4890-4896.

Duong, V. T., Thomas-Hall, S. R., & Schenk, P. (2015). Growth and lipid accumulation of microalgae from fluctuating brackish and sea water locations in South East Queensland – Australia. *Frontiers in Plant Science, 6*.

Fábregas, J., Domínguez, A., Regueiro, M., Maseda, A., & Otero, A. (2000). Optimization of culture medium for the continuous cultivation of the microalga Haematococcus pluvialis. *Applied Microbiology and Biotechnology, 53*(5), 530-535.

Fernández, Y., Arenillas, A., & Menéndez, J. Á. (2011). *Microwave Heating Applied to Pyrolysis, Advances in Induction and Microwave Heating of Mineral and Organic Materials, Stanisław Grundas (Ed.), ISBN: 978-953-307-522-8, InTech*: InTech.

Gai, C., Liu, Z., Han, G., Peng, N., & Fan, A. (2015). Combustion behavior and kinetics of low-lipid microalgae via thermogravimetric analysis. *Bioresource technology*, *181*, 148-154.

Gai, C., Zhang, Y., Chen, W.-T., Zhang, P., & Dong, Y. (2013). Thermogravimetric and kinetic analysis of thermal decomposition characteristics of low-lipid microalgae. *Bioresource technology, 150*, 139-148.

García, R., Pizarro, C., Lavín, A. G., & Bueno, J. L. (2013). Biomass proximate analysis using thermogravimetry. *Bioresource technology, 139*, 1-4.

Gardner, R., Peters, P., Peyton, B., & Cooksey, K. E. (2011). Medium pH and nitrate concentration effects on accumulation of triacylglycerol in two members of the chlorophyta. *Journal of Applied Phycology*, *23*(6), 1005-1016.

Georgianna, D. R., & Mayfield, S. P. (2012). Exploiting diversity and synthetic biology for the production of algal biofuels. *Nature*, *488*(7411), 329-335.

Gong, X., & Chen, F. (1997). Optimization of culture medium for growth of Haematococcus pluvialis. *Journal of Applied Phycology*, *9*(5), 437-444.

Gordillo, F. J., Goutx, M., Figueroa, F. L., & Niell, F. X. (1998). Effects of light intensity, CO2 and nitrogen supply on lipid class composition of Dunaliella viridis. *Journal of Applied Phycology, 10*(2), 135-144.

Goyal, H. B., Seal, D., & Saxena, R. C. (2008). Bio-fuels from thermochemical conversion of renewable resources: A review. *Renewable and sustainable energy reviews, 12*(2), 504-517.

Griffiths, M. J., & Harrison, S. T. (2009). Lipid productivity as a key characteristic for choosing algal species for biodiesel production. *Journal of Applied Phycology, 21*(5), 493-507.

Guillard, R. R. (1975). Culture of phytoplankton for feeding marine invertebrates *Culture of marine invertebrate animals* (pp. 29-60): Springer.

Guiry, M. D. (2012). How many species of algae are there? *Journal of Phycology, 48*(5), 1057-1063.

Hempel, N., Petrick, I., & Behrendt, F. (2012). Biomass productivity and productivity of fatty acids and amino acids of microalgae strains as key characteristics of suitability for biodiesel production. *Journal of Applied Phycology, 24*(6), 1407-1418.

Ho, S.-H., Chen, C.-Y., Lee, D.-J., & Chang, J.-S. (2011). Perspectives on microalgal CO2-emission mitigation systems — A review. *Biotechnology Advances, 29*(2), 189-198.

Ho, S.-H., Ye, X., Hasunuma, T., Chang, J.-S., & Kondo, A. (2014). Perspectives on engineering strategies for improving biofuel production from microalgae - A critical review. *Biotechnology Advances, 32*(8), 1448-1459.

Hu, M., Chen, Z., Guo, D., Liu, C., Xiao, B., Hu, Z., & Liu, S. (2015). Thermogravimetric study on pyrolysis kinetics of Chlorella pyrenoidosa and bloom-forming cyanobacteria. *Bioresource technology, 177*, 41-50.

Hu, Q., Sommerfeld, M., Jarvis, E., Ghirardi, M., Posewitz, M., Seibert, M., & Darzins, A. (2008). Microalgal triacylglycerols as feedstocks for biofuel production: perspectives and advances. *The Plant Journal, 54*(4), 621-639.

Hu, Z., Ma, X., & Chen, C. (2012). A study on experimental characteristic of microwave-assisted pyrolysis of microalgae. *Bioresource technology, 107*, 487-493.

Huesemann, M., Van Wagenen, J., Miller, T., Chavis, A., Hobbs, S., & Crowe, B. (2013). A screening model to predict microalgae biomass growth in photobioreactors and raceway ponds. *Biotechnology and bioengineering*, *110*(6), 1583-1594.

Hughes, E. O., Gorham, P., & Zehnder, A. (1958). Toxicity of a unialgal culture of Microcystis aeruginosa. *Canadian Journal of Microbiology, 4*(3), 225-236.

Juneja, A., Ceballos, R. M., & Murthy, G. S. (2013). Effects of Environmental Factors and Nutrient Availability on the Biochemical Composition of Algae for Biofuels Production: A Review. *Energies, 6*(9), 4607-4638.

Keller, M. D., Selvin, R. C., Claus, W., & Guillard, R. R. (1987). Media for the culture of oceanic ultraphytoplankton1, 2. *Journal of Phycology, 23*(4), 633-638.

Kirkwood, A. E., & Henley, W. J. (2006). Algal community dynamics and halotolerance in a terrestrial, hypersaline environment1. *Journal of Phycology*, *42*(3), 537-547.

Knothe, G. (2005). Dependence of biodiesel fuel properties on the structure of fatty acid alkyl esters. *Fuel processing technology, 86*(10), 1059-1070.

Larkum, A. W., Ross, I. L., Kruse, O., & Hankamer, B. (2012). Selection, breeding and engineering of microalgae for bioenergy and biofuel production. *Trends in biotechnology, 30*(4), 198-205.

Laurens, L. M., Quinn, M., Van Wychen, S., Templeton, D. W., & Wolfrum, E. J. (2012). Accurate and reliable quantification of total microalgal fuel potential as fatty acid methyl esters by in situ transesterification. *Analytical and bioanalytical chemistry, 403*(1), 167-178.

Lee, S., Kim, S.-B., Kim, J.-E., Kwon, G.-S., Yoon, B.-D., & Oh, H.-M. (1998). Effects of harvesting method and growth stage on the flocculation of the green alga Botryococcus braunii. *Letters in Applied Microbiology, 27*(1), 14-18.

Lee, Y.-K., Ding, S.-Y., Hoe, C.-H., & Low, C.-S. (1996). Mixotrophic growth ofChlorella sorokiniana in outdoor enclosed photobioreactor. *Journal of Applied Phycology, 8*(2), 163-169.

Lei, H., Ren, S., & Julson, J. (2009). The effects of reaction temperature and time and particle size of corn stover on microwave pyrolysis. *Energy & Fuels*, *23*(6), 3254-3261.

Li, D., Chen, L., Zhao, J., Zhang, X., Wang, Q., Wang, H., & Ye, N. (2010). Evaluation of the pyrolytic and kinetic characteristics of Enteromorpha prolifera as a source of renewable bio-fuel from the Yellow Sea of China. *Chemical Engineering Research and Design*, *88*(5), 647-652.

Li, Y., Chen, Y.-F., Chen, P., Min, M., Zhou, W., Martinez, B., & Ruan, R. (2011). Characterization of a microalga Chlorella sp. well adapted to highly concentrated municipal wastewater for nutrient removal and biodiesel production. *Bioresource technology*, *102*(8), 5138-5144.

Luque, R., Menéndez, J. A., Arenillas, A., & Cot, J. (2012). Microwave-assisted pyrolysis of biomass feedstocks: the way forward? *Energy & Environmental Science, 5*(2), 5481-5488.

Ma, F., & Hanna, M. A. (1999). Biodiesel production: a review. *Bioresource technology, 70*(1), 1-15.

Maddi, B., Viamajala, S., & Varanasi, S. (2011). Comparative study of pyrolysis of algal biomass from natural lake blooms with lignocellulosic biomass. *Bioresource technology, 102*(23), 11018-11026.

Maher, K., & Bressler, D. (2007). Pyrolysis of triglyceride materials for the production of renewable fuels and chemicals. *Bioresource technology, 98*(12), 2351-2368.

Maiti, S., Purakayastha, S., & Ghosh, B. (2007). Thermal characterization of mustard straw and stalk in nitrogen at different heating rates. *Fuel, 86*(10), 1513-1518.

Marcilla, A., Catalá, L., García-Quesada, J. C., Valdés, F., & Hernández, M. (2013). A review of thermochemical conversion of microalgae. *Renewable and sustainable energy reviews, 27*, 11-19.

Mayers, J. J., Flynn, K. J., & Shields, R. J. (2014). Influence of the N: P supply ratio on biomass productivity and time-resolved changes in elemental and bulk biochemical composition of Nannochloropsis sp. *Bioresource technology, 169*, 588-595.

Mayoral, M., Izquierdo, M., Andres, J., & Rubio, B. (2001). Different approaches to proximate analysis by thermogravimetry analysis. *Thermochimica Acta, 370*(1), 91-97.

Mohan, D., Pittman, C. U., & Steele, P. H. (2006). Pyrolysis of wood/biomass for bio-oil: a critical review. *Energy & Fuels, 20*(3), 848-889.

Montero, M. F., Aristizábal, M., & Reina, G. G. (2011). Isolation of high-lipid content strains of the marine microalga Tetraselmis suecica for biodiesel production by flow cytometry and single-cell sorting. *Journal of Applied Phycology, 23*(6), 1053-1057.

Motasemi, F., & Afzal, M. T. (2013). A review on the microwave-assisted pyrolysis technique. *Renewable and sustainable energy reviews, 28*, 317-330.

Na, J.-G., Lee, H., Oh, Y.-K., Park, J.-Y., Ko, C., Lee, S.-H., . . . Jeon, S. (2011). Rapid estimation of triacylglycerol content of Chlorella sp. by thermogravimetric analysis. *Biotechnology Letters, 33*(5), 957-960.

Pan, P., Hu, C., Yang, W., Li, Y., Dong, L., Zhu, L., & Fan, Y. (2010). The direct pyrolysis and catalytic pyrolysis of Nannochloropsis sp. residue for renewable bio-oils. *Bioresource technology, 101*(12), 4593-4599.

Parikh, J., Channiwala, S. A., & Ghosal, G. K. (2005). A correlation for calculating HHV from proximate analysis of solid fuels. *Fuel, 84*(5), 487-494.

Peng, L., Lan, C. Q., Zhang, Z., Sarch, C., & Laporte, M. (2015). Control of protozoa contamination and lipid accumulation in Neochloris oleoabundans culture: Effects of pH and dissolved inorganic carbon. *Bioresource technology, 197*, 143-151.

Pereira, H., Barreira, L., Mozes, A., Florindo, C., Polo, C., Duarte, C. V., & Varela, J. (2011). Microplate-based high throughput screening procedure for the isolation of lipid-rich marine microalgae. *Biotechnology for biofuels, 4*(1), 1-12.

Radakovits, R., Jinkerson, R. E., Darzins, A., & Posewitz, M. C. (2010). Genetic engineering of algae for enhanced biofuel production. *Eukaryotic cell, 9*(4), 486-501.

Rao, A. R., Dayananda, C., Sarada, R., Shamala, T., & Ravishankar, G. (2007). Effect of salinity on growth of green alga Botryococcus braunii and its constituents. *Bioresource technology, 98*(3), 560-564.

Renaud, S. M., Thinh, L.-V., & Parry, D. L. (1999). The gross chemical composition and fatty acid composition of 18 species of tropical Australian microalgae for possible use in mariculture. *Aquaculture, 170*(2), 147-159.

Rhee, G.-Y. (1978). Effects of N: P atomic ratios and nitrate limitation on algal growth, cell composition, and nitrate uptake 1. *Limnology and oceanography, 23*(1), 10-25.

Richmond, A. (2008). *Handbook of microalgal culture: biotechnology and applied phycology*: John Wiley & Sons.

Rizzo, A. M., Prussi, M., Bettucci, L., Libelli, I. M., & Chiaramonti, D. (2013). Characterization of microalga Chlorella as a fuel and its thermogravimetric behavior. *Applied Energy, 102*, 24-31.

Rodolfi, L., Chini Zittelli, G., Bassi, N., Padovani, G., Biondi, N., Bonini, G., & Tredici, M. R. (2009). Microalgae for oil: Strain selection, induction of lipid synthesis and outdoor mass cultivation in a low-cost photobioreactor. *Biotechnology and bioengineering, 102*(1), 100-112.

Ross, A., Jones, J., Kubacki, M., & Bridgeman, T. (2008). Classification of macroalgae as fuel and its thermochemical behaviour. *Bioresource technology, 99*(14), 6494-6504.

Saldarriaga, J. F., Aguado, R., Pablos, A., Amutio, M., Olazar, M., & Bilbao, J. (2015). Fast characterization of biomass fuels by thermogravimetric analysis (TGA). *Fuel, 140*, 744-751.

Salema, A. A., & Ani, F. N. (2011). Microwave induced pyrolysis of oil palm biomass. *Bioresource technology, 102*(3), 3388-3395.

Satoh, A., Kurano, N., & Miyachi, S. (2001). Inhibition of photosynthesis by intracellular carbonic anhydrase in microalgae under excess concentrations of CO2. *Photosynthesis research, 68*(3), 215-224.

Scott, S. A., Davey, M. P., Dennis, J. S., Horst, I., Howe, C. J., Lea-Smith, D. J., & Smith, A. G. (2010). Biodiesel from algae: challenges and prospects. *Current opinion in biotechnology, 21*(3), 277-286.

Sharara, M., & Sadaka, S. (2014). Thermogravimetric analysis of swine manure solids obtained from farrowing, and growing-finishing farms. *Journal of Sustainable Bioenergy Systems, 4*(01), 75.

Sharara, M. A., Holeman, N., Sadaka, S. S., & Costello, T. A. (2014). Pyrolysis kinetics of algal consortia grown using swine manure wastewater. *Bioresource technology, 169*, 658-666.

Sheehan, J., Dunahay, T., Benemann, J., & Roessler, P. (1998). *A look back at the US Department of Energy's aquatic species program: biodiesel from algae* (Vol. 328): National Renewable Energy Laboratory Golden.

Shuping, Z., Yulong, W., Mingde, Y., Chun, L., & Junmao, T. (2010). Pyrolysis characteristics and kinetics of the marine microalgae Dunaliella tertiolecta using thermogravimetric analyzer. *Bioresource technology, 101*(1), 359-365.

Silva, C. S., Seider, W. D., & Lior, N. (2015). Exergy efficiency of plant photosynthesis. *Chemical Engineering Science, 130*, 151-171.

Sobczuk, T. M., Camacho, F. G., Rubio, F. C., Fernández, F., & Grima, E. M. (2000). Carbon dioxide uptake efficiency by outdoor microalgal cultures in tubular airlift photobioreactors. *Biotechnology and bioengineering, 67*(4), 465-475.

Takagi, M., Karseno, & Yoshida, T. (2006). Effect of salt concentration on intracellular accumulation of lipids and triacylglyceride in marine microalgae Dunaliella cells. *Journal of Bioscience and Bioengineering, 101*(3), 223-226.

Thiansathit, W., Keener, T. C., Khang, S.-J., Ratpukdi, T., & Hovichitr, P. (2015). The kinetics of Scenedesmus obliquus microalgae growth utilizing carbon dioxide gas from biogas. *Biomass and Bioenergy, 76*, 79-85.

Tittel, J., Bissinger, V., Gaedke, U., & Kamjunke, N. (2005). Inorganic carbon limitation and mixotrophic growth in Chlamydomonas from an acidic mining lake. *Protist, 156*(1), 63-75.

Van de Velden, M., Baeyens, J., Brems, A., Janssens, B., & Dewil, R. (2010). Fundamentals, kinetics and endothermicity of the biomass pyrolysis reaction. *Renewable Energy, 35*(1), 232-242.

Van Wychen, S., & Laurens, L. (2013). Determination of Total Lipids as Fatty Acid Methyl Esters (FAME) by in situ Transesterification. *Contract, 303*, 275-3000.

Vasudevan, P. T., & Briggs, M. (2008). Biodiesel production—current state of the art and challenges. *Journal of Industrial Microbiology & Biotechnology, 35*(5), 421-430.

Vyazovkin, S., Burnham, A. K., Criado, J. M., Pérez-Maqueda, L. A., Popescu, C., & Sbirrazzuoli, N. (2011). ICTAC Kinetics Committee recommendations for performing kinetic computations on thermal analysis data. *Thermochimica Acta, 520*(1), 1-19.

Wan, Y., Chen, P., Zhang, B., Yang, C., Liu, Y., Lin, X., & Ruan, R. (2009). Microwave-assisted pyrolysis of biomass: Catalysts to improve product selectivity. *Journal of Analytical and Applied Pyrolysis, 86*(1), 161-167.

Wang, S. K., Stiles, A. R., Guo, C., & Liu, C. Z. (2014). Microalgae cultivation in photobioreactors: An overview of light characteristics. *Engineering in Life Sciences, 14*(6), 550-559.

Wijffels, R. H., & Barbosa, M. J. (2010). An outlook on microalgal biofuels. *Science(Washington), 329*(5993), 796-799.

Williams, P. J. l. B., & Laurens, L. M. (2010). Microalgae as biodiesel & biomass feedstocks: review & analysis of the biochemistry, energetics & economics. *Energy & Environmental Science, 3*(5), 554-590.

Wu, C., Budarin, V. L., Gronnow, M. J., De Bruyn, M., Onwudili, J. A., Clark, J. H., & Williams, P. T. (2014). Conventional and microwave-assisted pyrolysis of biomass under different heating rates. *Journal of Analytical and Applied Pyrolysis, 107*, 276-283.

Wu, K.-T., Tsai, C.-J., Chen, C.-S., & Chen, H.-W. (2012). The characteristics of torrefied microalgae. *Applied Energy, 100*, 52-57.

Xin, L., Hong-ying, H., Ke, G., & Ying-xue, S. (2010). Effects of different nitrogen and phosphorus concentrations on the growth, nutrient uptake, and lipid accumulation of a freshwater microalga Scenedesmus sp. *Bioresource technology, 101*(14), 5494-5500.

Yang, Y., & Gao, K. (2003). Effects of CO2 concentrations on the freshwater microalgae, Chlamydomonas reinhardtii, Chlorella pyrenoidosa and Scenedesmus obliquus (Chlorophyta). *Journal of Applied Phycology, 15*(5), 379-389.

Yang, Z., Sarkar, M., Kumar, A., Tumuluru, J. S., & Huhnke, R. L. (2014). Effects of torrefaction and densification on switchgrass pyrolysis products. *Bioresource technology, 174*, 266-273.

Yeesang, C., & Cheirsilp, B. (2011). Effect of nitrogen, salt, and iron content in the growth medium and light intensity on lipid production by microalgae isolated from freshwater sources in Thailand. *Bioresource technology, 102*(3), 3034-3040.

Yen, H.-W., Hu, I. C., Chen, C.-Y., & Chang, J.-S. (2014). Chapter 2 - Design of Photobioreactors for Algal Cultivation. In A. P.-J. L. C. R. Soccol (Ed.), *Biofuels from Algae* (pp. 23-45). Amsterdam: Elsevier.

Yin, C. (2012). Microwave-assisted pyrolysis of biomass for liquid biofuels production. *Bioresource technology, 120*, 273-284.

Zhang, Q., Wang, T., & Hong, Y. (2014). Investigation of initial pH effects on growth of an oleaginous microalgae Chlorella sp. HQ for lipid production and nutrient uptake. *Water Science & Technology, 70*(4), 712-719.

Zhao, X., Wang, M., Liu, H., Li, L., Ma, C., & Song, Z. (2012). A microwave reactor for characterization of pyrolyzed biomass. *Bioresource technology, 104*, 673-678.

Zhu, C., & Lee, Y. (1997). Determination of biomass dry weight of marine microalgae. *Journal of Applied Phycology, 9*(2), 189-194.

Zhu, X.-G., Long, S. P., & Ort, D. R. (2008). What is the maximum efficiency with which photosynthesis can convert solar energy into biomass? *Current opinion in biotechnology, 19*(2), 153-159.

Zhu, Y., & Dunford, N. T. (2013). Growth and biomass characteristics of Picochlorum oklahomensis and Nannochloropsis oculata. *Journal of the American Oil Chemists' Society, 90*(6), 841-849.

Table 1: List of the algae strains, cell sizes and growth media.

UTEX ID	Species	Group	Morphology	Size (µm)	Medium
SP 20	*Dunaliella sp.*	Green algae	Unicellular	10-14 × 4-6	5% F/2
SP 22	*Tetraselmis striata*	Green algae	Unicellular	11-14 × 8-11	F/2
SP 38	*Phormidium keutzingianum*	Cyanobacteria	Filamentous	1-3 × 3	BG11+ 1% NaCl
SP 46	*Pseudanabaena sp.*	Cyanobacteria	Filamentous	3-4 × 2	A+
SP 47	*Pseudanabaena sp.*	Cyanobacteria	Filamentous	1-2 × 1	A+
SP 48	*Pseudanabaena sp.*	Cyanobacteria	Filamentous	2-5 × 1-2	A+
SP 50	*Tychonema bornetii*	Cyanobacteria	Filamentous	20-70 × 10-12	5% F/2

Table 2: Growth characteristics of the algae strains.

Species	SP 20	SP 22	SP 38	SP 46	SP 47	SP 48	SP 50
Specific growth rate μ, /day	0.76^{a}	0.48^{c}	0.23^{e}	0.61^{b}	0.47^{c}	0.50^{c}	0.38^{d}
Doubling time t_d, day	0.91	1.44	3.08	1.14	1.49	1.32	1.84
Max biomass concentration X_{max}, g/L	0.62^{c}	0.38^{d}	0.38^{d}	1.32^{a}	0.58^{c}	0.85^{b}	0.72^{c}
Average biomass productivity ΔX, mg/(L · day)	51.8^{a}	25.3^{c}	17.9^{d}	55.9^{a}	26.9^{c}	42.0^{b}	51.2^{a}

Means with the same superscripts in a row are not significantly different (Tukey's HSD test, P>0.05).

Table 3: Ash and lipid contents of the algae strains.

	SP20	SP22	SP38	SP46	SP47	SP48	SP50
% ash w/o washing dry basis	13.7^{d}	21.3^{b}	12.0^{d}	13.2^{d}	15.2^{c}	19.1^{b}	34.0^{a}
% ash w/ washing dry basis	3.8^{d}	7.3^{a}	4.7^{c}	2.5^{e}	5.8^{b}	3.0^{e}	7.5^{a}
% lipid dry ash free basis	18.9^{a}	18.7^{a}	14.4^{b}	9.2^{d}	8.7^{d}	8.9^{d}	11.0^{c}

Means with the same superscripts in a row are not significantly different (Tukey's HSD test, $P>0.05$).

Table 4: Fatty acid composition of the algae strains.

	Fatty acid	SP20	SP22	SP38	SP46	SP47	SP48	SP50
Saturated fatty acids (% of total FAME)	C10:0	0.78 ± 0.01	ND	ND	ND	ND	ND	ND
	C12:0	2.12 ± 0.14	ND	ND	ND	ND	1.68 ± 0.05	ND
	C14:0	1.06 ± 0.05	1.16 ± 0.01	1.38 ± 0.02	ND	ND	ND	ND
	C16:0	32.51 ± 0.15	32.98 ± 0.07	30.95 ± 0.23	36.48 ± 0.05	34.84 ± 0.08	31.56 ± 0.02	32.52 ± 0.11
	C17:0	1.92 ± 0.01	2.61 ± 0.01	1.27 ± 0.03	ND	ND	ND	ND
	C18:0	1.49 ± 0.02	1.36 ± 0.01	1.06 ± 0.04	3.43 ± 0.01	2.74 ± 0.03	2.50 ± 0.02	ND
	subtotal	**39.9**	**38.1**	**34.7**	**39.9**	**37.6**	**35.7**	**32.5**
Mono-unsaturated fatty acids (% of total FAME)	C14:1	0.83 ± 0.04	ND	1.04 ± 0.03	ND	ND	ND	ND
	C15:1	ND	ND	ND	3.15 ± 0.10	3.83 ± 0.01	ND	3.46 ± 0.01
	C16:1	1.05 ± 0.02	1.19 ± 0.00	5.94 ± 0.11	3.19 ± 0.02	3.22 ± 0.04	11.75 ± 0.04	10.81 ± 0.02
	C17:1	2.03 ± 0.12	ND	2.30 ± 0.03	3.57 ± 0.06	5.14 ± 0.06	ND	ND
	C18:1 n9	8.84 ± 0.04	25.69 ± 0.03	3.17 ± 0.09	36.78 ± 0.05	23.20 ± 0.06	27.84 ± 0.04	26.24 ± 0.02
	C20:1	ND	2.16 ± 0.04	ND	ND	ND	ND	ND
	subtotal	**12.8**	**29.0**	**12.5**	**46.7**	**35.4**	**39.6**	**40.5**
Polyunsaturated fatty acids (% of total FAME)	C18:2	14.94 ± 0.05	9.29 ± 0.00	15.15 ± 0.03	13.40 ± 0.05	18.14 ± 0.14	16.43 ± 0.01	18.23 ± 0.04
	C18:3 n3	3.31 ± 0.01	ND	ND	ND	ND	ND	ND
	C18:3 n6	29.12 ± 0.14	15.20 ± 0.04	35.95 ± 0.05	ND	8.90 ± 0.04	8.24 ± 0.10	8.74 ± 0.09
	C20:3 n3	ND	1.48 ± 0.04	ND	ND	ND	ND	ND
	C20:4	ND	ND	1.78 ± 0.08	ND	ND	ND	ND
	C20:5	ND	6.88 ± 0.03	ND	ND	ND	ND	ND
	subtotal	**47.4**	**32.85**	**52.88**	**13.4**	**27.04**	**24.67**	**26.97**
Total FAMEs (%AFDW)		**7.76**	**10.40**	**6.77**	**3.69**	**4.85**	**5.29**	**4.48**

ND stands for Not Detected.

Table 5: Proximate analysis results by TGA (on as received basis) and HHV estimation

	SP20	SP22	SP38	SP46	SP47	SP48	SP50
Moisture %	6.8^{d}	8.3^{c}	12.2^{a}	9.2^{c}	10.1^{b}	9.9^{b}	6.9^{d}
Volatile Matter %	62.4^{b}	66.5^{a}	67.5^{a}	66.4^{a}	64.4^{b}	61.9^{b}	66.5^{a}
Fixed Carbon %	26.0^{a}	18.0^{c}	10.6^{d}	18.8^{c}	19.2^{c}	23.9^{b}	20.7^{c}
Ash %	4.8^{d}	7.2^{b}	9.7^{a}	5.7^{c}	6.3^{c}	4.3^{e}	5.9^{c}
HHV, dry basis (MJ/kg)	20.3^{a}	18.2^{c}	16.2^{d}	18.7^{b}	18.7^{b}	20.0^{a}	18.9^{b}

Means with the same superscripts in a row are not significantly different (Tukey's HSD test, P>0.05).

Table 6:.Characteristics of the peaks in 20 ^{o}C/min DTG curves.

	SP20		SP22		SP38		SP46		SP47		SP48		SP50	
	T_p (^{o}C)	-dW/dT (%/^{o}C)	T_p (^{o}C)	-dW/dT (%/^{o}C)	T_p (^{o}C)	-dW/dT (%/^{o}C)	T_p (^{o}C)	-dW/dT (%/^{o}C)	T_p (^{o}C)	-dW/dT (%/^{o}C)	T_p (^{o}C)	-dW/dT (%/^{o}C)	T_p (^{o}C)	-dW/dT (%/^{o}C)
1st peak	226.3	0.93	215.0	0.52	177.0	0.34	232.0	0.63	201.0	0.50	254.3	0.53	232.0	0.65
2nd peak			246.0	0.55	206.0	0.37			254.3	0.63				
3rd peak					247.0	0.39								

Notes: -dW/dT: maximum weight loss rates; T_p : the corresponding temperatures for the peaks.

Table 7: The apparent activation energies of the algae strains.

	Degree of conversion	0.2	0.3	0.4	0.5	0.6	0.7	0.8	Average E_a (kJ/mol)
SP20	E_a (kJ/mol)	109.0	125.6	124.1	126.7	127.9	134.9	162.8	130.1
	R^2	0.991	1.000	1.000	1.000	0.993	0.991	0.995	
SP22	E_a (kJ/mol)	135.1	132.9	137.1	142.9	149.0	165.4	252.3	159.3
	R^2	0.982	0.997	0.999	0.999	0.997	0.996	1.000	
SP38	E_a (kJ/mol)	67.9	76.3	91.7	105.6	116.5	130.1	131.7	102.8
	R^2	1.000	1.000	0.999	0.997	0.998	0.999	0.997	
SP46	E_a (kJ/mol)	153.2	141.8	151.3	151.0	158.3	194.4	294.0	177.7
	R^2	0.997	1.000	0.998	0.999	0.995	0.996	0.972	
SP47	E_a (kJ/mol)	131.4	150.3	155.8	141.2	147.7	150.6	216.5	156.2
	R^2	0.988	0.985	0.981	0.995	0.989	0.996	0.987	
SP48	E_a (kJ/mol)	109.2	140.6	152.2	154.8	161.1	253.6	300.2	181.7
	R^2	0.958	0.980	0.967	0.973	0.971	0.959	0.953	
SP50	E_a (kJ/mol)	147.4	141.5	152.3	156.5	163.1	169.3	230.9	165.8
	R^2	0.964	0.958	0.969	0.974	0.989	0.993	1.000	

Table 8: Relative proportions (area %) of the main compounds of four bio-oil samples

Group	Compound name	Formula	Area %			
			450 °C	600 °C [1]	750 °C	600 °C [2]
Acid	**Subtotal**		**14.16**	**19.64**	**30.40**	**24.03**
	Palmitoleic acid	$C_{16}H_{30}O_2$	3.65	5.40	4.62	2.45
	n-Hexadecanoic acid	$C_{16}H_{32}O_2$	5.45	6.75	10.13	20.87
	9-Octadecenoic acid, (E)-	$C_{18}H_{34}O_2$	5.07	7.49	12.25	ND
Aliphatic hydrocarbons	**Subtotal**		**22.73**	**14.25**	**8.56**	**10.31**
	1-Butene, 3-methyl-	C_5H_{10}	3.21	1.52	2.04	ND
	1-Butene	C_4H_8	1.20	0.70	ND	ND
	Propane, 2-cyclopropyl-	C_6H_{12}	5.58	5.61	1.81	ND
	Cyclohexane, 1,1,2-trimethyl-	C_9H_{18}	1.11	ND	ND	ND
	Pentadecane	$C_{15}H_{32}$	2.65	1.37	ND	1.12
	Heptadecane	$C_{17}H_{36}$	1.62	ND	ND	ND
	1,13-Tetradecadiene	$C_{14}H_{26}$	1.96	1.45	ND	2.05
	1-Nonadecene	$C_{19}H_{38}$	5.40	3.61	4.71	ND
Aromatic hydrocarbons	**Subtotal**		**1.66**	**2.34**	**6.23**	**0.0**
	Toluene	C_7H_8	ND	1.40	4.07	ND
	Bicyclo[4.2.0]octa-1,3,5-triene	C_8H_8	ND	0.94	2.16	ND
	Naphthalene, 1,2,3,4-tetrahydro-1,1,6-trimethyl-	$C_{13}H_{18}$	1.66	ND	ND	ND
Phenols	**Subtotal**		**15.22**	**14.35**	**17.82**	**17.80**
	Phenol	C_6H_5OH	5.86	5.42	6.68	4.22
	Phenol, 2-methyl-	C_7H_8O	1.28	1.22	1.22	1.11
	p-Cresol	C_7H_8O	6.40	6.21	9.93	9.32
Others	**Subtotal**		**25.75**	**19.15**	**17.72**	**16.89**
	2-Propenal	C_3H_4O	7.61	ND	ND	ND
	1-Methoxy-3-(2-hydroxyethyl)nonane	$C_{12}H_{26}O_2$	3.69	1.84	3.19	3.50
	Oxirane, (1-methylethyl)-	$C_5H_{10}O$	ND	5.87	3.51	ND
	2-Furanmethanol	$C_5H_6O_2$	2.03	3.19	1.68	ND
	Ethanol, 2-(9-octadecenyloxy)	$C_{20}H_{40}O_2$	12.43	7.68	9.35	11.52

Table 8: Relative proportions (area %) of the main compounds of four bio-oil samples (continued from the previous page)

Group	Compound name	Formula	Area %			
			450 °C	600 °C[1]	750 °C	600 °C[2]
Organic nitrogen compounds	**Subtotal**		**20.47**	**30.27**	**20.48**	**31.07**
	Pyridine	C_5H_5N	ND	2.07	2.18	ND
	Pyrrole	C_4H_5N	0.77	1.61	1.89	ND
	Pyridine, 2-methyl-	C_6H_7N	ND	1.74	1.95	ND
	Pyrazine, methyl-	$C_5H_6N_2$	1.37	2.40	ND	ND
	4-Methylcyclohexylamine	$C_7H_{15}N$	2.71	2.51	ND	ND
	Pentanamide, 4-methyl-	$C_6H_{13}NO$	ND	1.10	ND	1.60
	2,4-Dihydroxypyridine	$C_5H_5NO_2$	1.03	ND	ND	ND
	Benzyl nitrile	C_8H_7N	2.96	2.22	2.49	0.87
	2-Piperidinone	C_5H_9NO	ND	4.52	ND	3.45
	Benzenepropanenitrile	C_9H_9N	1.93	1.31	ND	1.27
	Indole	C_8H_7N	5.10	3.81	5.88	5.44
	1H-Indole, 3-methyl-	C_9H_9N	1.51	1.09	1.67	2.48
	Hexadecanamide	$C_{16}H_{33}NO$	2.08	1.84	2.95	7.08
	9-Octadecenamide, (Z)-	$C_{18}H_{35}NO$	1.01	1.02	1.47	6.60

Note: 600 °C [1] is the bio-oil directly collected in the condensation flask; 600 °C [2] is the bio-oil recovered after solvent washing and evaporation.

Figure 1: Mole fraction of inorganic carbon species (i.e., d CO_2, HCO_3^-, and CO_3^{2-}) under different medium pH (assuming gas and liquid phase equilibrium at 25 ^oC and 1 atmosphere) (Peng et al., 2015).

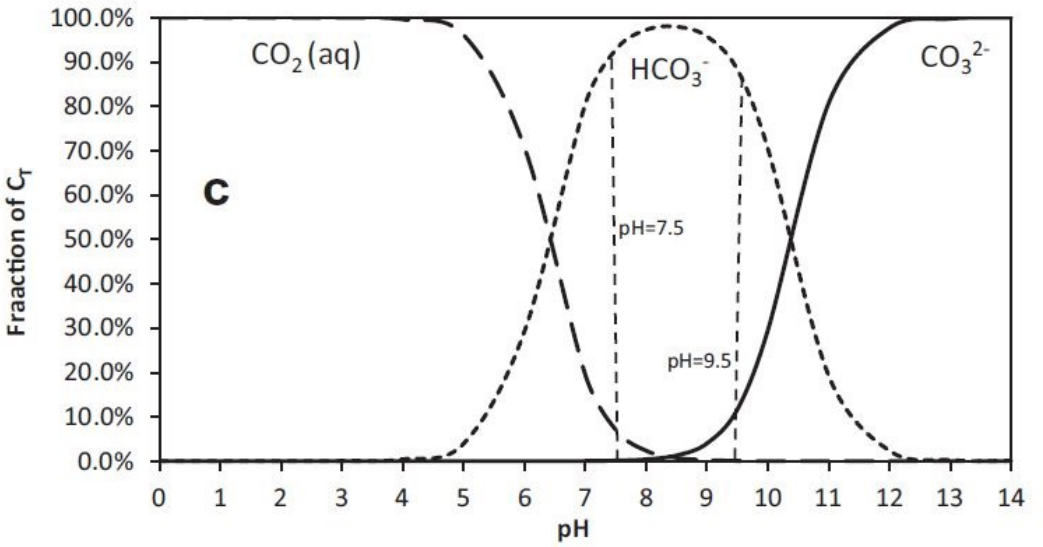

Figure 2: Relationship between photosynthesis rate and light intensity.

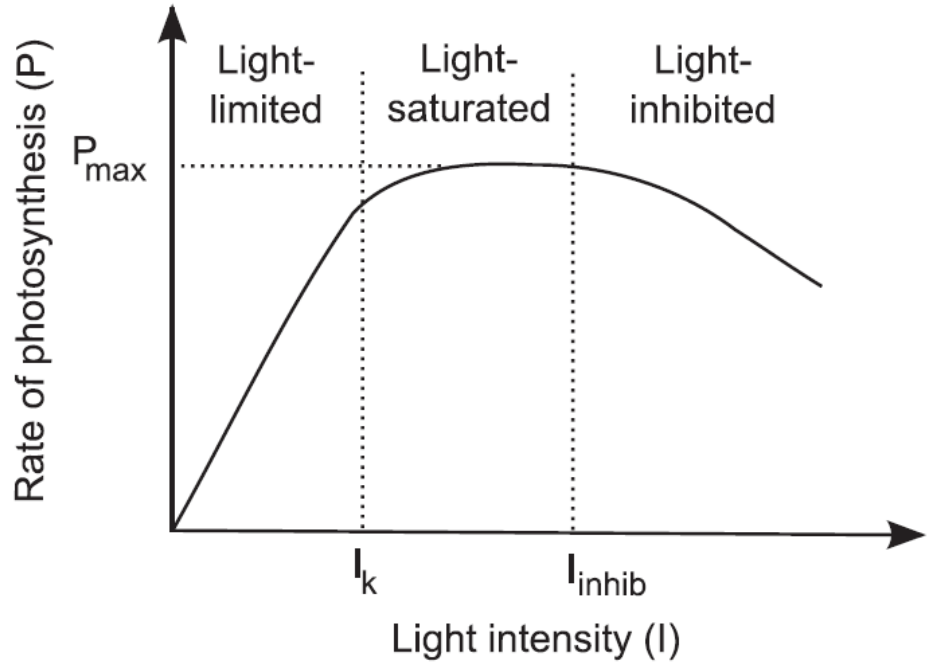

P-I relationship: light-limited ($I<I_k$), light-saturated ($I_k<I<I_{inhib}$), and light-inhibited ($I>I_{inhib}$) regimes of microalgae light response (Wang et al., 2014) .

Figure 3: PAR Observation at the North Coast of California for Sep. 12-14, 2015 (top) and Daily averages for 2015 (bottom)

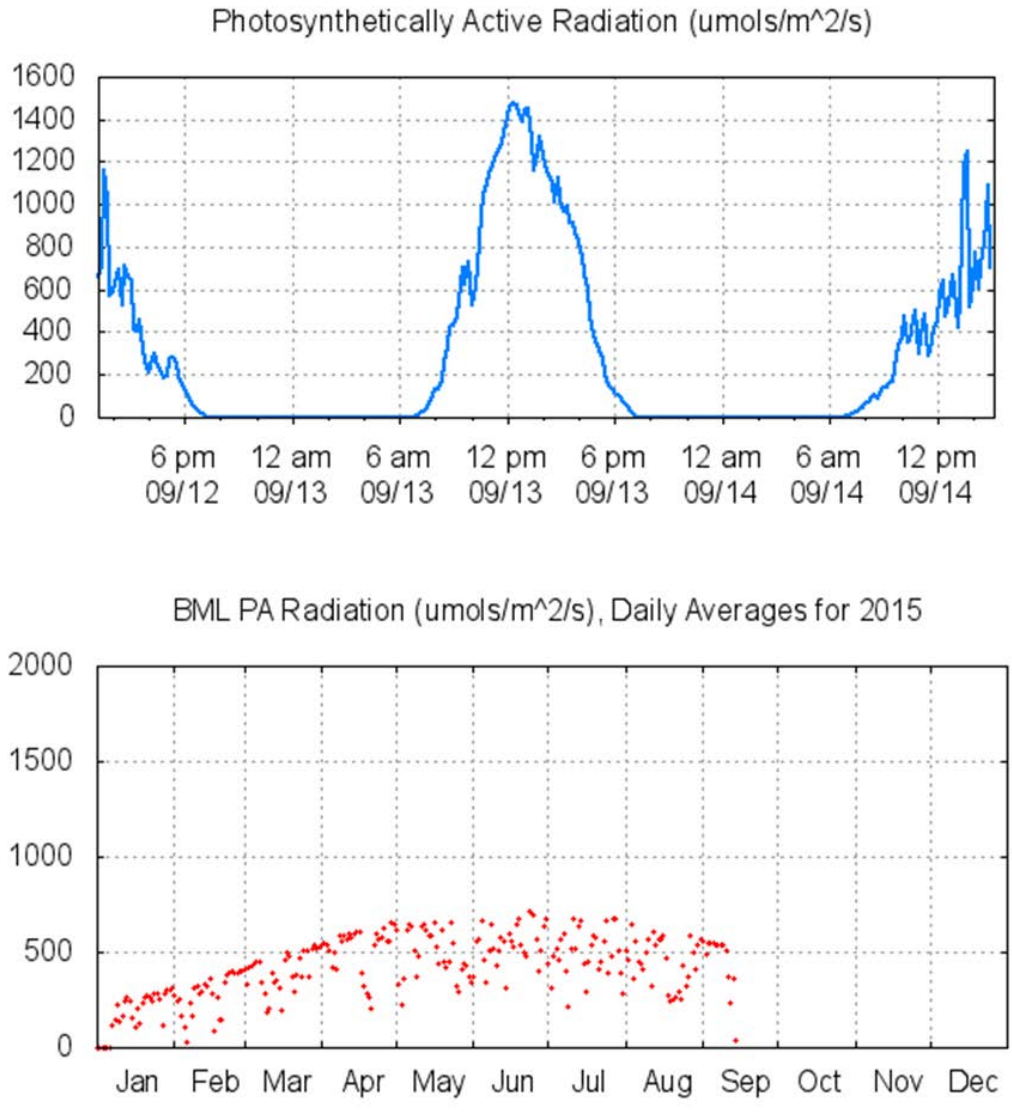

Data provided by the University of California, Davis, Bodega Marine Laboratory (http://bml.ucdavis.edu/boon/)

Figure 4: Pathways for conversion of algae biomass to biofuel.

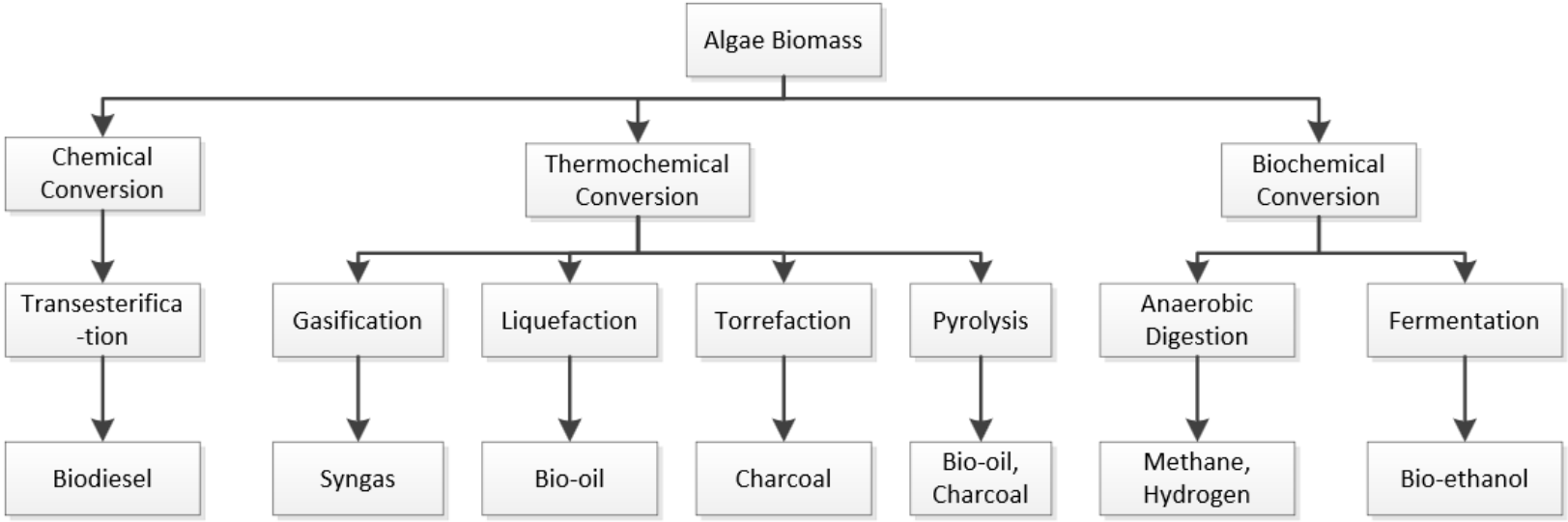

Figure 5. Schematic diagram of a TGA curve to be used for proximate analysis.

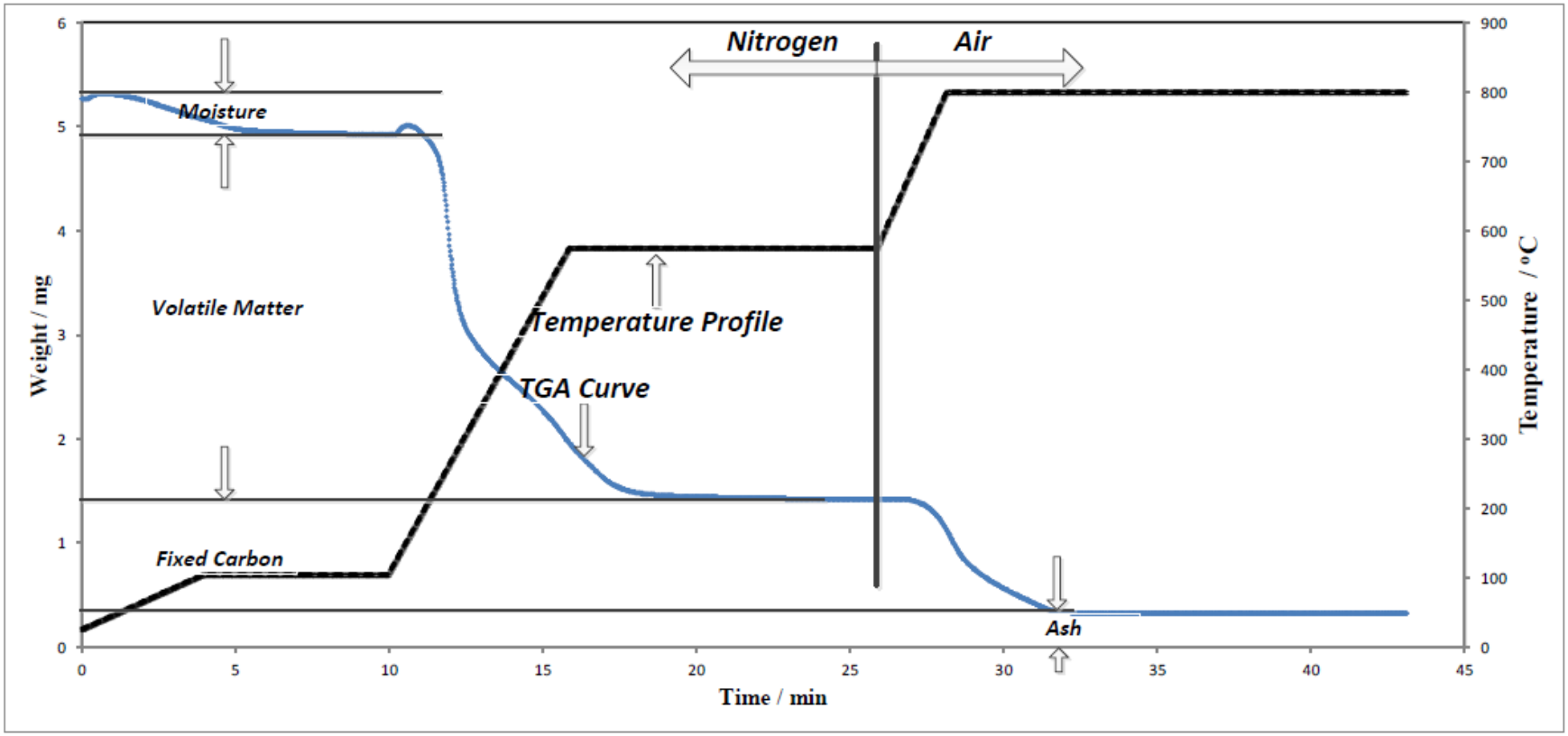

Figure 6: The schematic diagram of microwave-assisted pyrolysis experimental set-up.

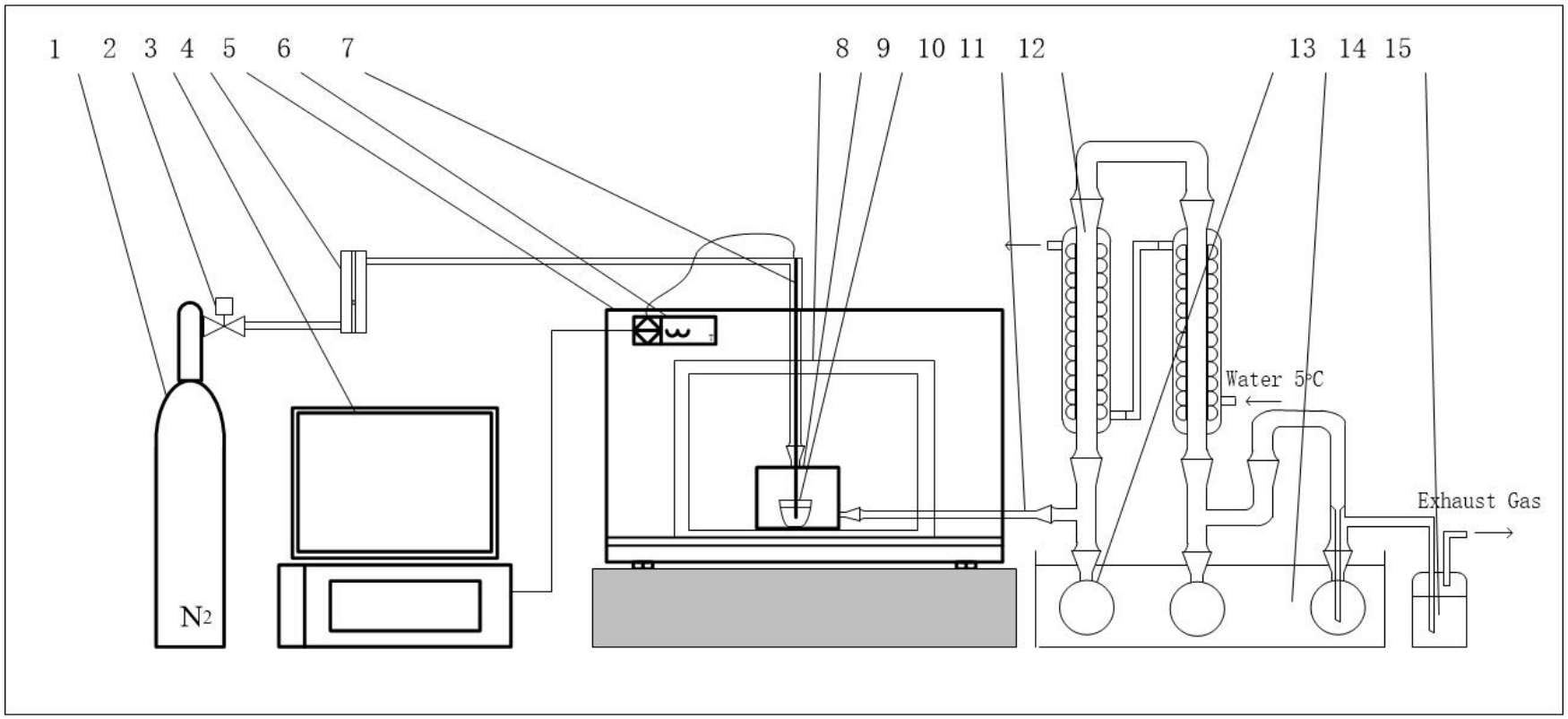

(1) N_2 cylinder, (2) regulator, (3) computer, (4) gas flowmeter, (5) microwave oven, (6) process controller, (7) thermocouple, (8) muffle, (9) quartz reactor, (10) quartz crucible, (11) quartz tube, (12) condenser system, (13) liquid collection flask, (14) ice bath, (15) water bottle

Figure 7: Growth curve (a) and semi-log growth curve (b) of SP20.

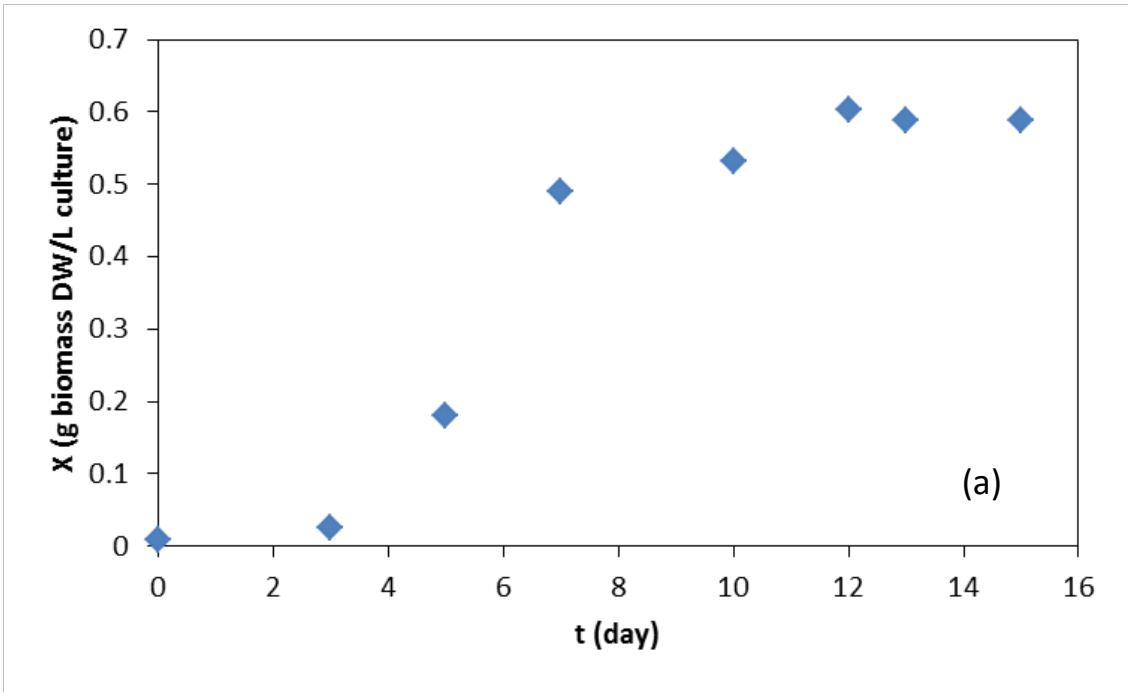

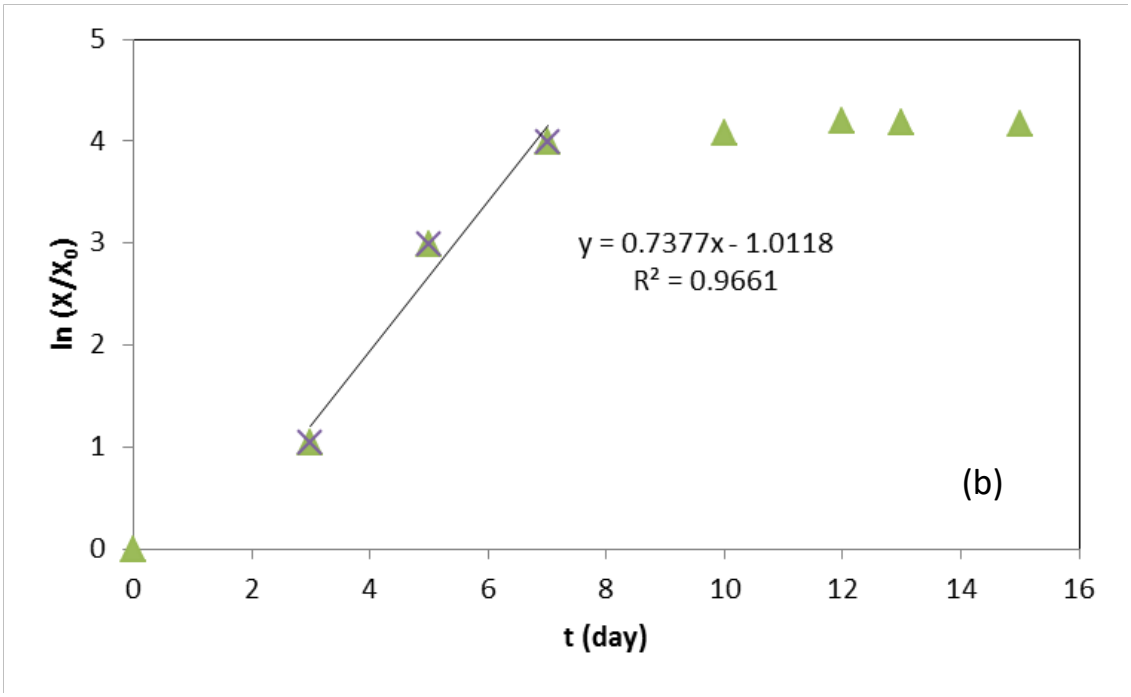

Figure 8: Growth curve (a) and semi-log growth curve (b) of SP22.

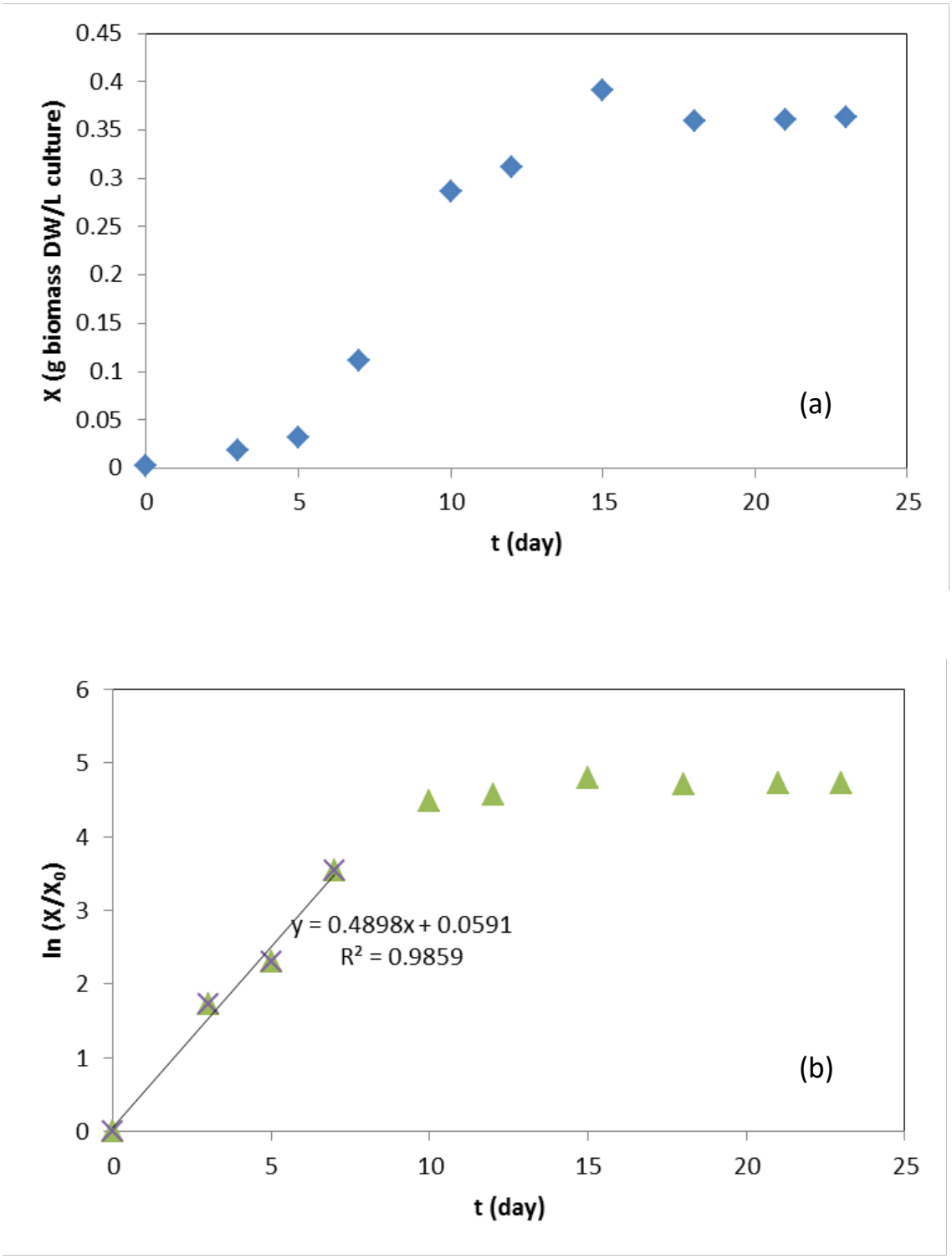

Figure 9: Growth curve (a) and semi-log growth curve (b) of SP38.

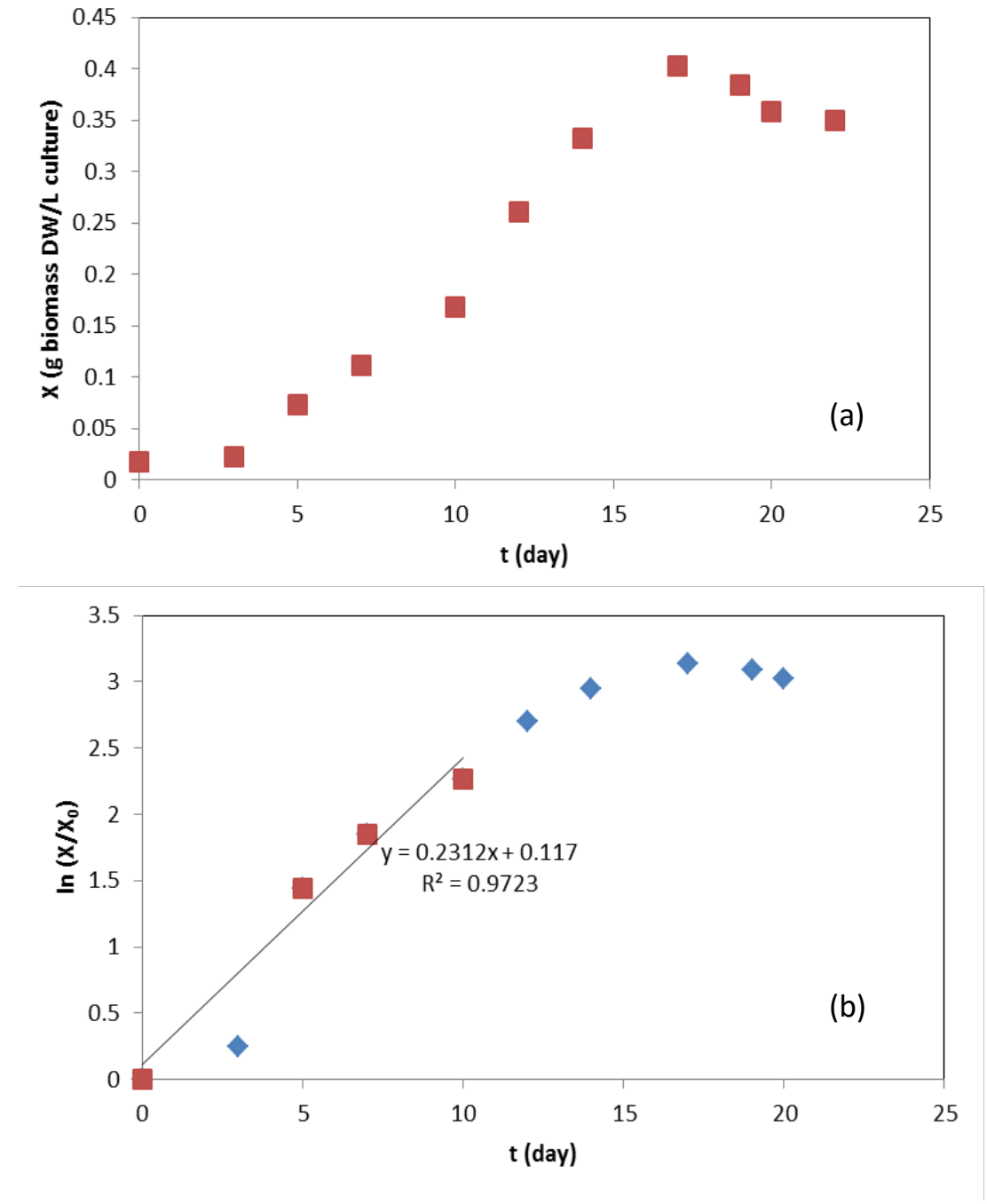

Figure 10: Growth curve (a) and semi-log growth curve (b) of SP46.

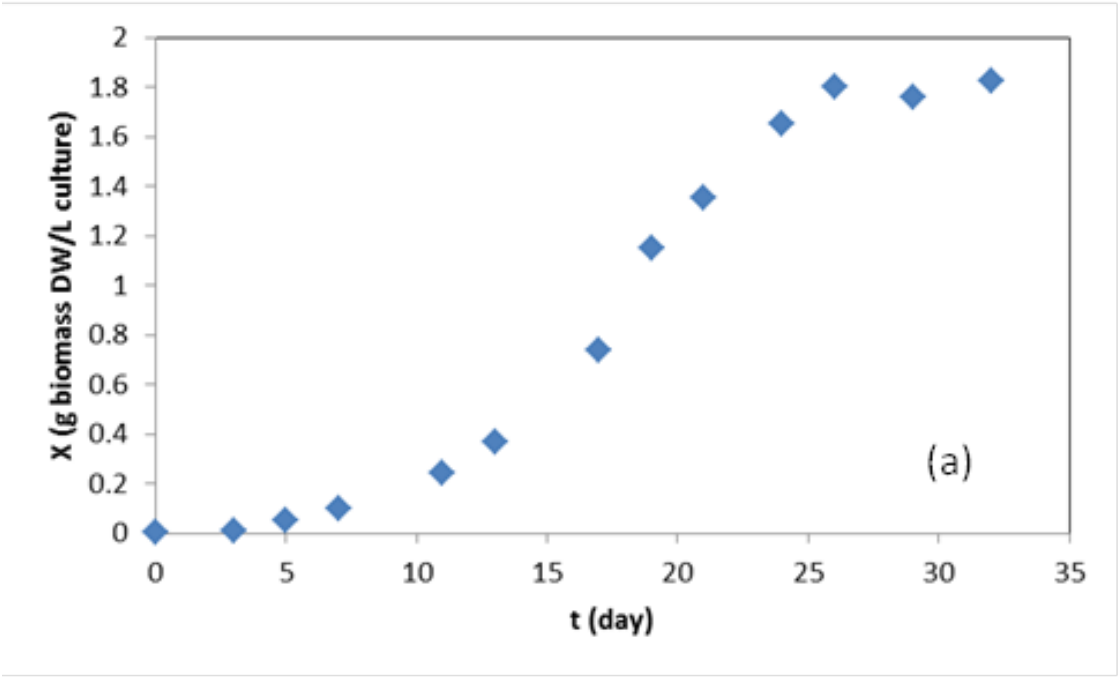

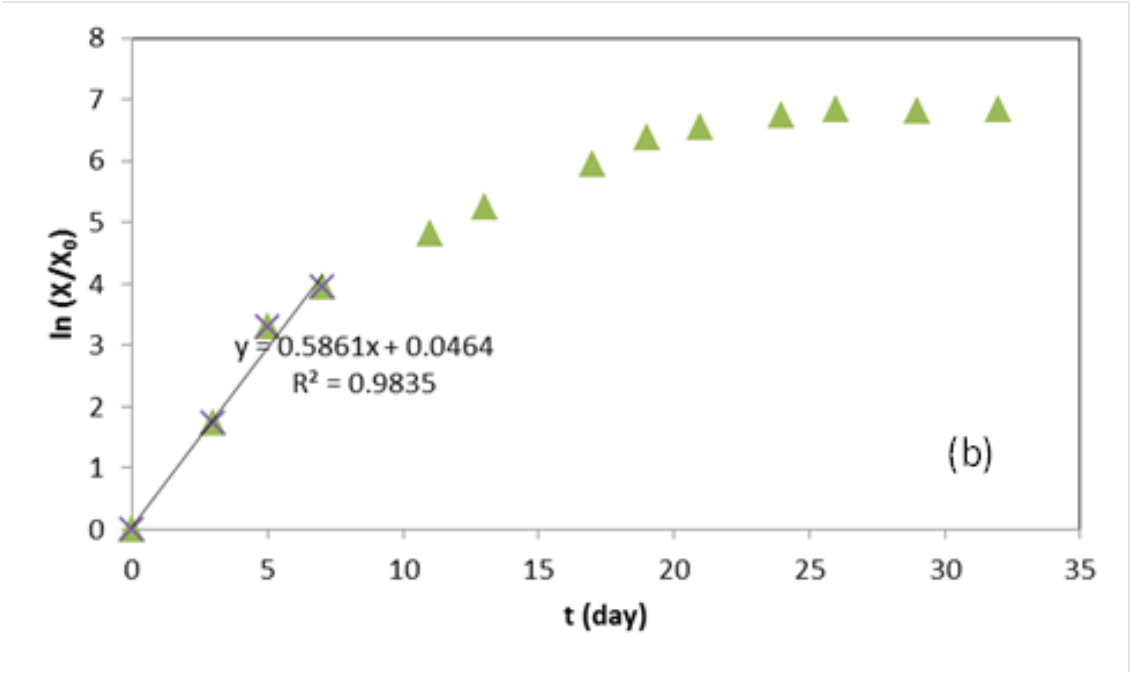

Figure 11: Growth curve (a) and semi-log growth curve (b) of SP47.

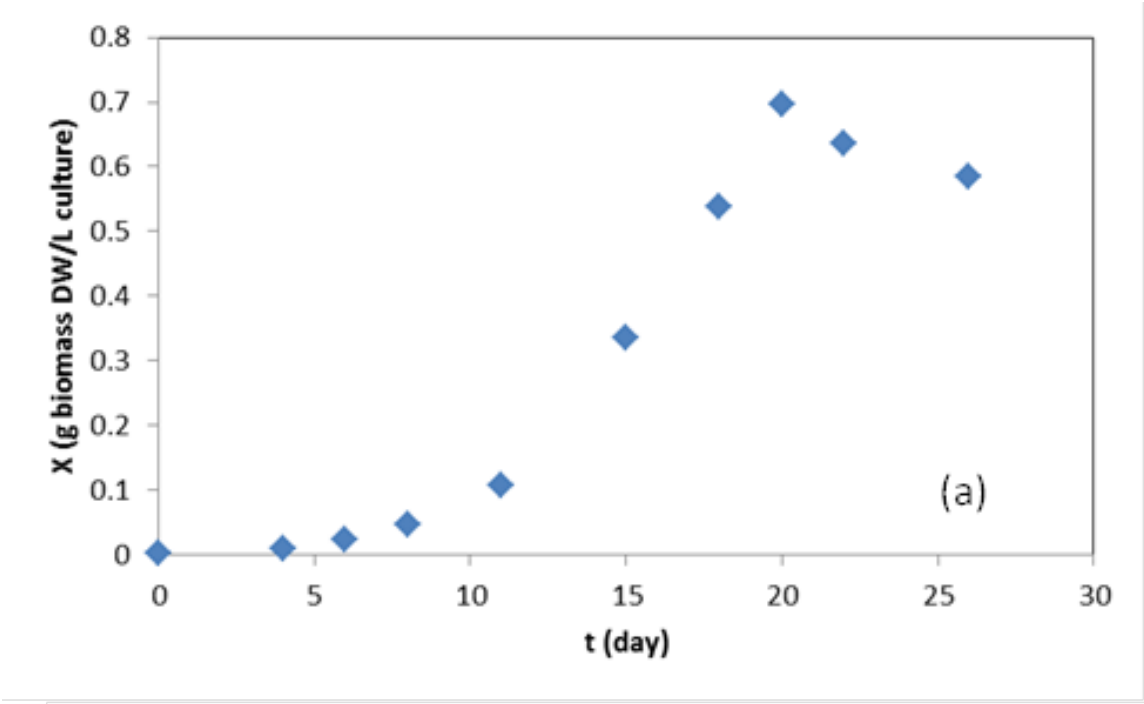

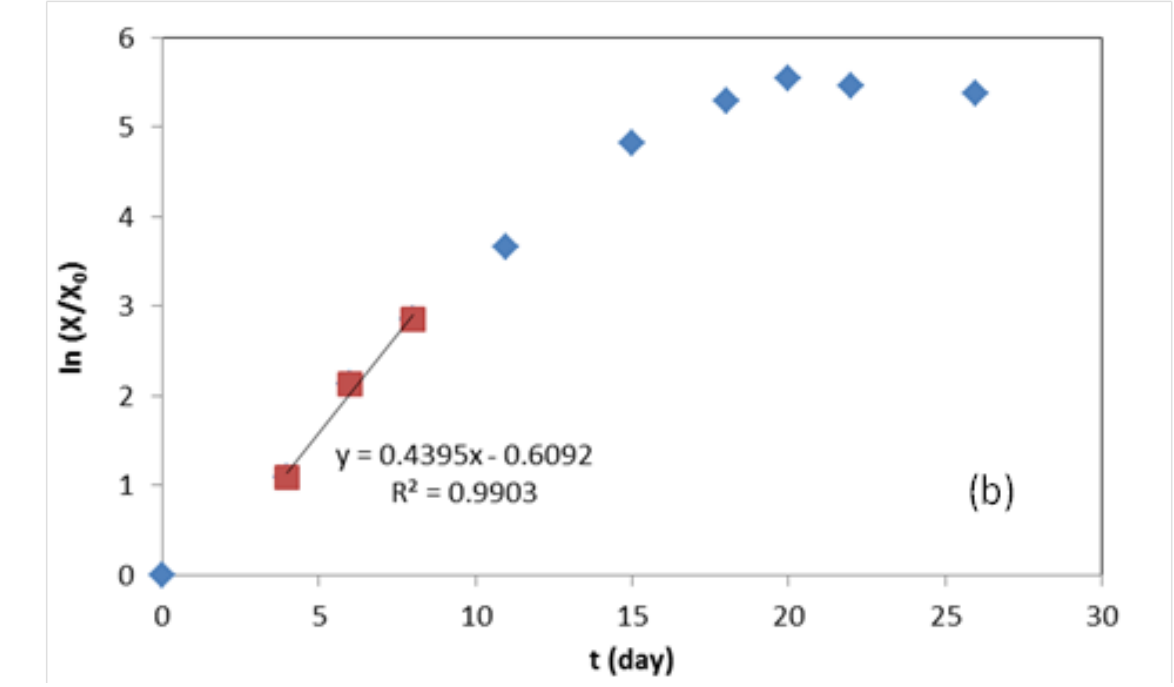

Figure 12: Growth curve (a) and semi-log growth curve (b) of SP48.

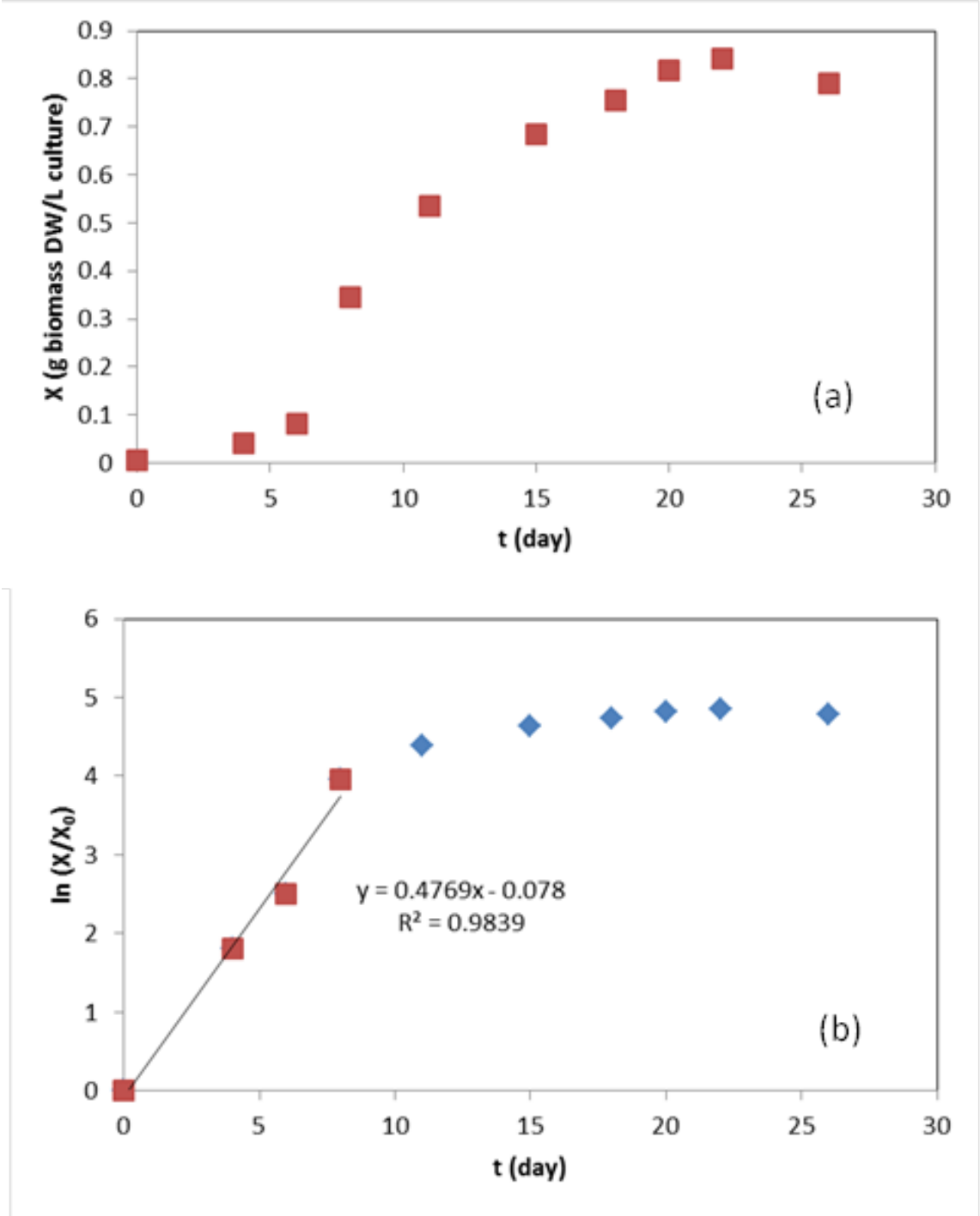

Figure 13: Growth curve (a) and semi-log growth curve (b) of SP50.

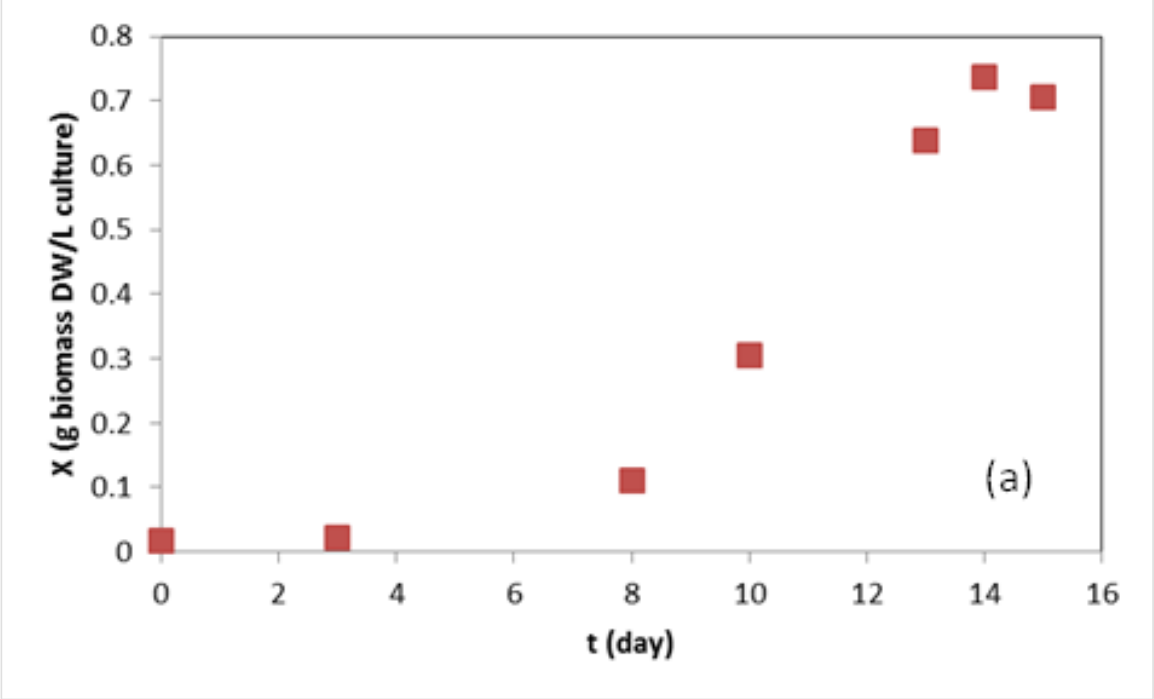

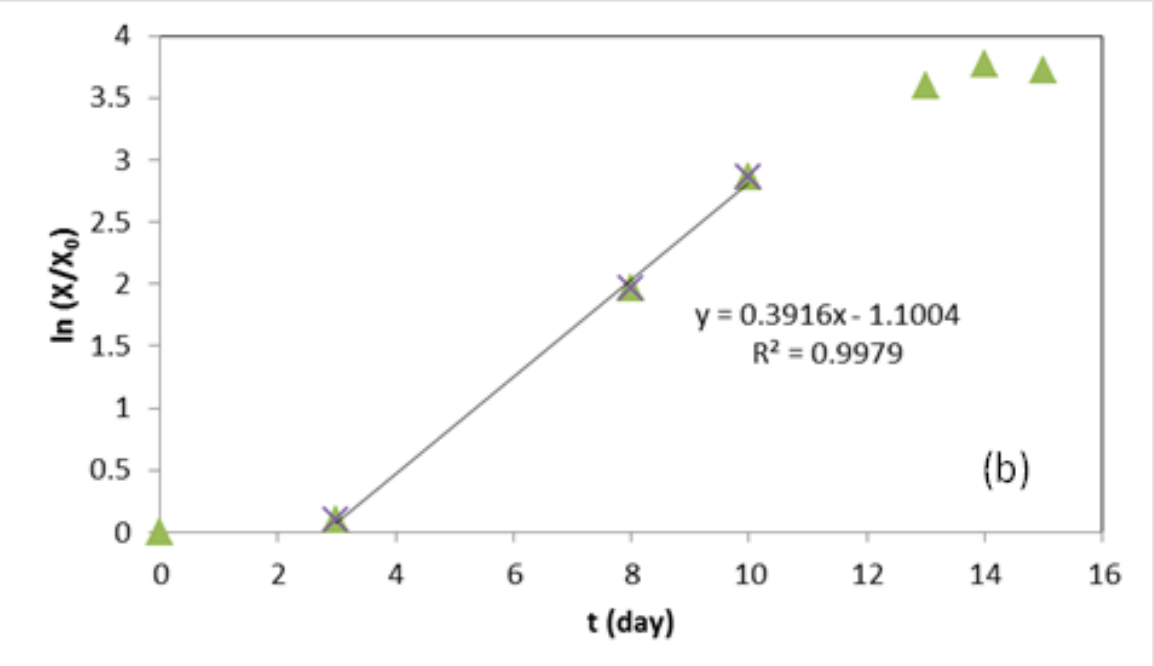

Figure 14: Semi-log growth curve and pH curve of SP20.

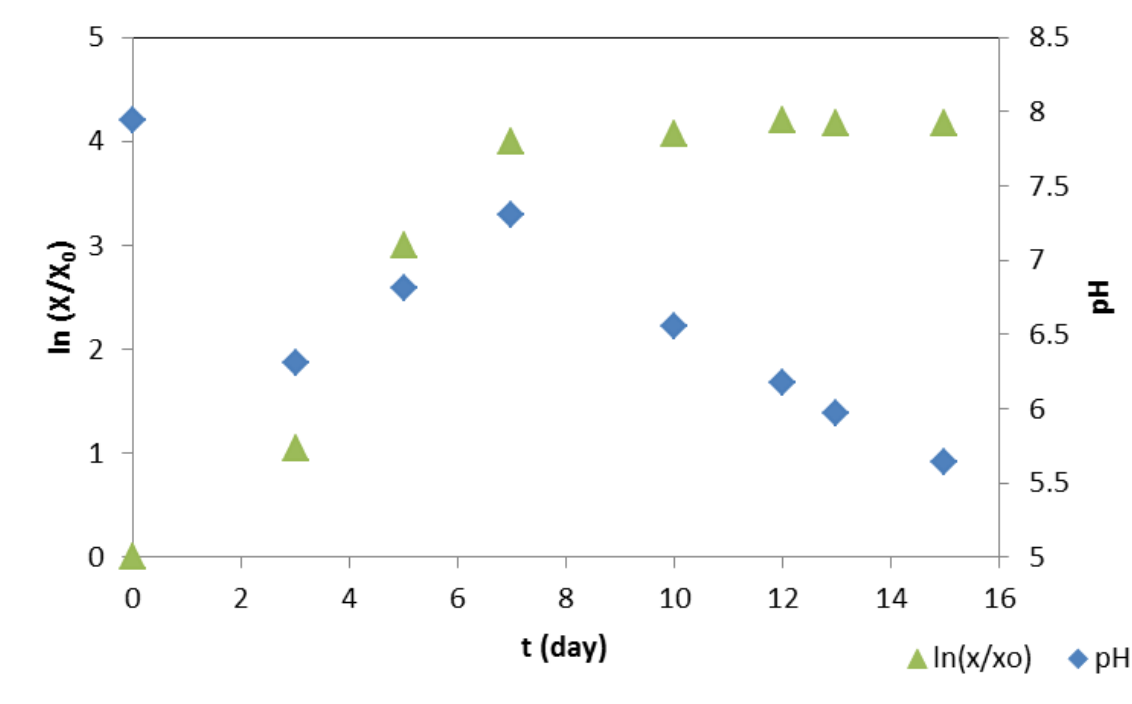

Figure 15: Semi-log growth curve and pH curve of SP22.

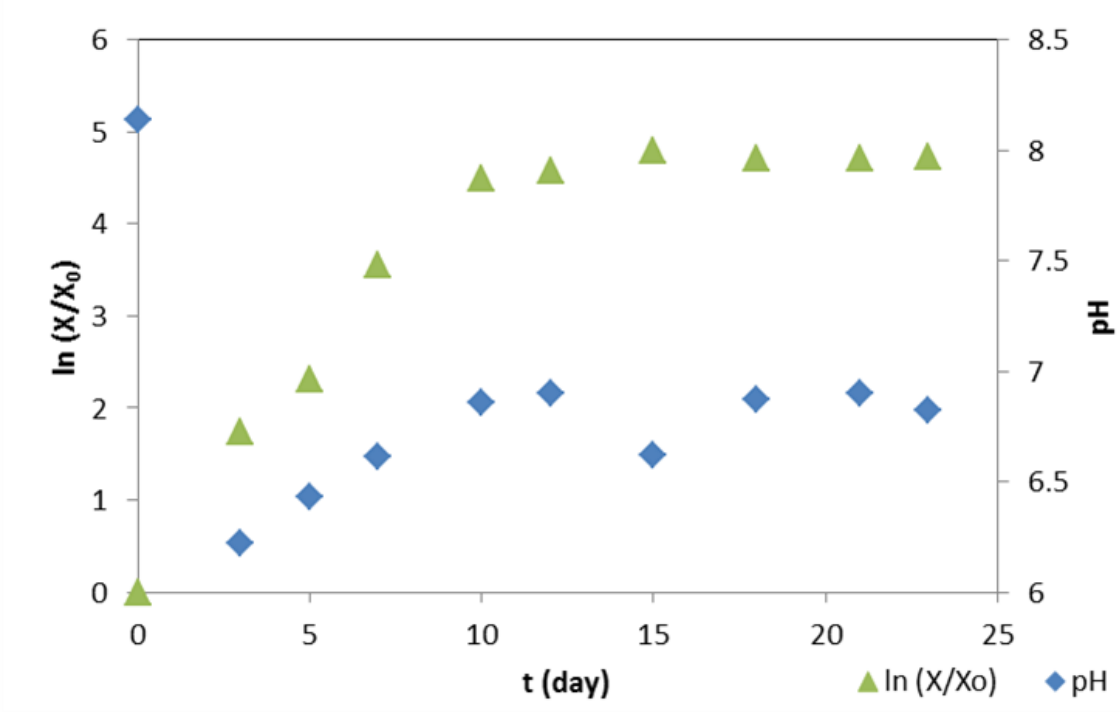

Figure 16: Semi-log growth curve and pH curve of SP38.

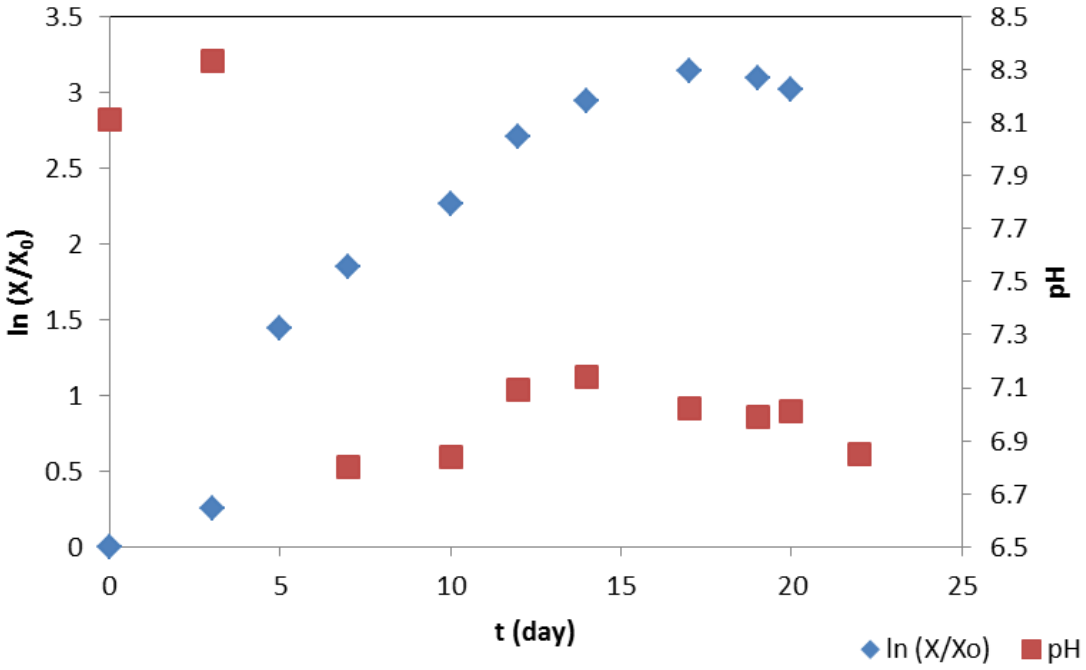

Figure 17: Semi-log growth curve and pH curve of SP46.

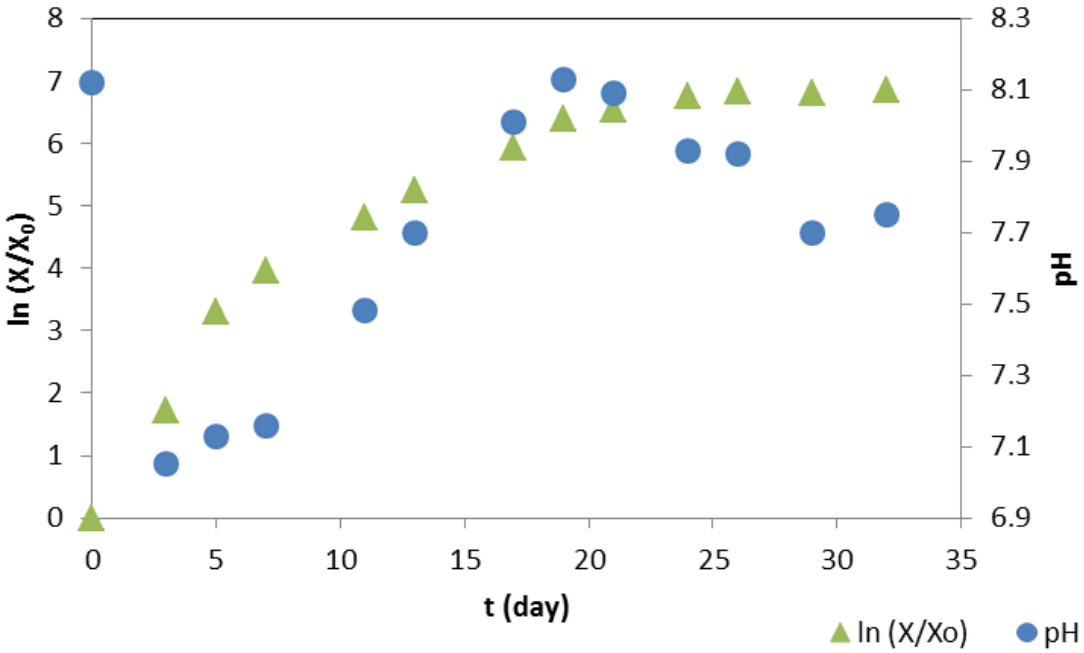

Figure 18: Semi-log growth curve and pH curve of SP47.

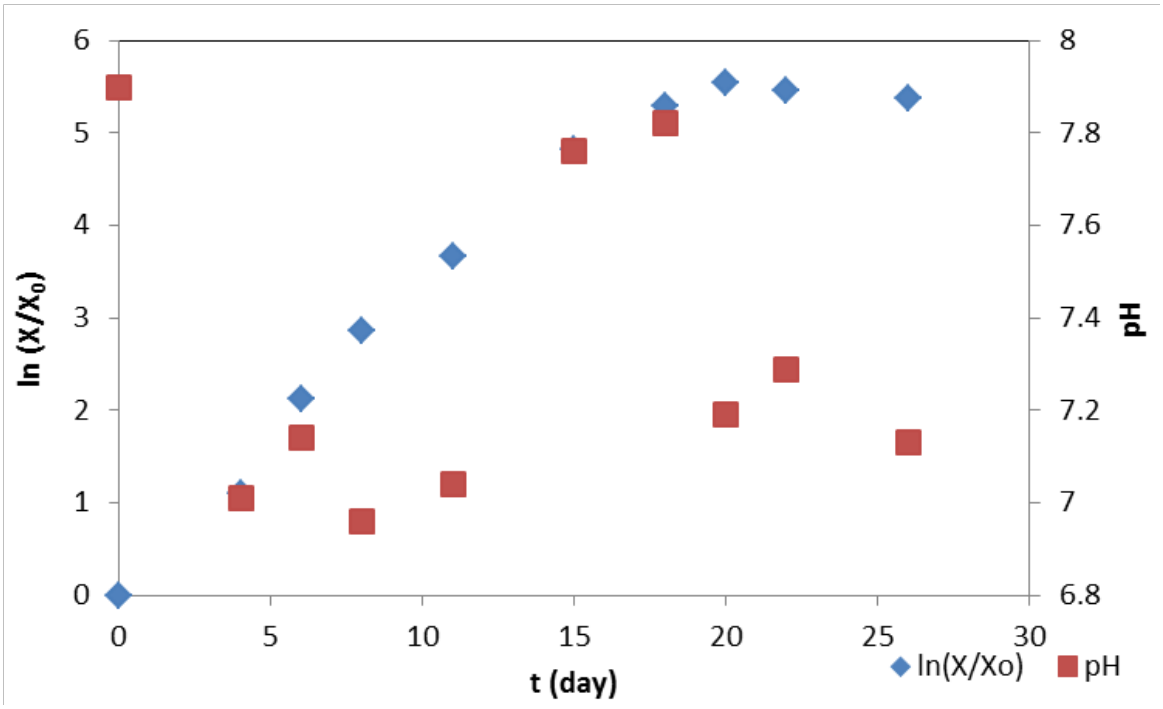

Figure 19: Semi-log growth curve and pH curve of SP48.

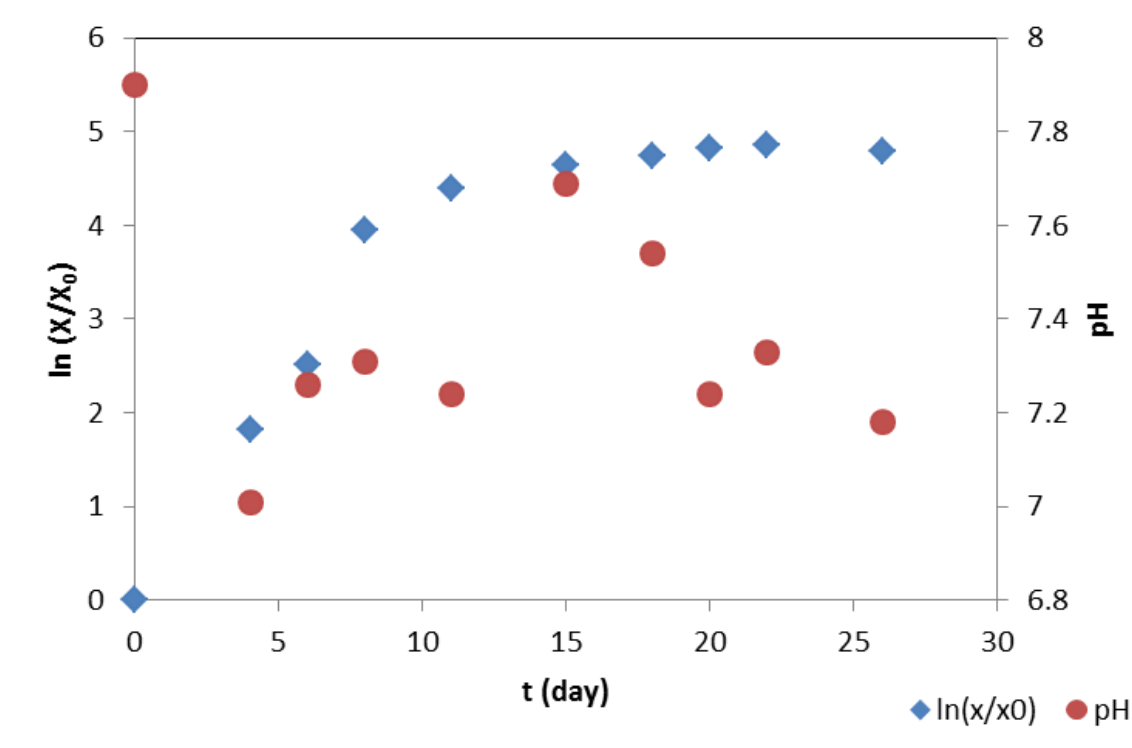

Figure 20: Semi-log growth curve and pH curve of SP50.

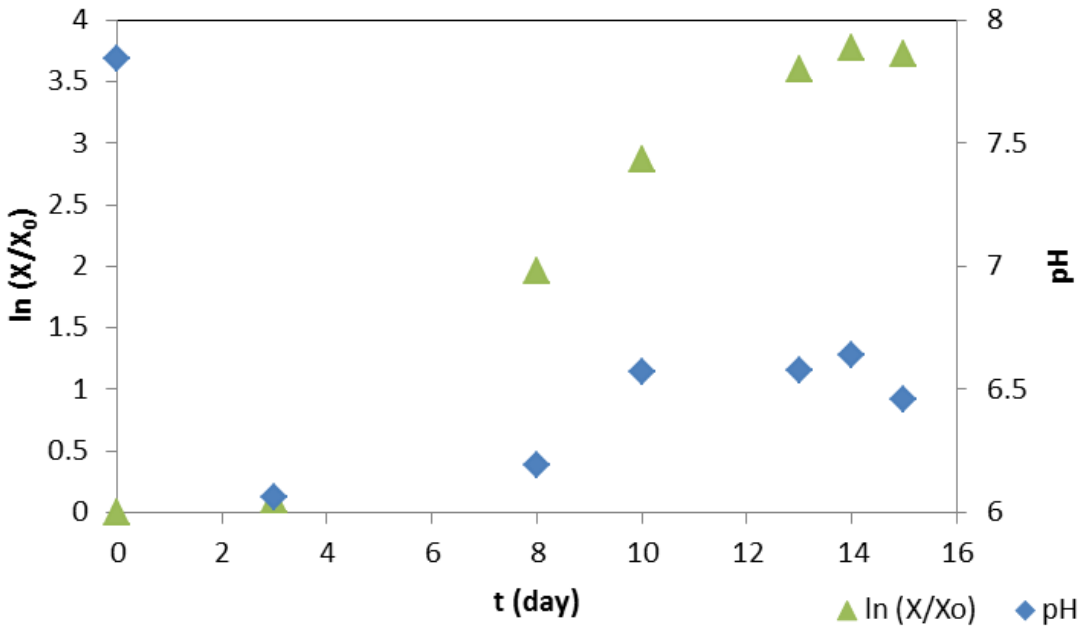

Figure 21: TG curves of SP20 biomass at three heating rates (20, 40, and 80 ^{o}C/min).

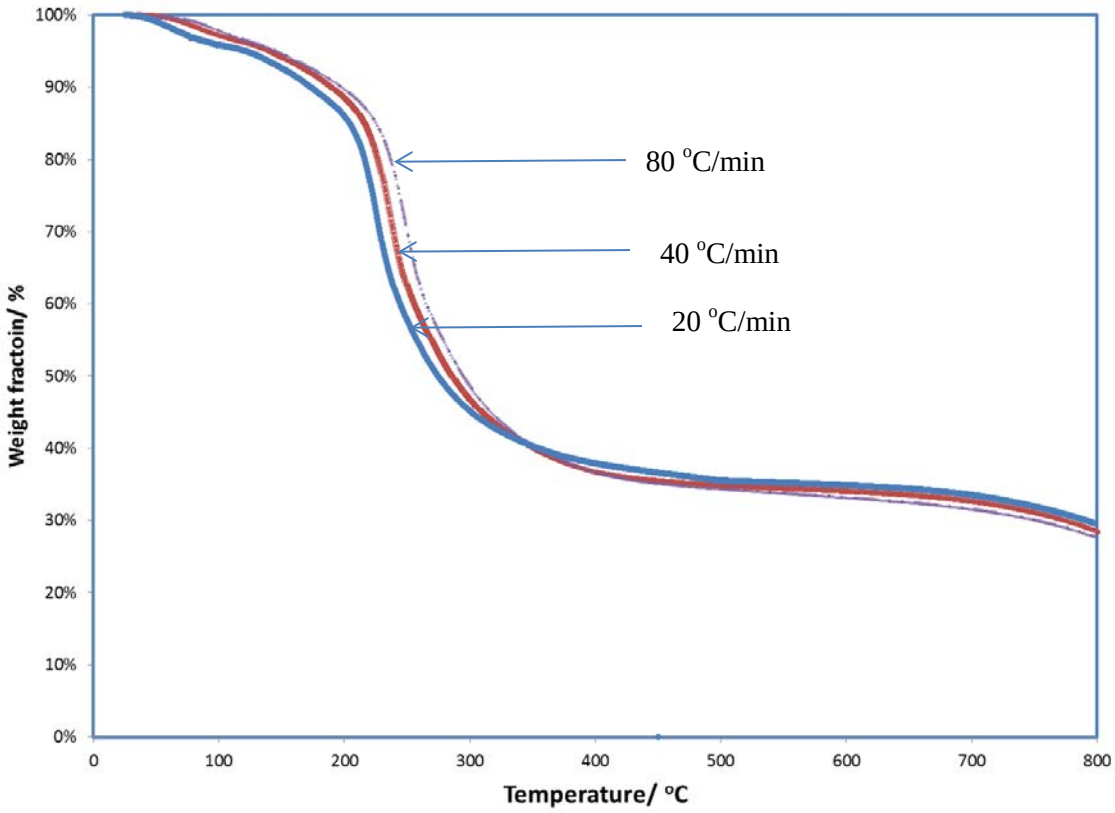

Figure 22: TG curves of SP22 biomass at three heating rates (20, 40, and 80 ^{o}C/min) .

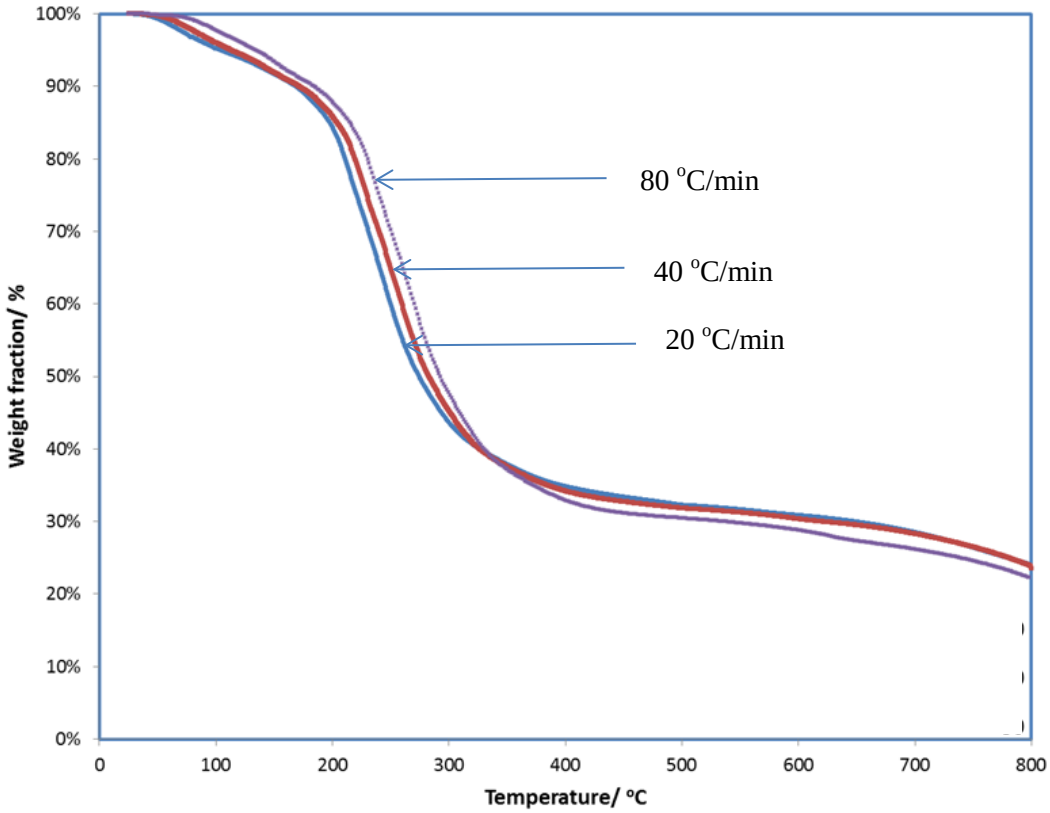

Figure 23: TG curves of SP38 biomass at three heating rates (20, 40, and 80 ^{o}C/min) .

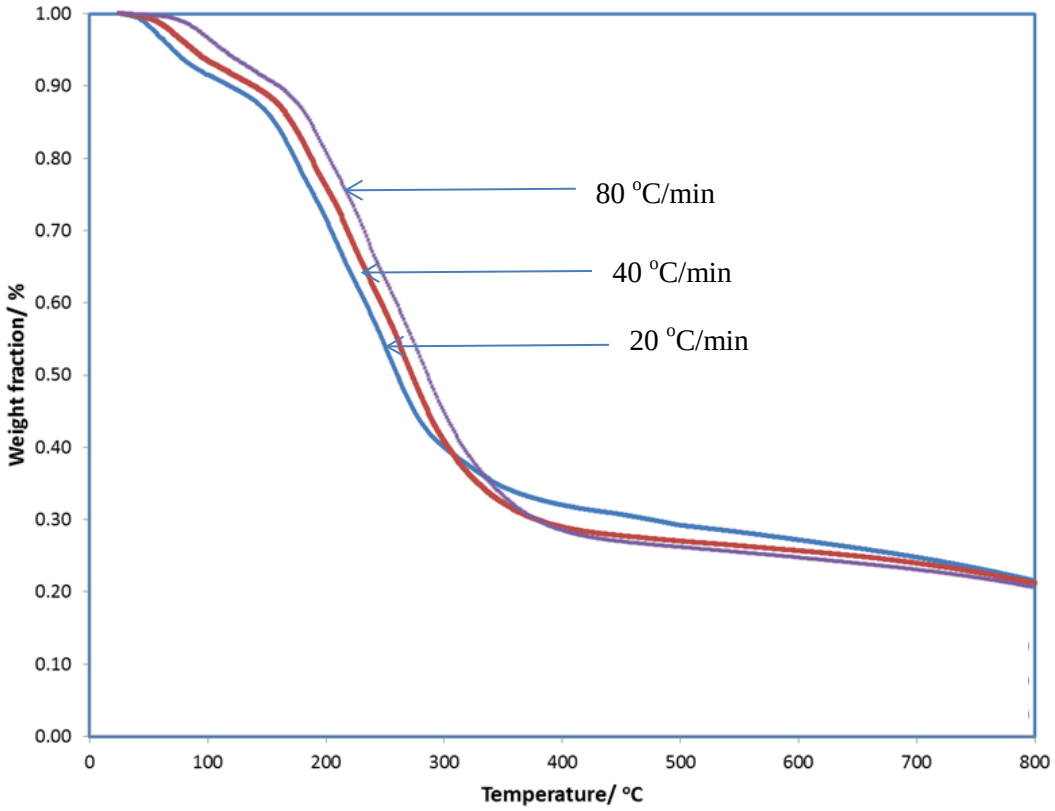

Figure 24: TG curves of SP46 biomass at three heating rates (20, 40, and 80 ^{o}C/min) .

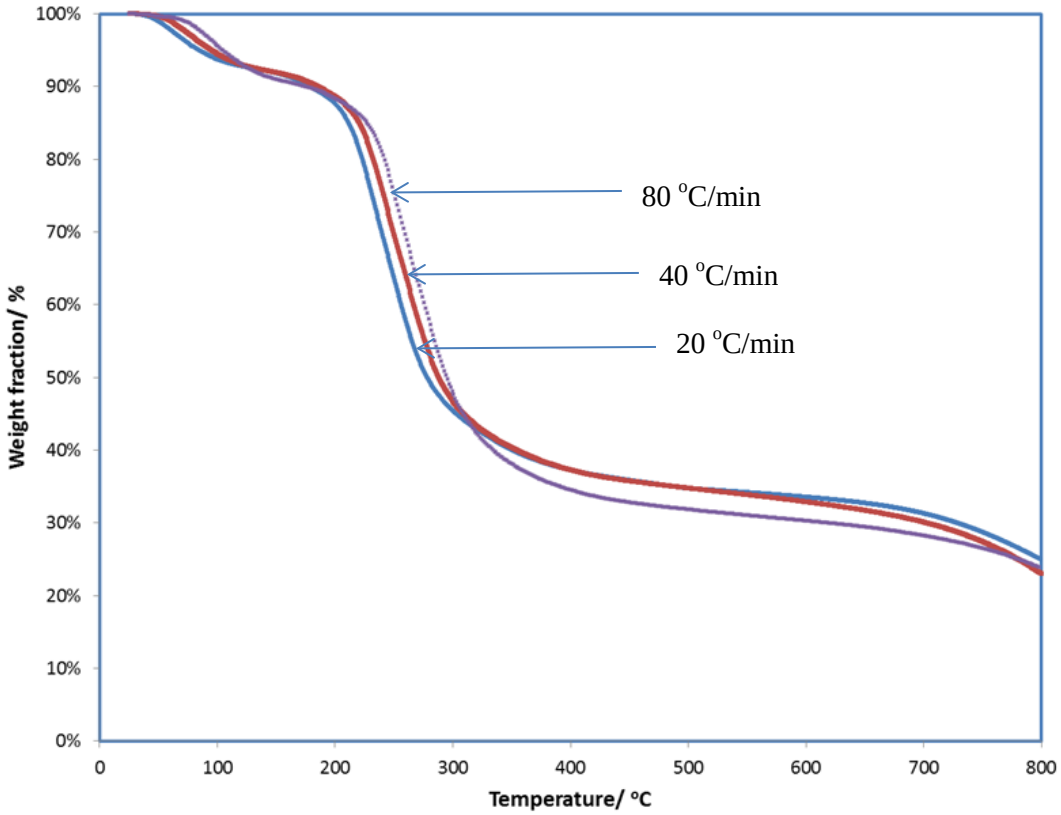

Figure 25: TG curves of SP47 biomass at three heating rates (20, 40, and 80 ^{o}C/min) .

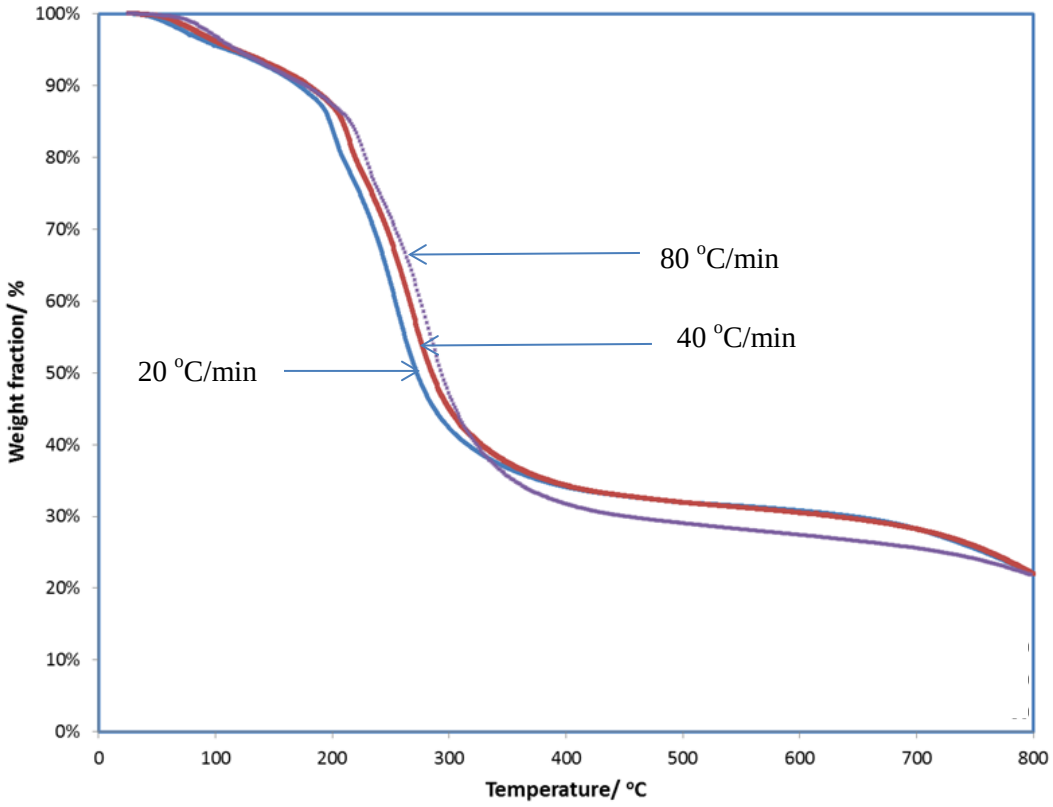

Figure 26: TG curves of SP48 biomass at three heating rates (20, 40, and 80 ^{o}C/min) .

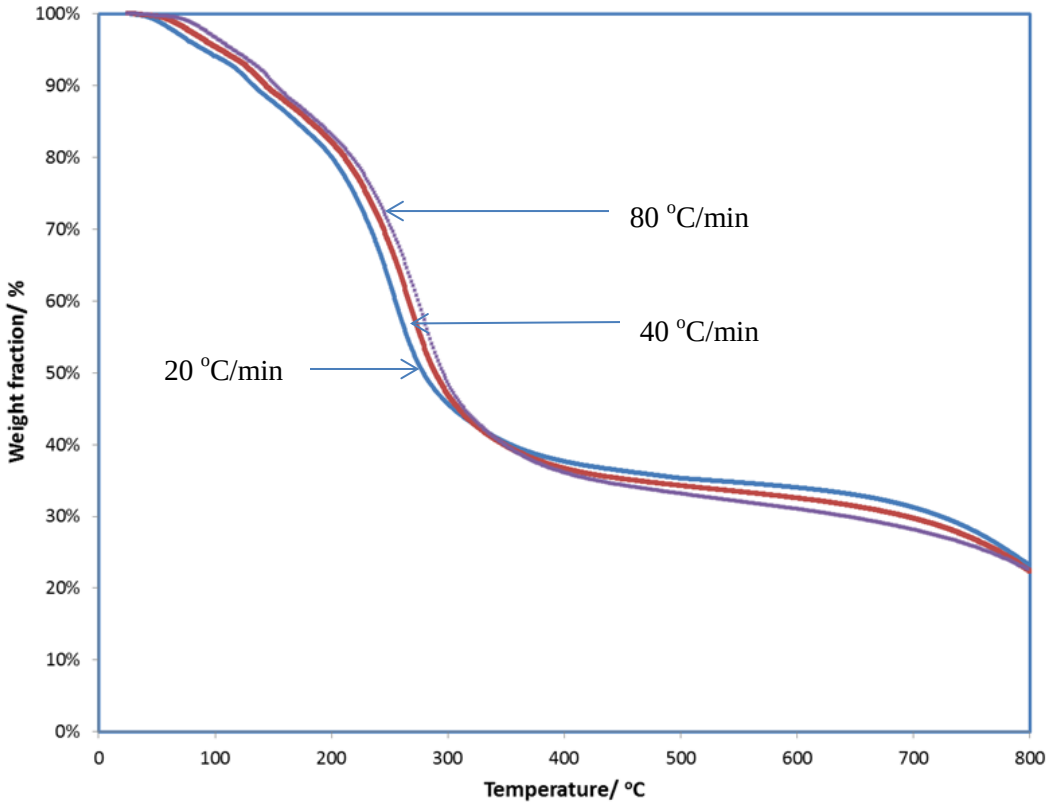

Figure 27: TG curves of SP50 biomass at three heating rates (20, 40, and 80 ^{o}C/min).

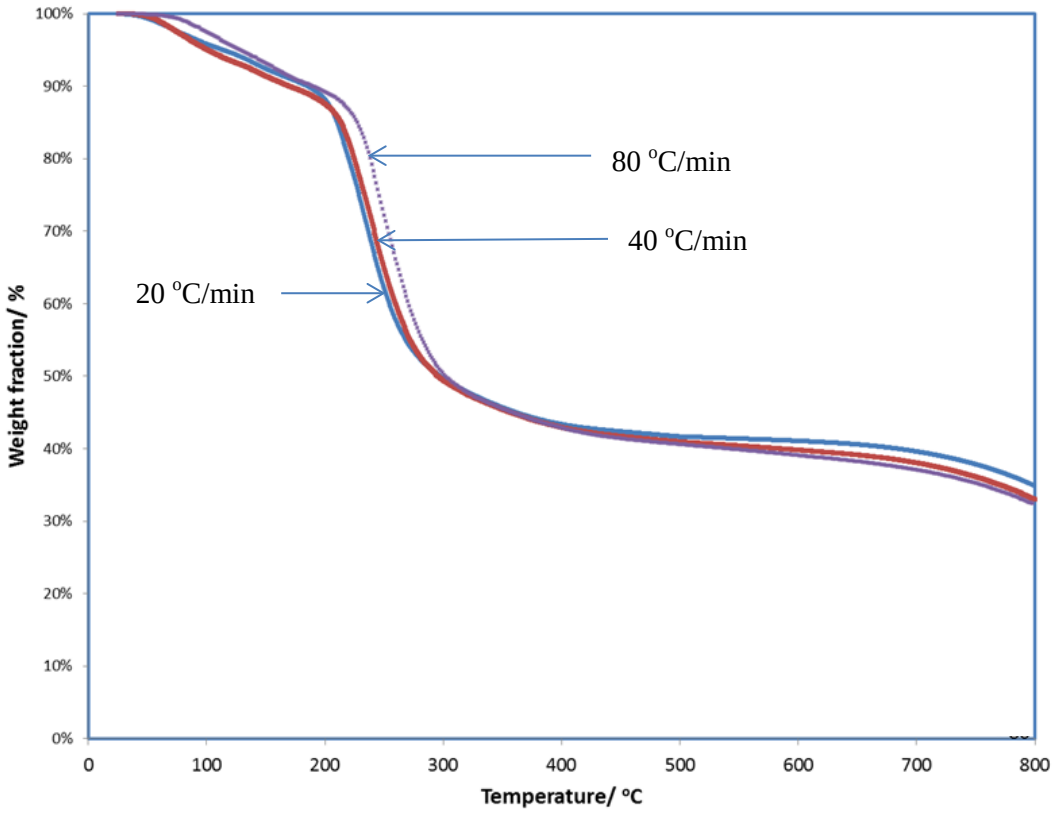

Figure 28: DTG curves of SP20 biomass at three heating rates (20, 40, and 80 ^{o}C/min).

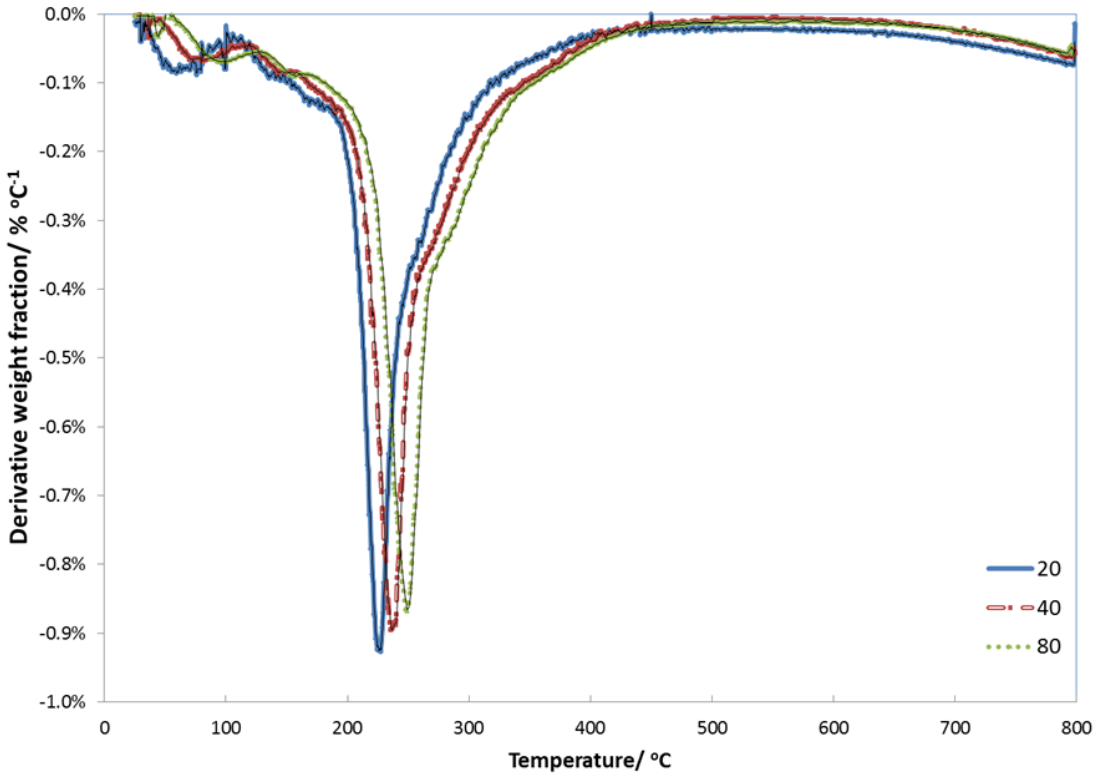

Figure 29: DTG curves of SP22 biomass at three heating rates (20, 40, and 80 ^{o}C/min).

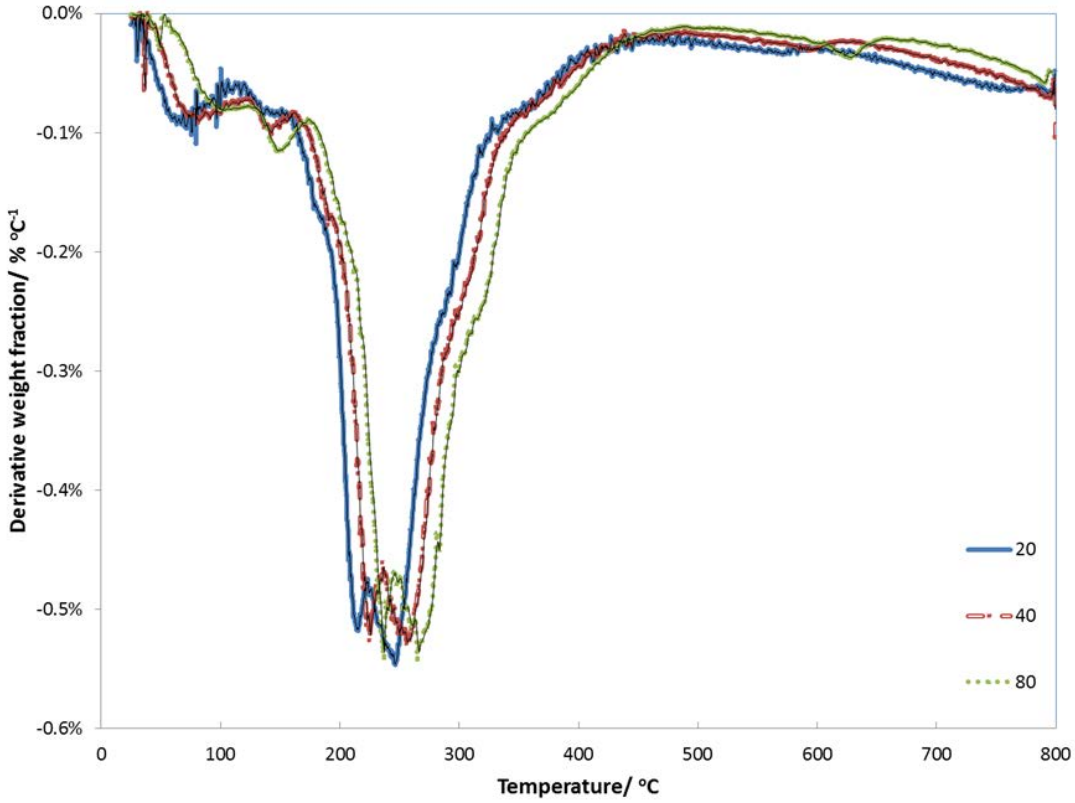

Figure 30: DTG curves of SP38 biomass at three heating rates (20, 40, and 80 ^{o}C/min).

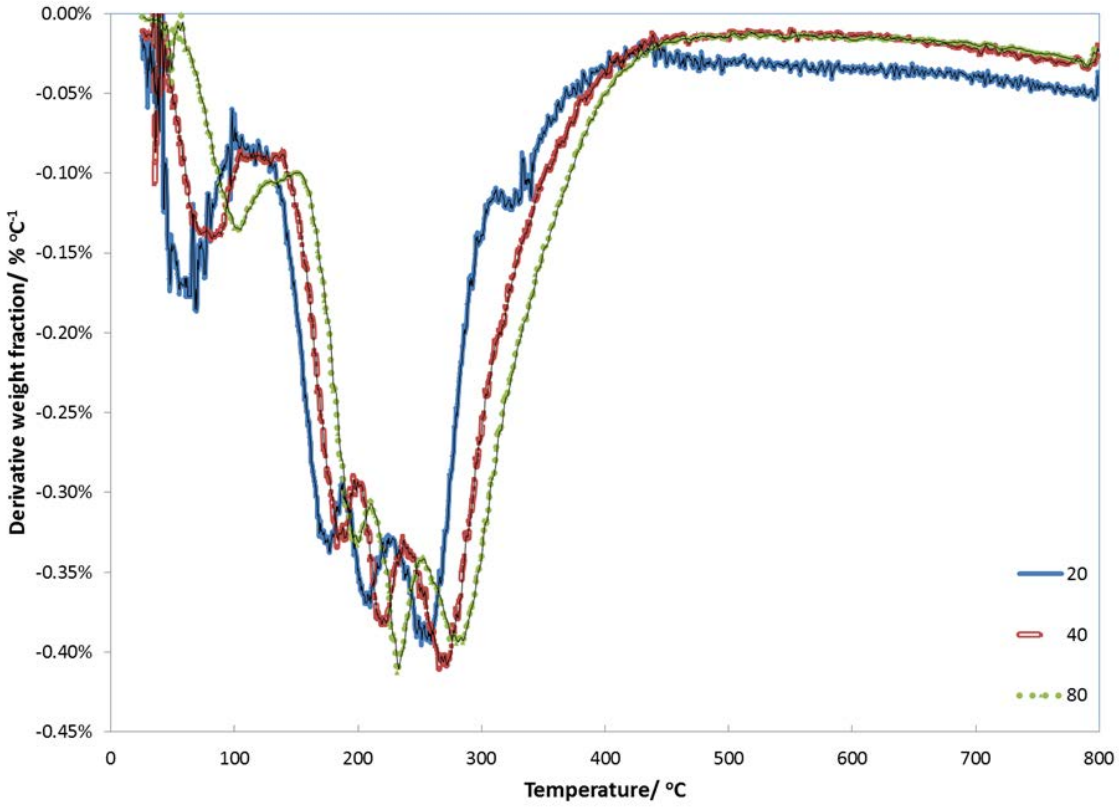

Figure 31: DTG curves of SP46 biomass at three heating rates (20, 40, and 80 ^{o}C/min).

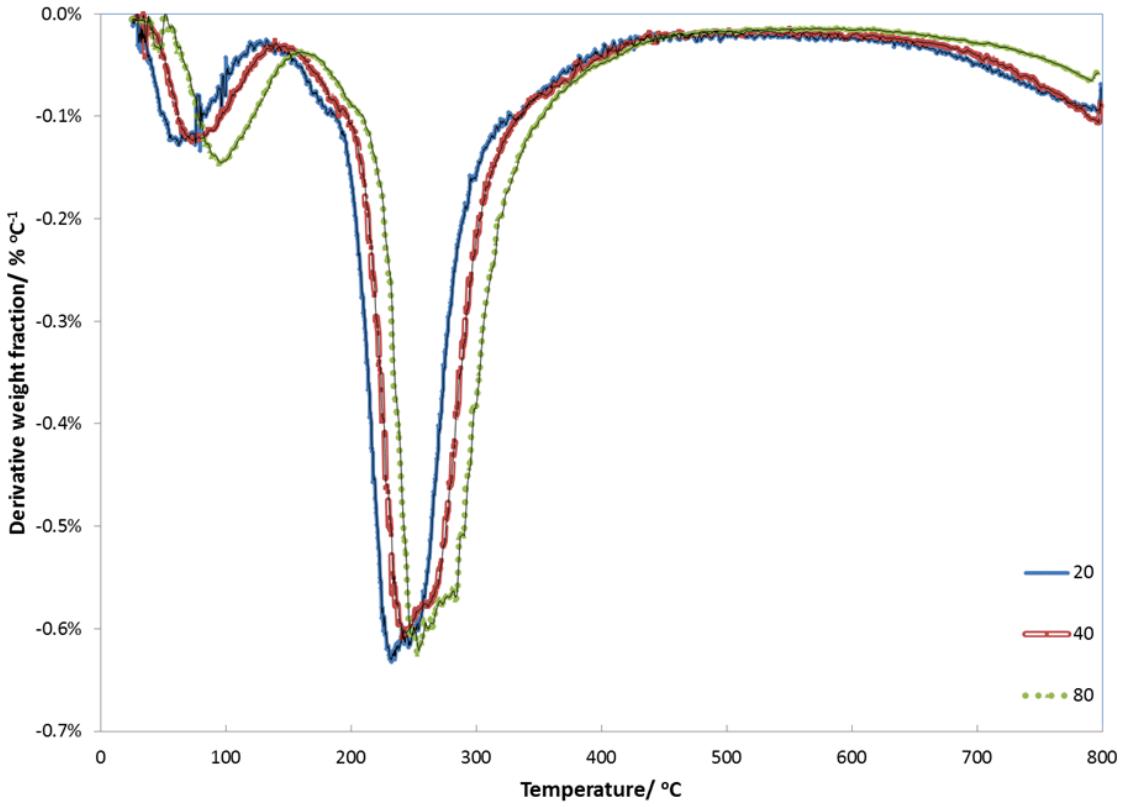

Figure 32: DTG curves of SP47 biomass at three heating rates (20, 40, and 80 ^{o}C/min).

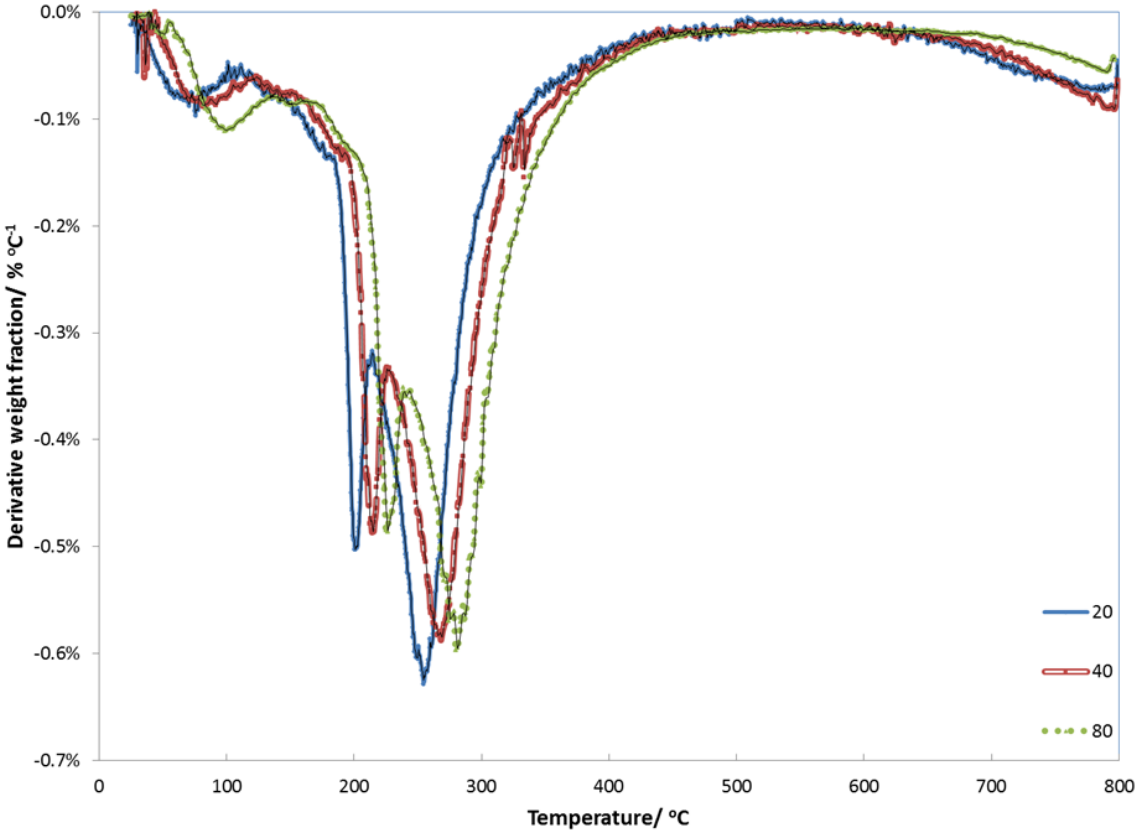

Figure 33: DTG curves of SP48 biomass at three heating rates (20, 40, and 80 ^{o}C/min).

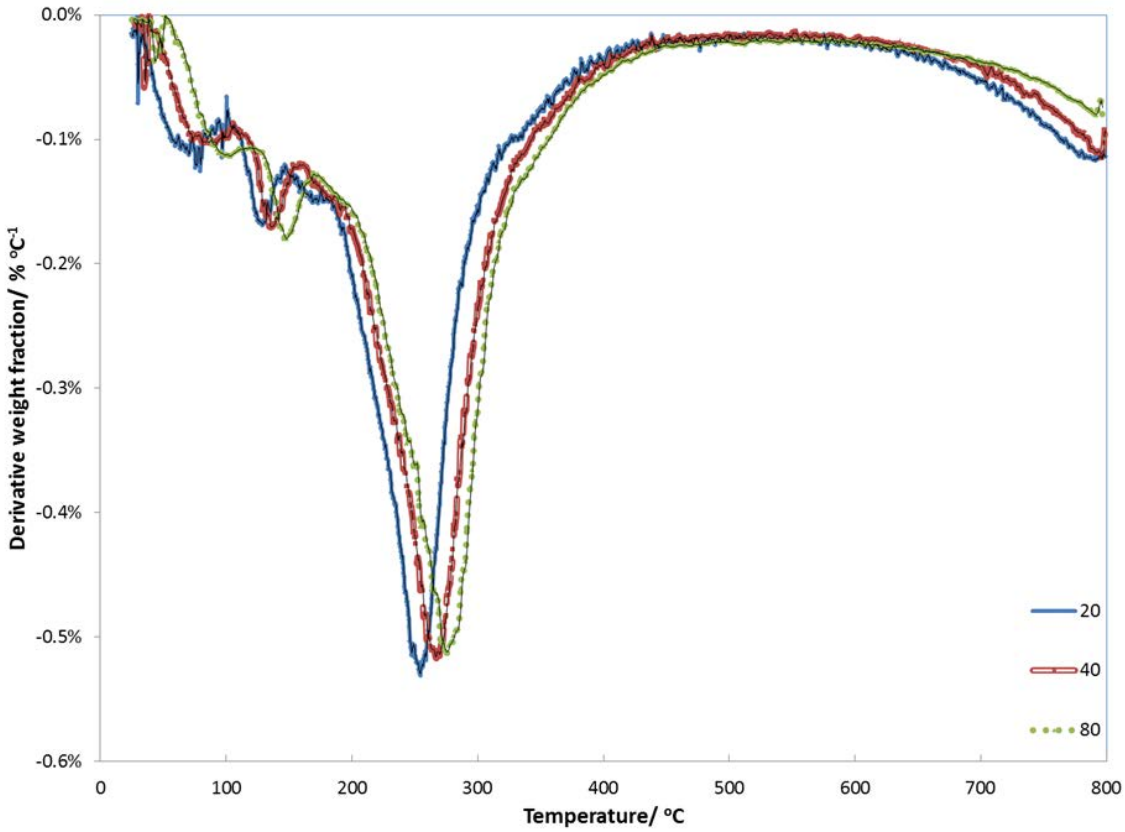

Figure 34: DTG curves of SP50 biomass at three heating rates (20, 40, and 80 ^{o}C/min).

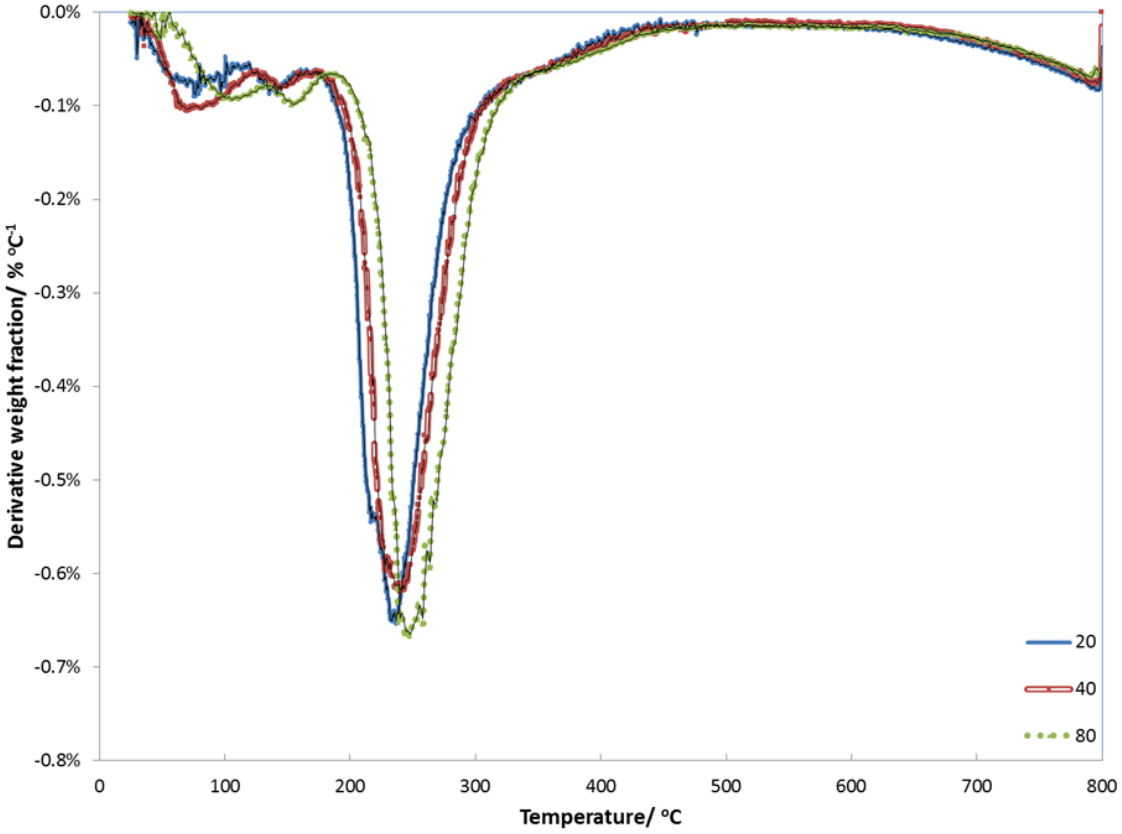

Figure 35: Plot of $\ln(\beta/T^2)$ versus 1/T at three heating rates for SP20 biomass.

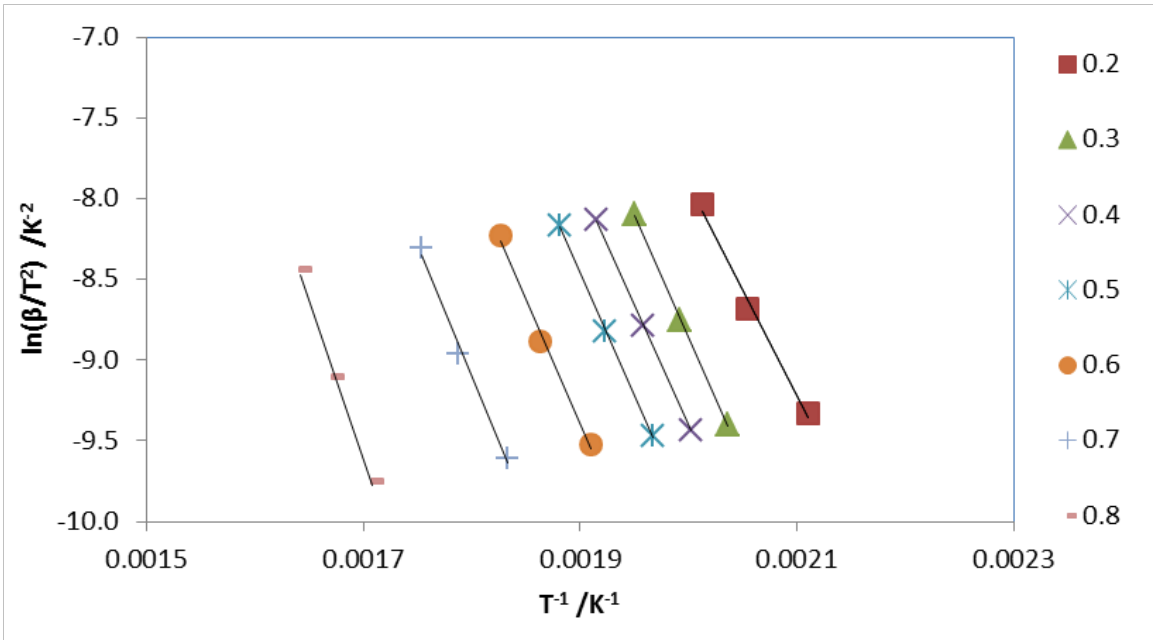

Figure 36: Plot of $\ln(\beta/T^2)$ versus 1/T at three heating rates for SP22 biomass.

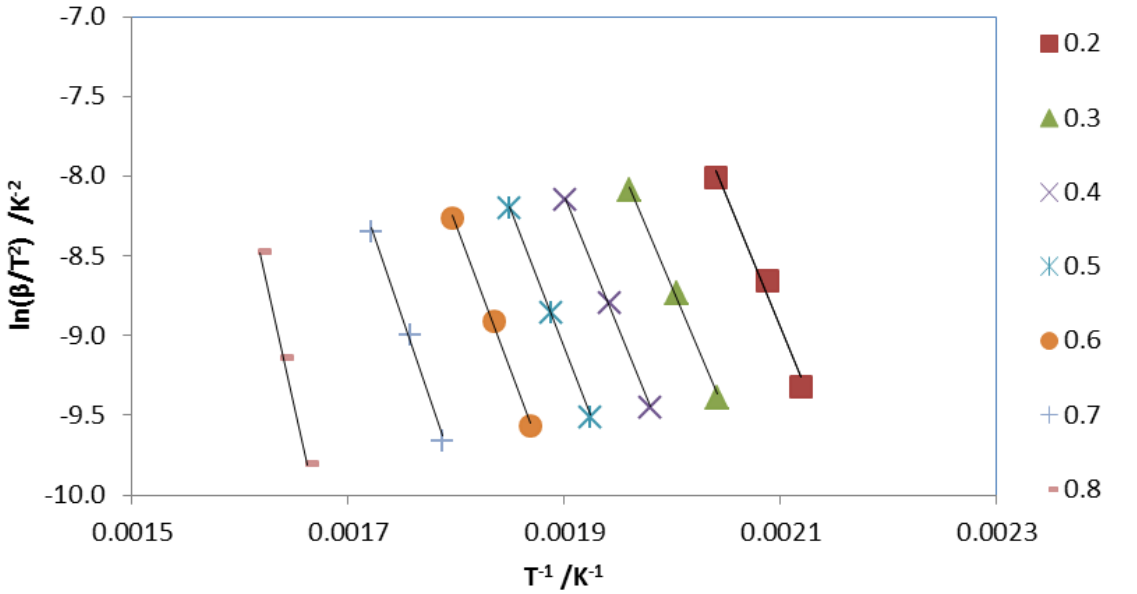

Figure 37: Plot of $\ln(\beta/T^2)$ versus 1/T at three heating rates for SP38 biomass.

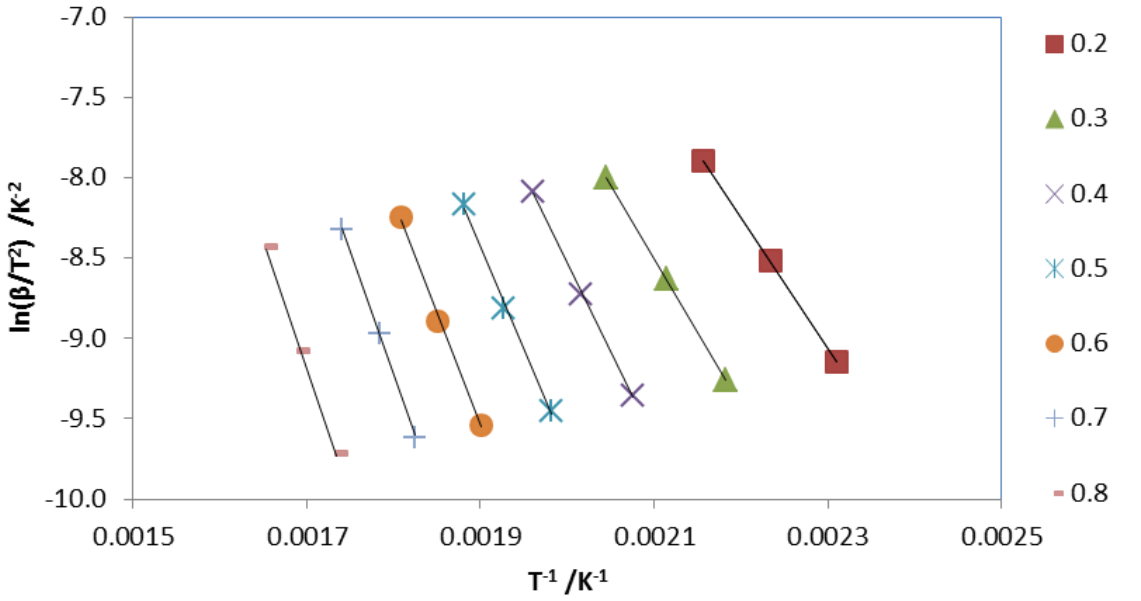

Figure 38: Plot of $\ln(\beta/T^2)$ versus 1/T at three heating rates for SP46 biomass.

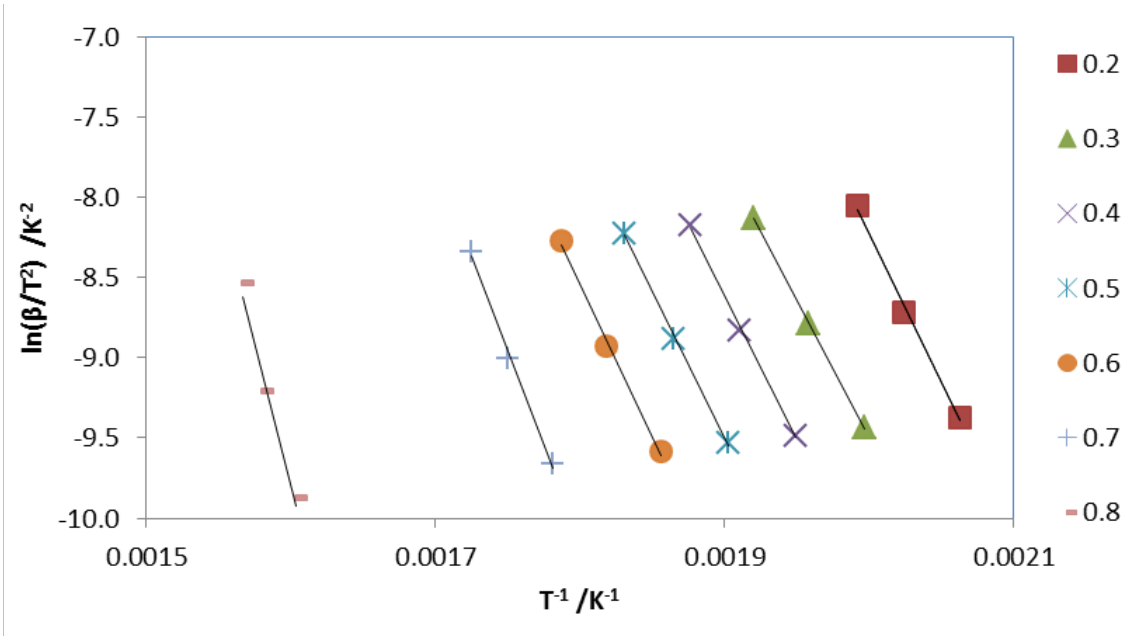

Figure 39: Plot of $\ln(\beta/T^2)$ versus 1/T at three heating rates for SP47 biomass.

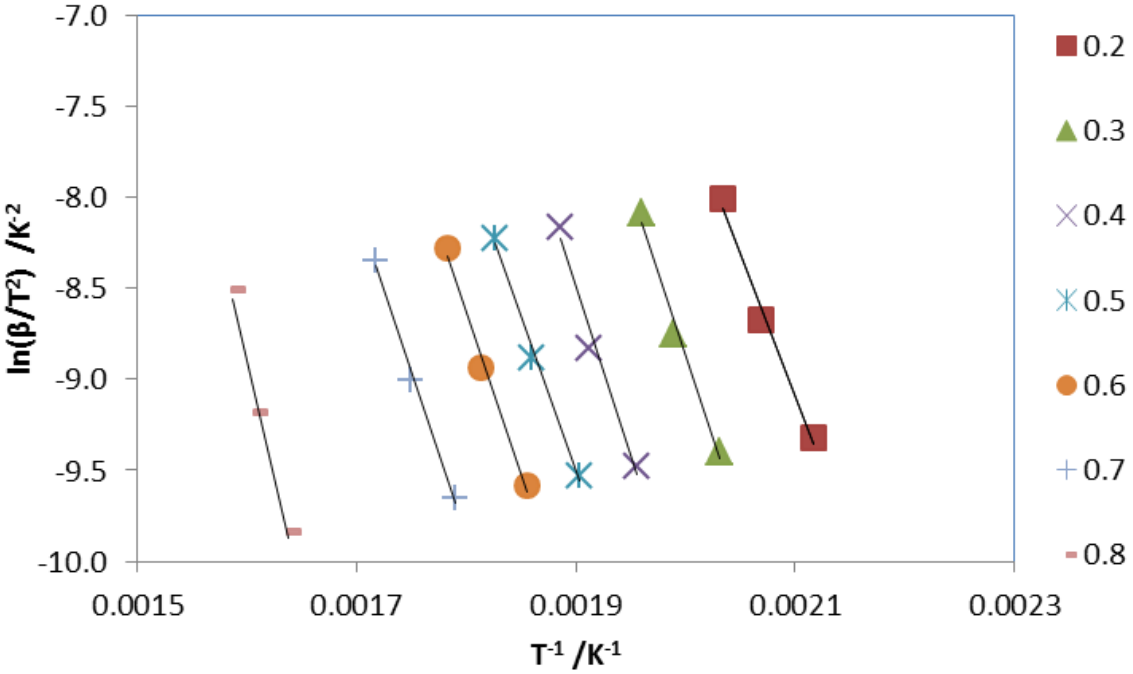

Figure 40: Plot of $\ln(\beta/T^2)$ versus 1/T at three heating rates for SP48 biomass.

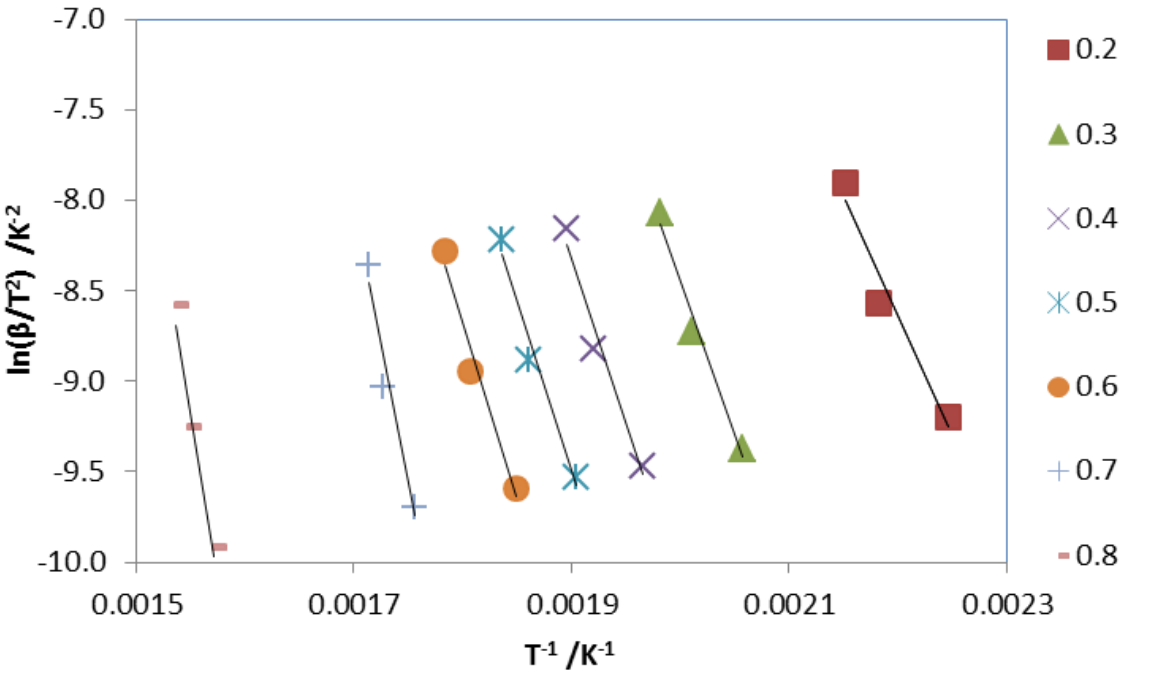

Figure 41: Plot of $\ln(\beta/T^2)$ versus 1/T at three heating rates for SP50 biomass.

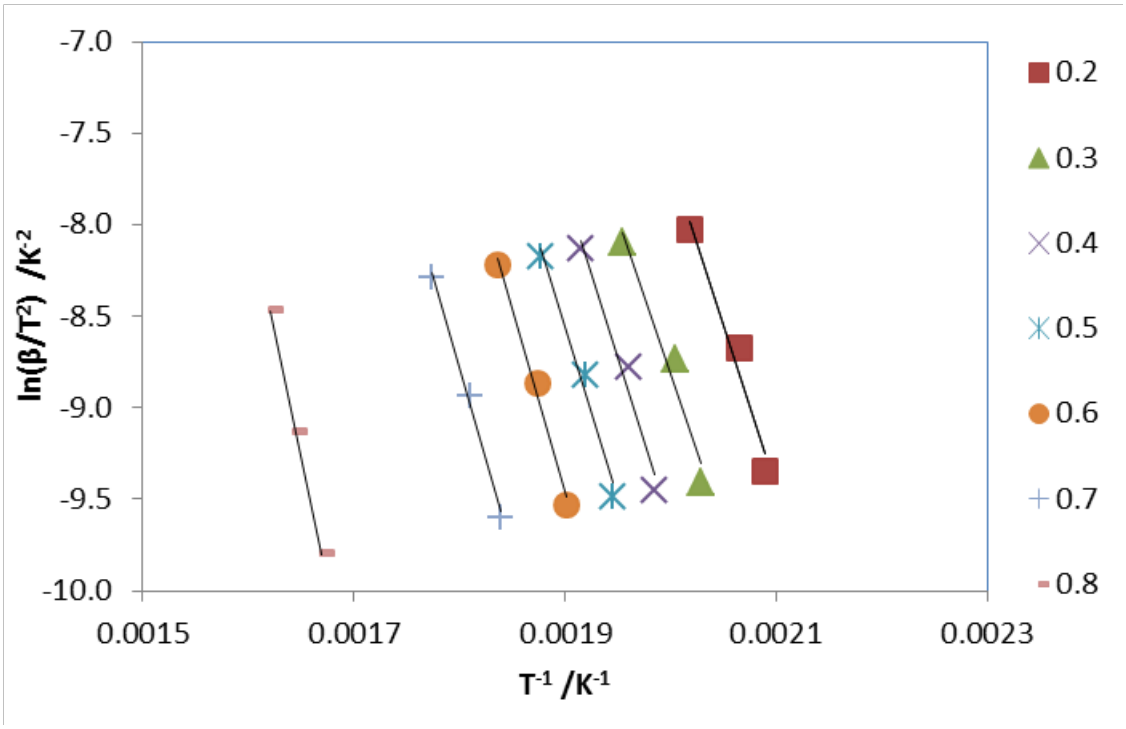

Figure 42: Temperature profiles of the pyrolysis experiments with three final temperatures, 450, 600, and 750 ^{o}C.

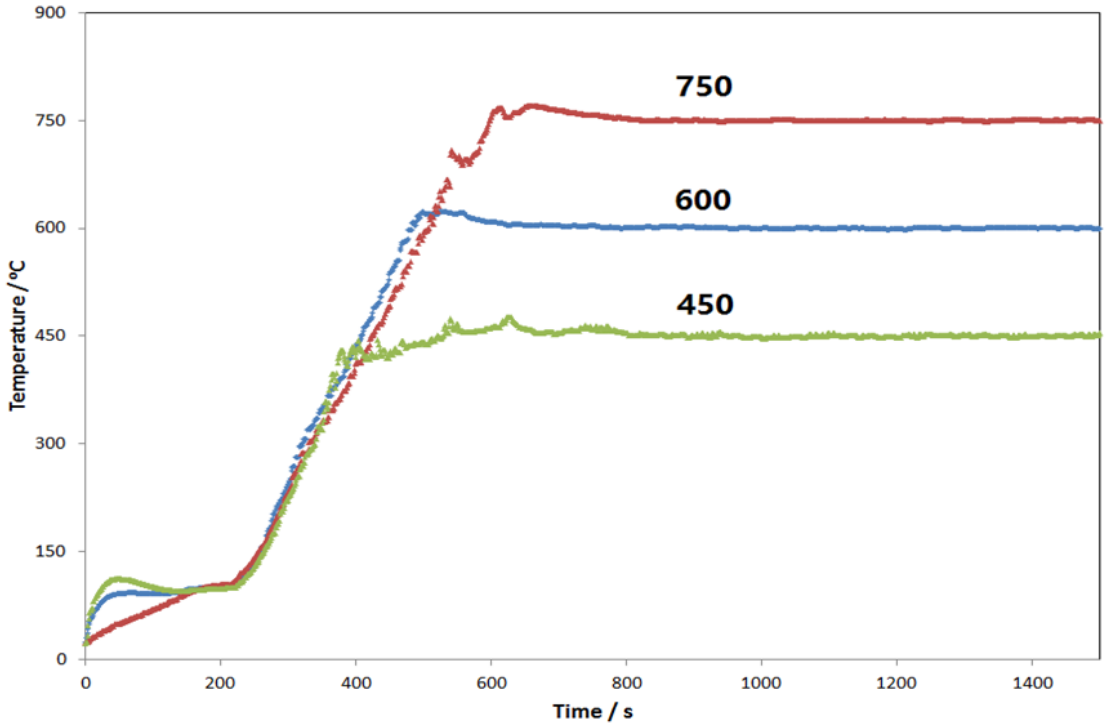

Figure 43: Product yields of microwave assisted pyrolysis under different temperatures.

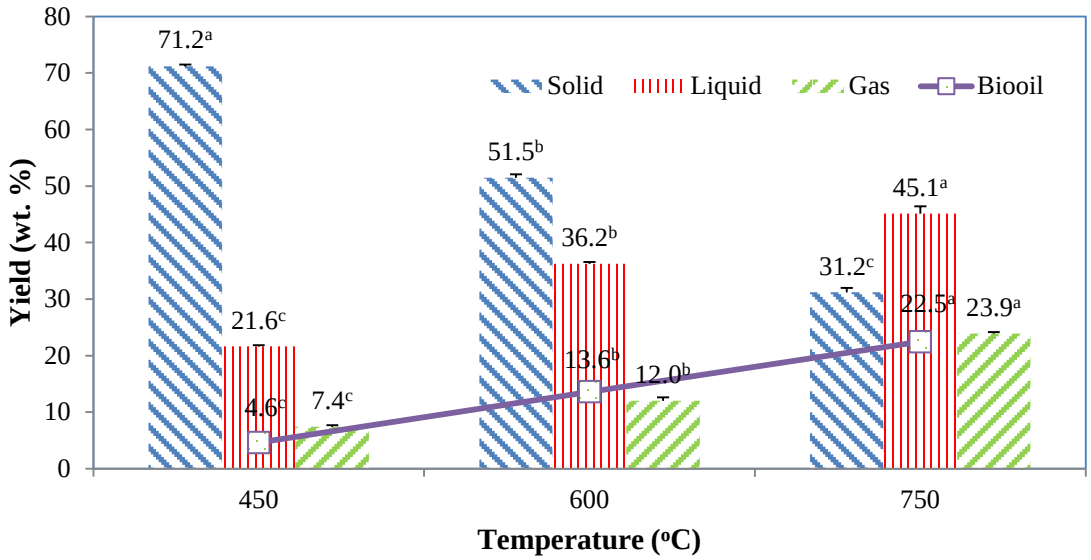

Error bars stand for standard deviations. Means with the same superscripts for each product are not significantly different (Tukey's HSD test, P>0.05).

Picture 1: Microscopic pictures of the seven algae species (SP20, SP22, SP38, SP46, SP47, SP48, SP50 shown in pictures 1 to7, respectively).

Picture 2: Bioreactors and the growth chamber.

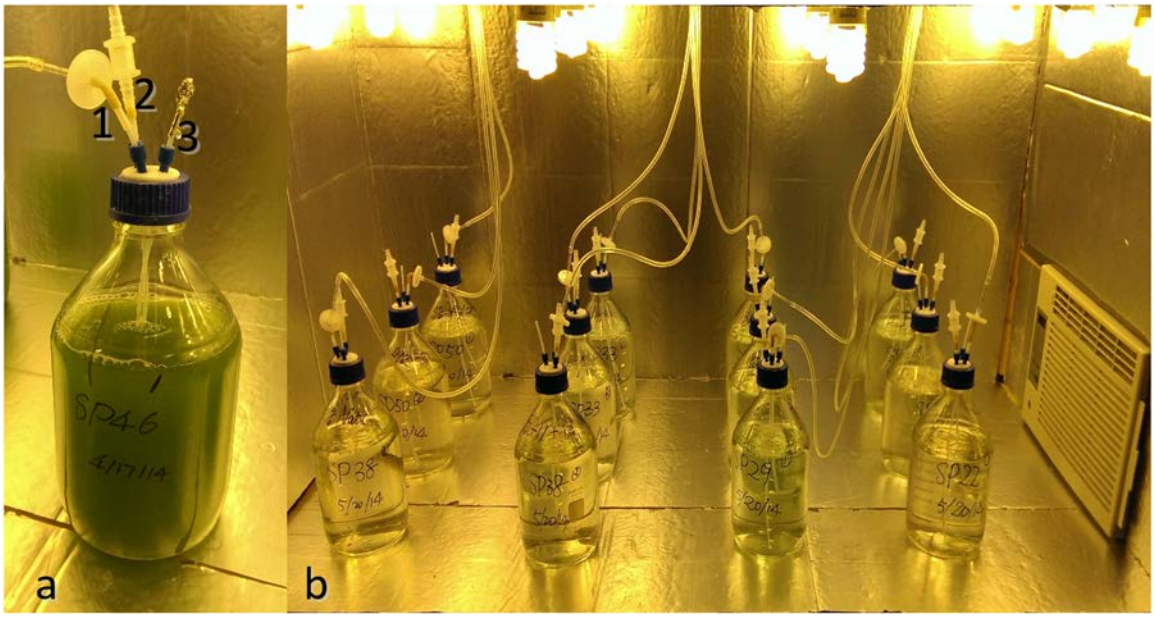

a: To minimize the risk of biological contamination, the bioreactor was designed to be an enclosed system with three opening on the cap: opening #1 for the inlet of the 0.2-µm filtered air flow, opening #2 for the outlet of air through a one-way valve, and opening #3 for taking samples. b: Bioreactors were organized in the growth chamber in an way that ensures equal amount of radiation is available for each culture.

Picture 3: Liquid products of microwave-assisted pyrolysis (bio-oil, i.e. the dark phase, and the aqueous product, i.e. the light-color phase)

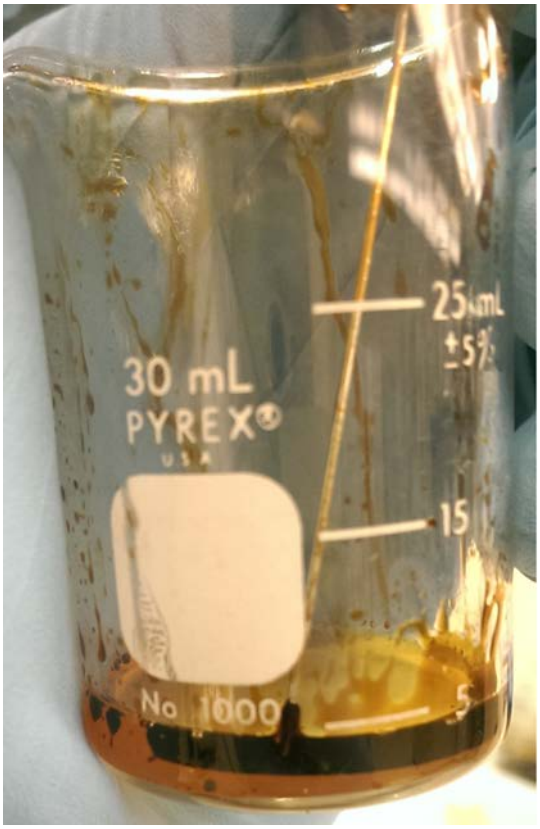

APPENDICES

CULTURE MEDIA RECIPE

A+ Medium

#	Component	Amount	Stock Solution Concentration	Final Concentration
1	NaCl	18 g/L		0.308 M
2	$MgSO_4 \cdot 7H_2O$	5 g/L		0.02 M
3	$Na_2EDTA \cdot 2H_2O$	10 mL/L	0.3 g/100 mL	0.08 mM
4	KCl	10 mL/L	6 g/100 mL	8.05 mM
5	$CaCl_2 \cdot 2H_2O$	10 mL/L	3.7 g/100 mL	2.52 mM
6	$NaNO_3$	10 mL/L	10 g/100 mL	11.8 mM
7	KH_2PO_4	10 mL/L	0.5 g/100 mL	0.37 mM
8	Trizma Base pH 8.2	10 mL/L	10 g/100 mL	8.26 mM
9	A+ Trace Components	10 mL/L		

BG11+ 1% NaCl Medium

#	Component	Amount	Stock Solution Concentration	Final Concentration
1	K2HPO4	10 mL/L	0.8 g/200 mL	0.22 mM
2	MgSO4·7H2O	10 mL/L	0.15 g/200 mL	0.03 mM
3	CaCl2·2H2O	10 mL/L	0.72 g/200 mL	0.24 mM
4	Citric Acid·H2O	10 mL/L	0.12 g/200 mL	0.012 mM
5	Ferric Ammonium Citrate	10 mL/L	0.12 g/200 mL	0.02 mM
6	Na2EDTA·2H2O	10 mL/L	0.02 g/200 mL	0.002 mM
7	Na2CO3	10 mL/L	0.4 g/200 mL	0.18 mM
8	BG-11 Trace Metals Solution	1 mL/L		
9	NaCl	10 g/L		0.17 M

F/2 Medium

#	Component	Amount	Stock Solution Concentration	Final Concentration
1	$NaNO_3$	1 mL	7.5 g/100 mL dH20	880 µM
2	$NaH_2PO_4 \cdot H_2O$	1 mL	0.5 g/100 mL dH20	36 µM
3	$Na_2SiO_3 \cdot 9H_2O$	1 mL	3 g/100 mL dH20	106 µM
4	Trace Metals Solution	1 mL/L		
5	Vitamin B12	1 mL/L		
6	Biotin Vitamin Solution	1 mL/L		
7	Thiamine Vitamin Solution	1 mL/L		
8	Seawater (non-sterized)	1 L		

5 % F/2 Medium

#	Component	Amount	Stock Solution Concentration	Final Concentration
1	$NaNO_3$	1 mL	7.5 g/100 mL dH20	880 µM
2	$NaH_2PO_4 \cdot H_2O$	1 mL	0.5 g/100 mL dH20	36 µM
3	$Na_2SiO_3 \cdot 9H_2O$	1 mL	3 g/100 mL dH20	106 µM
4	Trace Metals Solution	1 mL/L		
5	Vitamin B12	1 mL/L		
6	Biotin Vitamin Solution	1 mL/L		
7	Thiamine Vitamin Solution	1 mL/L		
8	Seawater (non-sterized)	1 L		
9	Natural Seasalt	15g/ L		

Note: The recipe was provided by the Culture Collection of Algae at the University of Texas at Austin http://utex.org/.

VITA

Nan Zhou

Candidate for the Degree of

Master of Science

Thesis: CHARACTERIZATION AND MICROWAVE ASSISTED PYROLYSIS OF OKLAHOMA NATIVE MICROALGAE STRAINS FOR BIO-OIL PRODUCTION

Major Field: Biosystems Engineering

Biographical:

Personal Data: Born in Rudong, Jiangsu, China, on January 5, 1992, the son of Hongwei Zhou and Aiping Yu

Education:

Completed the requirements for the Master of Science in Biosystems Engineering at Oklahoma State University, Stillwater, Oklahoma in December 2015.

Completed the requirements for the Bachelor of Science degree in Energy and Power Engineering from Xi'an Jiaotong University, Xi'an, Shaanxi, China in June 2013.

Experience: Graduate Research Assistant at Oklahoma State University Stillwater, OK, August 2013 to July 2015.

Professional Memberships: ASABE